

# Role of *npas4l* and Hif pathway in endothelial cell specification and specialization in vertebrates

---



MAX-PLANCK-GESELLSCHAFT

Dissertation  
zur Erlangung des Doktorgrades  
der Naturwissenschaften

vorgelegt beim Fachbereich 15  
der Goethe-Universität  
in Frankfurt am Main

von  
Michele Marass  
aus Trieste, Italien

Frankfurt 2018  
(D30)

vom Fachbereich Biowissenschaften (FB15) der Johann  
Wolfgang Goethe - Universität als Dissertation angenommen.

Dekan: Prof. Dr. Sven Klimpel

Gutachter: Prof. Dr. Didier Y. R. Stainier  
Prof. Dr. Virginie Lecaudey

Datum der Disputation :

## **REVIEWERS**

Prof. Dr. Didier Stainier, Ph.D.  
Department of Developmental Genetics  
Max Planck Institute for Heart and Lung Research  
Bad Nauheim, Germany

and

Prof. Dr. Virginie Lecaudey, Ph.D.  
Department of Developmental Biology of Vertebrates  
Institute of Cell Biology and Neuroscience  
Johann Wolfgang Goethe University  
Frankfurt am Main, Germany

## ERKLÄRUNG

Ich erkläre hiermit, dass ich mich bisher keiner Doktorprüfung im Mathematisch-Naturwissenschaftlichen Bereich unterzogen habe.

Frankfurt am Main, den .....

(Unterschrift)

## Versicherung

Ich erkläre hiermit, dass ich die vorgelegte Dissertation über

**Role of *npas4l* and Hif pathway in endothelial cell specification and specialization in vertebrates**

selbständig angefertigt und mich anderer Hilfsmittel als der in ihr angegebenen nicht bedient habe, insbesondere, dass alle Entlehnungen aus anderen Schriften mit Angabe der betreffenden Schrift gekennzeichnet sind.

Ich versichere, die Grundsätze der guten wissenschaftlichen Praxis beachtet, und nicht die Hilfe einer kommerziellen Promotionsvermittlung in Anspruch genommen zu haben.

Einen Teil der vorliegende Ergebnisse der Arbeit sind in folgendem Publikationsorgan veröffentlicht:

Gerri\* and Marass\* et al., Hif-1 $\alpha$  and Hif-2 $\alpha$  regulate hemogenic endothelium and hematopoietic stem cell formation in zebrafish *Blood* Jan 2018; 131:963-973,

© the American Society of Hematology (\*Joint first author.)

doi:<https://doi.org/10.1182/blood-2017-07-797795>

Frankfurt am Main, den .....

(Unterschrift)

This thesis is dedicated to the memory of my grandfather

## Table of contents

<b>1</b>	<b>Introduction</b>	<b>13</b>
<b>1.1</b>	<b>The cardiovascular system</b>	<b>14</b>
1.1.1	Discovery of the cardiovascular system – The history	15
1.1.2	Evolution of the blood vascular system	17
<b>1.2</b>	<b>Model Organisms to study vascular development</b>	<b>18</b>
1.2.1	Zebrafish as model organism	19
1.2.2	Mouse as model organism	19
<b>1.3</b>	<b>Molecular mechanisms directing vascular development in vertebrates</b>	<b>20</b>
1.3.1	Vasculogenesis	20
1.3.2	Angiogenesis and vascular remodeling	23
<b>1.4</b>	<b>Endothelial cell origin</b>	<b>27</b>
1.4.1	Mesodermal differentiation	28
1.4.2	The hemangioblast	29
1.4.3	<i>cloche</i> mutant	30
<b>1.5</b>	<b>Endothelial cell specialization</b>	<b>32</b>
1.5.1	Morphological and functional heterogeneity of endothelial cells	32
1.5.2	Hematopoiesis	33
1.5.3	Hemogenic endothelium and HSC formation	35
<b>1.6</b>	<b>bHLH-PAS transcription factors</b>	<b>37</b>
1.6.1	Structure and regulation of bHLH-PAS transcription factors	37
1.6.2	Hypoxia inducible factors	39
<b>2</b>	<b>Aim of the study</b>	<b>42</b>
<b>3</b>	<b>Material and Methods</b>	<b>45</b>
<b>3.1</b>	<b>Materials</b>	<b>46</b>
3.1.1	Antibiotics	46

3.1.2	Antibodies	46
3.1.3	Buffers	46
3.1.4	Chemicals	47
3.1.5	Enzymes	48
3.1.6	Growth media	48
3.1.7	Kits	49
3.1.8	Laboratory supplies	49
3.1.9	Microscopes	50
3.1.10	Laboratory equipment	50
3.1.11	Morpholinos	51
3.1.12	Primers	51
3.1.13	Plasmids	53
3.1.14	Softwares	54
3.1.15	Zebrafish lines	54
3.1.16	Mouse lines	54
3.1.17	Cell lines	55
<b>3.2</b>	<b>Methods</b>	<b>55</b>
3.2.1	Zebrafish maintenance	55
3.2.2	Zebrafish breeding	55
3.2.3	Preparation of injection needles	56
3.2.4	Microinjection	56
3.2.5	Quantitative real-time PCR	56
3.2.6	Drug treatment	57
3.2.7	Measurement of nucleic acid concentrations	57
3.2.8	DNA sequencing	57
3.2.9	TA cloning	57
3.2.10	DNA restriction digestion	58
3.2.11	DNA ligation	58
3.2.12	Plasmid DNA preparation	58
3.2.13	<i>in situ</i> hybridization: probe synthesis	58
3.2.14	<i>in situ</i> hybridization	59

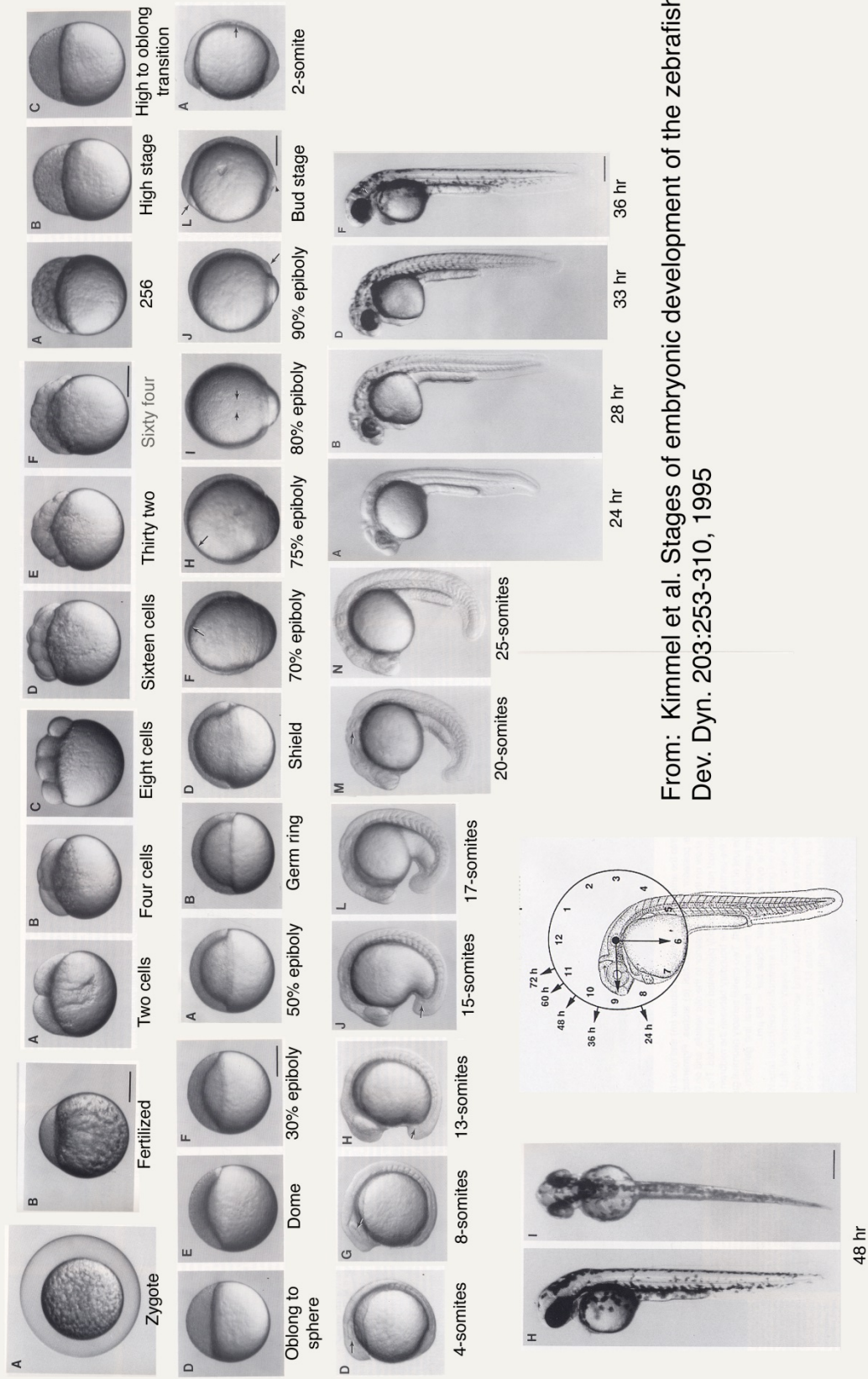
3.2.15	Mouse maintenance	59
3.2.16	Chromatin immunoprecipitation sequencing (ChIP-seq)	59
3.2.17	Assay for transposase-accessible chromatin with high-throughput sequencing (ATAC-seq)	62
3.2.18	RNA extraction and cDNA synthesis of zebrafish embryos	63
3.2.19	Mouse embryos dissection	63
3.2.20	Mouse embryos RNA isolation	64
3.2.21	gRNA design	64
3.2.22	gRNA assembly and synthesis	64
3.2.23	Heat shock treatments	65
3.2.24	mRNA synthesis	65
3.2.25	Mutant generation and alleles recovered	66
<b>4</b>	<b>Results</b>	<b>67</b>
<b>4.1</b>	<b>Upstream regulators of <i>npas4l</i> and angioblast differentiation</b>	<b>68</b>
4.1.1	<i>npas4l</i> spatiotemporal expression analysis reveals an early induction of <i>npas4l</i> in the ventral mesoderm.	68
4.1.2	Drug screening identify BMP and FGF signaling pathways to be involved in <i>npas4l</i> regulation	69
4.1.3	<i>in silico</i> binding motif prediction combined with transcriptome analysis of BCI-treated embryos suggest a role for <i>eomesa</i> upstream of <i>npas4l</i>	73
4.1.4	<i>eomesa</i> can induce <i>npas4l</i> expression <i>in vivo</i>	74
4.1.5	<i>Eomes</i> function is conserved in mammals and can lead to angioblast differentiation <i>in vitro</i>	75
4.1.6	Proposed model	78
<b>4.2</b>	<b>Identification and characterization of downstream targets of <i>npas4l</i></b>	<b>79</b>
4.2.1	<i>npas4l</i> overexpression followed by transcriptome analysis reveals its primary and secondary target genes	79



4.2.2	Chromatin immunoprecipitation sequencing identifies direct targets of Npas4l	83
4.2.3	Chromatin accessibility analysis in <i>npas4l</i> mutant does not suggest that Npas4l can act as a pioneer factor	87
4.2.4	Early transcriptome analysis of <i>npas4l</i> mutants reveals the reduction of early hematopoietic and endothelial markers	88
4.2.5	Combined analysis of different datasets reveals the downstream targets of Npas4l	92
4.2.6	Generation of mutants using CRISPR/Cas9 technology targeting the identified candidate genes downstream of <i>npas4l</i>	93
4.2.7	Proposed model	96
<b>4.3</b>	<b>Identification of the functional ortholog of <i>npas4l</i> in mammals: role of HIFs in endothelial cell differentiation</b>	97
4.3.1	<i>in vitro</i> identification of <i>npas4l</i> -homolog genes downstream of <i>Eomes</i>	97
4.3.2	Role of <i>Hif-1<math>\alpha</math></i> and <i>Hif-2<math>\alpha</math></i> in mouse <i>Etv2</i> regulation and endothelial cell specification	98
<b>4.4</b>	<b>Role of Hifs in endothelial cell specialization in zebrafish</b>	100
4.4.1	<i>Vasculogenesis and angiogenesis are not affected in hif-1<math>\alpha</math> and hif-2<math>\alpha</math> mutant</i>	100
4.4.2	<i>hif-1<math>\alpha</math></i> and <i>hif-2<math>\alpha</math></i> mutants show reduced expression of HSC markers	101
4.4.3	Hypoxia induces hemogenic endothelium specification and hematopoietic stem cell formation	101
4.4.4	Defects in hemogenic endothelial specification in <i>hif-1<math>\alpha</math></i> and <i>hif-2<math>\alpha</math></i> morphants	104
4.4.5	Notch signaling acts downstream of Hif pathway in HSC development	107
4.4.6	Proposed Model	111

<b>5</b>	<b>Discussion</b>	<b>113</b>
5.1	Upstream regulators of <i>npas4l</i> and angioblast differentiation	114
5.2	Identification and characterization of downstream targets of <i>npas4l</i>	117
5.3	Identification of a functional ortholog of <i>npas4l</i> in mammals: role of HIFs in endothelial cell differentiation	120
5.4	Role of Hifs in endothelial cell specialization in zebrafish	122
<b>6</b>	<b>Conclusions</b>	<b>125</b>
	I. Zusammenfassung	129
	II. English summary	137
	III. References	144
	Acknowledgments	156
	Curriculum Vitae	158

# Zebrafish developmental stages



From: Kimmel et al. Stages of embryonic development of the zebrafish  
Dev. Dyn. 203:253-310, 1995

## Commonly used abbreviations

Abbreviation	Description
EMT	Epithelial-to-mesenchyme transition
LPM	Lateral plate mesoderm
bHLH	Basic helix-loop-helix domain
DA	Dorsal aorta
ATAC	Assay for Transposase-Accessible Chromatin
<i>dll4</i>	delta-like-4
DMOG	Dimethylloxaloylglycine
dpf	Days post fertilization
E6.5	Mouse Embryonic day 6.5
EC	Endothelial cell
ECM	Extracellular matrix
EHT	Endothelial-to-hematopoietic transition
Etv2	ETS Variant 2
HIF	Hypoxia-inducible factor
HE	Hemogenic endothelium
HECs	Hemogenic endothelial cells
hpf	Hours post fertilization
HSC	Hematopoietic stem cell
ISV	Intersegmental vessel
kdrl	Kinase insert domain receptor like
Lmo2	LIM domain only 2
NICD	Notch intracellular domain
<i>Npas4l</i>	Neuronal Pas domain protein 4 like
N-TAD	N-terminal transactivating domain
ChIP	Chromatin immunoprecipitation
P5	Mouse postnatal day 5
PAS	Per-Arnt-Sim domain
PCV	Posterior cardinal vein
<i>shh</i>	sonic hedgehog
TGFB	Transforming Growth Factor Beta
<i>vegfa</i>	vascular endothelial growth factor A
Vegfr2	Vascular endothelial growth factor receptor 2
YS	Yolk Sac

## Nomenclature guide

Species	gene symbol	protein symbol
<b>Zebrafish (<i>Danio rerio</i>)</b>	<i>etv2</i>	Etv2
<b>Mouse (<i>Mus musculus</i>)</b>	<i>Etv2</i>	ETV2

# 1. INTRODUCTION

---

Part of this thesis includes a research originally published in *Blood*. Gerri\* and Marass\* et al., Hif-1 $\alpha$  and Hif-2 $\alpha$  regulate hemogenic endothelium and hematopoietic stem cell formation in zebrafish *Blood* Jan 2018; 131:963-973, © the American Society of Hematology (\*Joint first author.) doi: <https://doi.org/10.1182/blood-2017-07-797795>

<http://www.bloodjournal.org/content/early/2018/01/16/blood-2017-07-797795?sso>

## **1.1 The cardiovascular system**

The cardiovascular system is one of the first tissues to develop in the vertebrate embryo and it is critical for the removal of waste products and the delivery of oxygen and nutrients to the growing and mature organs. The blood is pumped by the heart in a closed circuit of arteries, veins and interconnecting capillaries forming an intricate but finely regulated network (Marcelo, Goldie, and Hirschi 2013). The large arteries carry the oxygenated blood from the left ventricle to the peripheral tissues. The oxygen is exchanged at the level of the capillaries and the oxygen-poor blood returns to the heart, into the right atrium. From the right ventricle, the blood will move to the alveoli, to be oxygenated, going into the left atrium, and back in the circle. In order to maintain homeostasis in the whole body, sustaining the blood flow, all vessels share some common characteristics. Anatomically, blood vessels are generally constituted by three layers: *tunica intima*, *tunica media* and *tunica adventitia*. The *tunica intima* is formed by endothelial cells (ECs), a specific type of epithelium covering the luminal side of vessels. *Tunica media* contains smooth

muscle cells and elastin fibers. The outermost layer of the blood vessel is the *tunica adventitia*, composed of fibro-elastic connective tissue. The intermediate and the most external layer are fundamental in providing structural support and elasticity to the blood vessels, in order to control the blood flow (Pugsley and Tabrizchi 2000).

### **1.1.1 Discovery of the cardiovascular system – The history**

Since ancient Greece, Greek physicians and philosophers investigated the nature of the cardiovascular system. It was observed, in fact, that living beings need some sort of nourishment in order to grow and survive. Specifically, Aristotle and others (4<sup>th</sup> century BC) described how, in animals, the blood was the major player in transporting the nutrients (*trophe*) around the whole body, flowing within blood vessels (*phlepsin*). Interestingly, the heart was considered the principle (*arche*) and the pulsating core of this system, and arteries and veins were known to have distinct properties as early as 340 BC (Boylan 2015). Only four centuries later (2<sup>nd</sup> century AD), Galen described for the first time that the arterial blood was mixed with “fresh air” coming from the lungs. Although the discoveries made before the fall of the Roman Empire were remarkable, given the limited tools available to investigate biology, the model of the cardiovascular system was certainly not flawless. Venous blood was believed to be originated in the liver, arterial blood generated in the heart and the cardiovascular system was considered open-ended. The concept of a closed circuit arrived with William Harvey, in the 17<sup>th</sup> century. Harvey proved that arteries receive blood from veins through the heart, performing experiments on fish and snakes. He tied the vein entering the heart and he noticed that the heart

became pale and there was no blood left in arteries. He then wanted to prove this concept in humans (Aird 2011). He employed tight ligature to compress the veins and the arteries of an arm and he observed loss of pulse and a cold, pale hand because the blood couldn't reach the periphery. Next, he used a medium-tight ligature to compress selectively the veins. In the latter case the hand became swollen and purple in color (Figure 1), thus suggesting that the blood was arriving at the extremities, but couldn't go back to the heart (Harvey et al. 1653). He published his exciting observations in *Exercitatio anatomica de motu cordis et sanguinis in animalibus*, in 1628.

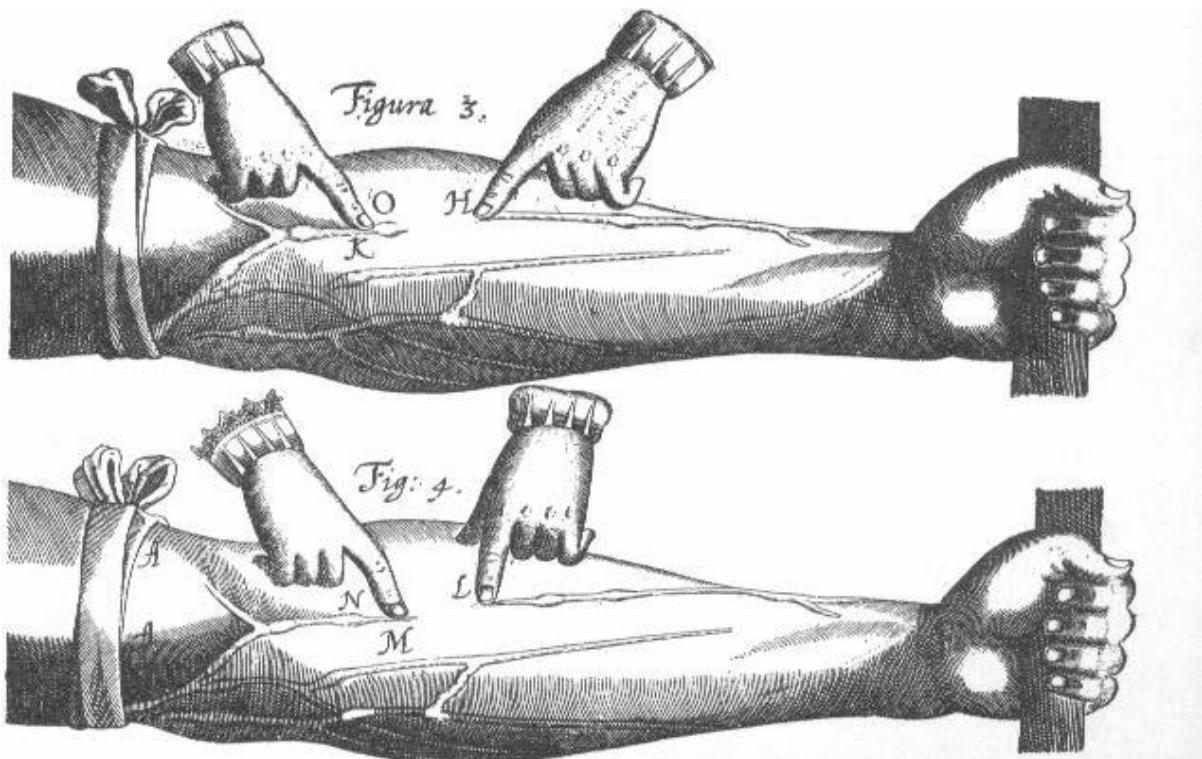


**Figure 1. *de motu cordis*: William Harvey's experiment on a human.** He proved that blood enters the arm by the arteries; venous blood flows only from the



periphery towards the heart, revealing the function of the valves in the veins, which prevent backflow of the passing blood (Harvey et al. 1653).

### **1.1.2 Evolution of the blood vascular system**

Animalia kingdom (Metazoa) emerged on planet earth between 700 and 800 million years ago. Interestingly, the embryonic development of animal species for the following 100 years was significantly different from the one we can observe in the modern animals. “Primitive” animals, like Porifera, a phylum including sponges, do not undergo a proper gastrulation and progressive fate determination (Nakanishi, Sogabe, and Degnan 2014). Cnidaria and Ctenophora were also present 700-800 million years ago; in these phyla, gastrulation occurs and it gives rise to two germ layers: endoderm and ectoderm and they are therefore called “diploblastic”. Concomitant to the emergence of a new body plan around 600 million years ago, Bilateria developed a third germ layer during embryogenesis, the mesoderm; hence these animals are considered triploblasts. Nutrients supplying and gas exchange occurs in diploblastic animals by diffusion. This strategy does not require a circulatory system, but it can efficiently work only when the body size of the animal is very limited. Although few triploblasts, like flatworms, are acelomates and rely on diffusion to nourish the tissues, during evolution, with the increase in body size and in body weight, some primitive triploblasts formed internal cavities, called coelomas. Eucoelomates developed a circulatory system, consisting of a coelum filled with fluid, physically separating endoderm-derived tissues and ectoderm-derived tissues. The luminal layer of this coelum consists of an epithelium called mesothelium,

differentiated from the mesoderm. Interestingly, in some animals, the coelom regresses in the adult, and the mesodermal cells reaggregate to form the blood vessels. In fact, early eucoelomates were the first animals on the planet to have a blood vascular system. The striking difference between primitive and modern eucoelomates is the presence of an open vascular system in the former, where there is no clear distinction between circulating fluid and interstitial fluid and the latter, characterized by a closed circulatory circuit. Blood, which content may vary greatly among species, flows in cavities, such as hemocels, vessels, and pumping organs; in absence of a heart, the flow is mediated by peristalsis, for example in annelids. The most luminal layer of the cavities where blood flows changed during evolution, invertebrates exhibit a layer of extracellular matrix facing the lumen, whereas vertebrates developed a *tunica intima*, consisting of so-called ECs (Monahan-Earley, Dvorak, and Aird 2013). The endothelium is involved in a plethora of biological processes in vertebrates such as controlling vasoconstriction and vasodilatation, modulating vessel permeability and hemostasis (Michiels 2003). Similarly to the mesothelium, also endothelium differentiates from the mesoderm, in a process that will be discussed further below.

## **1.2 Model Organisms to study vascular development**

Model organisms have been used since the dawn of biology to describe and study biological phenomena in more accessible and simpler living beings. Different model organisms provide advantages to study various biological processes assuming that a certain mechanism is conserved, at least in part, in other species.

### **1.2.1 Zebrafish as a model organism**

Zebrafish (*Danio rerio*) is a freshwater fish, belonging to the family of *Cyprinidae*, originally from Indian sub-continent. Zebrafish presents many peculiar advantages compared to other model organisms. Zebrafish females lay many eggs – up to 300 every week – and embryos develop externally, making them easy to be observed and manipulated. The development of most organs and the tissues occurs in the first day of embryogenesis; heart, vessels and neurons are visible already at 24 hours after the insemination of the oocyte. During the first few days after fertilization the embryos do not present pigmentation, allowing a live-analysis of organogenesis using bright-field or confocal microscopy, which confers a sub-cellular resolution of developing systems (Gutierrez-Lovera et al. 2017). These features, combined with the ease in generating transgenic fluorescence reporters and mutants using genome editing techniques, e.g. CRISPR/Cas9 technology, make zebrafish an ideal model to study vascular development.

### **1.2.2 Mouse as a model organism**

Over the course of the past century, Mouse (*Mus musculus*) has represented the preferred mammalian model to study genetics, development, and diseases. Besides having a short generation time - they reach sexual maturity at around 5 weeks - it takes 3 weeks for a female to give birth, meaning that they can expand quickly, allowing the scientist to perform experiments that require a high number of animals is needed (Nguyen and Xu 2008). Among other classical model organisms, namely

*Escherichia coli*, Yeast (*Saccharomyces cerevisiae*), Fly (*Drosophila melanogaster*) and Frog (*Xenopus leavis*), the mouse has the advantage of being evolutionary the closest one to *Homo sapiens*, sharing a number of anatomical, physiological and genetic features with human. Importantly, in 1987 Capecchi and Thomas described how to introduce a site-oriented mutation in a mouse embryo, revolutionizing the way to study genetics in a mammalian model (Thomas and Capecchi 1987). The mouse genome was sequenced and assembled in 2002 (Mouse Genome Sequencing et al. 2002) and the genome assembly highlighted the similarities in terms of sequence and synteny between human and mouse, making easier to study gene function and also to generate murine models to study human diseases.

### **1.3 Molecular mechanisms directing vascular development in vertebrates**

The formation of a functional vascular system in vertebrates requires several sequential processes: vasculogenesis, angiogenesis, and vascular remodeling. Subsequently, ECs may undergo a specialization event, in order to adapt to the environment and answer the peculiar needs of the supplied organs (Ellertsdottir et al. 2010).

#### **1.3.1 Vasculogenesis**

As described above, the most important cell type constituting the vasculature is the endothelium. ECs differentiate from their progenitors, called angioblasts.

Angioblasts, in zebrafish, specify from the ventral mesoderm and migrate from the lateral plate mesoderm (LPM) during somitogenesis towards the midline, ventrally to the hypochord and dorsally to the endodermal layer. In the midline, angioblasts coalesce, fuse and form tubes, which are the first axial vessels developed in the embryo, called dorsal aorta (DA) and posterior cardinal vein (PCV) (Vogel and Weinstein 2000). This process that gives rise to the formation of vessels *de novo*, is defined as vasculogenesis. Arterial and venous progenitors originate at distinct locations and migrate in two separate waves. The first angioblast wave is formed in the LPM at around 4 somite-stage and will constitute the DA, the second one, detectable at 10-somite stage, will form the PCV (Kohli et al. 2013).

These two populations are exposed to different concentrations of morphogens, such as vascular endothelial growth factor (Vegf), transforming growth factor beta (TGFB) and sonic hedgehog (Shh). In fish, a signaling cascade including Sonic, Vegf and Notch pathways has been described to drive the specification and the maturation of axial vessels. Shh is a soluble factor expressed in the notochord, and it induces the expression of *vegfr* in the somites. Vegf binds to Vegfr2, expressed in ECs, and activate Notch signaling, responsible for the induction of well-known arterial markers, such as *efnb2a*, and the consequent maintenance of arterial identity of the DA (Lawson, Vogel, and Weinstein 2002). In line with this model, *ptch1;ptch2* mutants, that exhibit an upregulation of Shh signaling, show ectopic arterial markers at the expense of venous markers, causing the formation of a second axial artery and the loss of a PCV (Wilkinson et al. 2012). Conversely, *vegfaa* mutants fail to form a lumenized DA and *efnb2a* is not detectable in the trunk region (Rossi et al. 2016). In

mouse, vasculogenesis occurs initially in the embryonic yolk sac at around embryonic stage 6.5 (E6.5), and only later at around E8.0 in the embryo proper. Starting from E6.5 mesodermal cells differentiate from the primitive streak during gastrulation, and FGF signaling plays a fundamental role in the migration of the primitive streak, promoting the epithelial-to-mesenchyme transition (EMT) of these cells (Yamaguchi et al. 1994) (Ciruna and Rossant 2001). BMP signaling is another pathway described to be instrumental for mesoderm differentiation, and its role will be discussed later in the introduction. In the mouse yolk sac, the visceral endoderm releases soluble factors that induce the specification of angioblasts and hematopoietic cells in the blood islands. Here, primitive ECs proliferate to cover the entirety of YS, forming the so-called capillary plexus (Jones, le Noble, and Eichmann 2006). In the embryo proper, from E8.0, the molecular mechanisms promoting vasculogenesis are similar to zebrafish. Angioblasts expressing *Vegfr2* organize in stripes and migrate from the lateral plate mesoderm towards the midline (Fish and Wythe 2015), but being the development internal, the vascular network of the embryo proper has to connect with the external plexus as depicted in Figure 2 in order to allow a functional blood flow between the mother and the embryos (Goldie, Nix, and Hirschi 2008). *Vegf-a* and *Vegfr2* have been described to be involved in the formation of blood islands in the YS as well as in the angioblast proliferation and migration in the embryo proper (Shalaby et al. 1995; Ferrara et al. 1996). *Etv2* mutant lacks both hematopoietic and vascular tissues in the whole embryo, suggesting a high similarity between the molecular cues directing intraembryonic and extraembryonic vasculogenesis (Figure 2) (Lee et al. 2008).

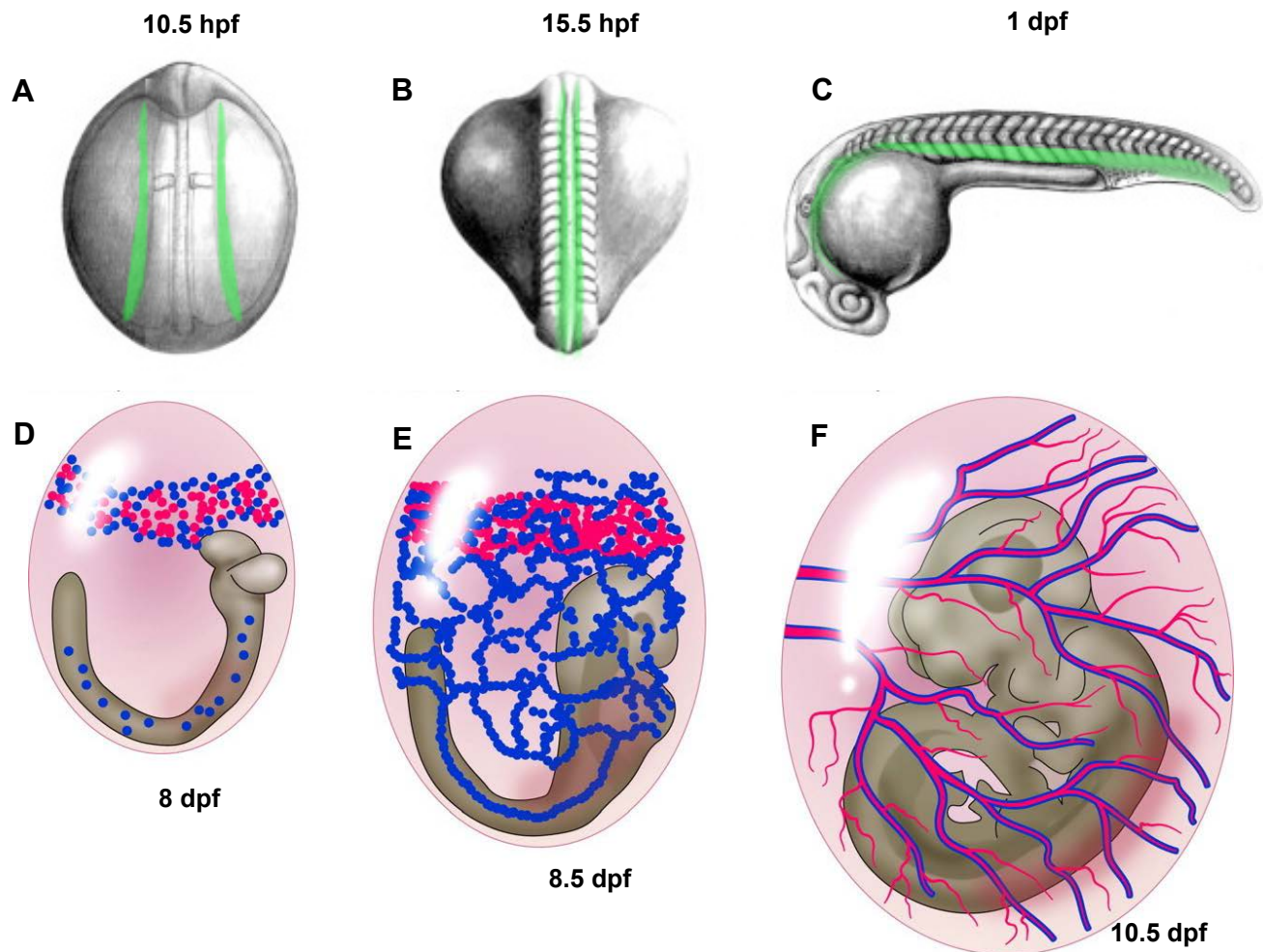


**Figure 2. Vasculogenesis in vertebrates**

In A,B,C angioblasts in zebrafish are highlighted in green. Angioblasts migrate from the LPM towards the midline, where they coalesce to form the axial vessels. A and B are seen from the dorsal view, C from the lateral view. (Stickney, Barresi, and Devoto 2000)

In D,E,F early mouse embryonic stages are depicted, side view. Blood cell precursors are marked in red, EC precursors in blue. (Jones, le Noble, and Eichmann 2006)

### 1.3.2 Angiogenesis and vascular remodeling

Angiogenesis is the process through which new blood vessels develop from vessels previously formed (Phng and Gerhardt 2009).

In zebrafish, after the formation of the axial vessels, most of the vascular network is formed via budding or sprouting of ECs starting from pre-existing vessels. At first, some ECs of the DA acquire motile features and exhibit protrusions, enriched in filamentous actin, called filopodia. These ECs sprout from the dorsal wall of the DA at around 22 hours post fertilization (hpf), and they migrate dorsally to form the intersegmental vessels (ISVs). ISVs line the somite boundaries and, once reached the dorsal floor of the neural tube, they fuse, through a process called anastomosis, to form the dorsal longitudinal anastomotic vessels (DLAVs). The venous ISVs sprout from the PCV from 32 hpf, these venous ECs migrate and connect to the pre-existing arterial ISV. The most ventral ECs of the arterial ISV regress and disappear, resulting in the formation of a venous ISV (Isogai et al. 2003) (Figure 3).

The first ECs sprouting from the DA are known as tip cells: they are migratory and have a low proliferation rate, in the forming ISVs they are the leading cells and are in contact to the so-called stalk cells, less motile but proliferative. These two types of cells are not only morphologically different, but also transcriptionally. Tip cells express high levels of *vegfr2*, compared to stalk cells. This feature causes tip cells to be more sensitive to Vegf-a. Vegf-a in fact, binding to Vegfr2, activates the Vegf signaling in tip cells and delta-like-4 (*dll4*) expression is induced (Ellertsdottir et al. 2010). Dll4 is a transmembrane ligand for the Notch receptor, the latter expressed in stalk cells. After Dll4 binds Notch1 of the neighboring cell, Notch receptor is cleaved and the Notch intracellular domain (NICD) is translocated into the nucleus, where can act as transcription factor. The NICD can induce not only genes associated with proliferation but also a soluble form of Vegfr1, which binds to the Vegf-a ligand, and



acts as a decoy receptor, in order to avoid the activation of Vegf signaling in the stalk cells. Loss-of-function models for *dll4* or *vegfr1* show a similar ectopic sprouting phenotype, due to the presence of an abnormal number of ECs with tip cell identity (Krueger et al. 2011) (Matsuoka et al. 2016) (Hogan et al. 2009).

To study developmental angiogenesis in mammals, the most popular model is represented by the mouse retinal angiogenesis, due to the ease in harvesting a consistent number of retinas in a short time. Newborn pups have an immature retinal vasculature. Angiogenesis is the main responsible for the vascular coverage of the retina; indeed, the vascular plexus is nearly absent at birth and covers most of the retina at 8 days postnatally (Figure 3A). The increase in the resolution of confocal microscopes and the availability of more reliable monoclonal antibodies have substantially helped the scientists in analyzing high-definition pictures of the angiogenic event in different settings (Catita et al. 2015). Similarly to zebrafish, Vegf pathway plays a central role in the migration and proliferation of ECs. Vessels expressing *Vegfr2* expand in a radial way following VEGF-A gradient (Ferrara, Gerber, and LeCouter 2003). Many molecular pathways are conserved between ISVs sprouting in zebrafish and mouse retinal vascularization. Besides Vegf pathway, also Notch1 signaling has been extensively studied in both settings (Blanco and Gerhardt 2013). Perturbation of Notch signaling has dramatic consequences on angiogenesis and artery specification (Jakobsson et al. 2010). Cell-autonomous expression of *Cxcr4* and *Vegfa* downstream to Notch signaling was shown to be key in sprouting angiogenesis (Pitulescu et al. 2017). Recently, Ralf Adams' Laboratory found that tip cells can migrate in opposite direction of the

sprouting, and they can be incorporated into arteries, contributing arterial growth (Pitulescu et al. 2017). Angiogenesis is followed by remodeling and pruning of vessels, processes that will give rise to the mature and functional vascular plexi (Hughes and Chang-Ling 2000) (Kobayashi et al. 2013). Notably, angiogenesis and vascular remodeling often occurs simultaneously, in an orchestrated manner. Notably, shortly after birth, two concomitant vascular processes occur in the mouse's eye: vascular regression in the hyaloid vasculature and concomitant growth of the intraretinal vasculature (Stahl et al. 2010).

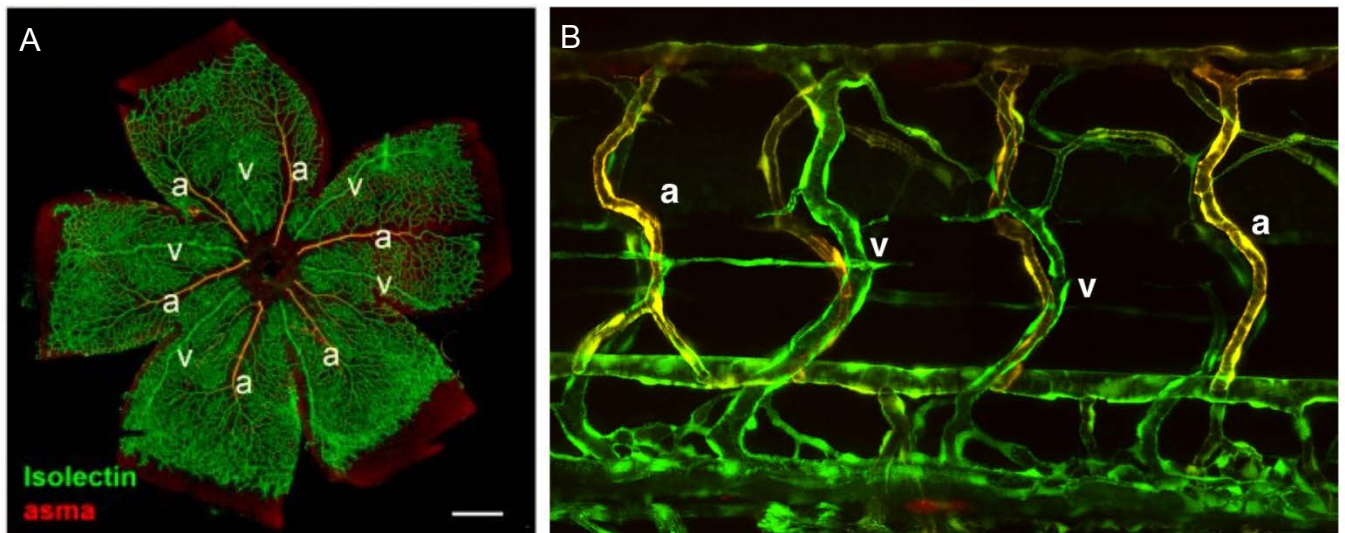


**Figure 3. Models of angiogenesis in vertebrates**

A) Retinal vasculature in mouse at P5; arteries are highlighted in red by Alpha Smooth Muscle Actin staining; Isolectin staining, in green, marks the whole vasculature. (Tual-Chalot et al. 2014)

B) Intersegmental vessels in a 5 dpf zebrafish embryos. *TgBAC(etv2:EGFP)* is expressed in all EC (green). The expression of *Tg(-0.8flt1:tdTomato)* is restricted to the arteries, therefore the arteries appear yellow. a = artery; b = vein.

## 1.4 Endothelial cell origin

### 1.4.1 Mesodermal differentiation

Mesoderm (from Greek *mesos* “middle” and *derma* “skin”, “layer”) is a germ layer formed during gastrulation between endoderm and ectoderm and give rise to a multitude of tissues including blood, ECs, muscles, and the tubular cells of the kidneys (Kimelman 2006). One of the most important signaling pathways involved in mesoderm specification and patterning, conserved among vertebrates, is the BMP signaling (Winnier et al. 1995). (Faure et al. 2002) (Pyati, Webb, and Kimelman 2005). Downstream or in parallel to BMP signaling pathway and its transcriptional effectors SMADs, many transcription factors are known to play a role in mesoderm differentiation, such as Brachyury, Eomes and Mixl1 that were identified to be key for the establishment of the mesodermal layer (Faial et al. 2015) (Pereira et al. 2011). Brachyury loss-of-function models show severe defects in mesoderm formation. In mice, a mutation in the *Bra* locus leads to the lack of the notochord resulting in a shorter body axis; *Bra* mutants have abnormal somites and all tissues derived from the mesoderm are affected (Stott, Kispert, and Herrmann 1993). Interestingly, also zebrafish mutants for the homolog of the mouse brachyury exhibit a very similar phenotype. These mutants identified through forward genetic screen were called “no-tail”, as the embryos do not develop the notochord and the caudal region of the body (Schulte-Merker et al. 1994). Similarly, *Eomes* mouse mutants have defects in axis formation and endoderm patterning (Arnold et al. 2008). Moreover, cardiac and vascular progenitors are impaired (Costello et al. 2011). In zebrafish, maternal

zygotic *eomesa* mutants exhibit defects in mesoderm-derived tissues, further highlighting the importance of this T-Box transcription factor in early mesodermal and endodermal patterning and specification (Xu et al. 2014).

### **1.4.2 The hemangioblast**

The precursors of ECs are the angioblasts, which specify from the mesoderm in proximity and concomitantly to the blood precursors. In mouse embryos, starting from E7.0, mesodermal cells migrate in the yolk sac forming clusters of cells called blood islands that will give rise to both primitive erythrocytes and ECs (Rossmann, Zhou, and Zon 2016).

Several models were described in the literature to explain the development of blood and ECs in the early vertebrate embryo, but up to date, the relationship between these two cell types have not been fully elucidated.

The term “hemangioblast” was coined by Murray in 1932, citing previous studies performed by Sabin, Maximov, and Ranvier. Murray called hemangioblast a mesodermal mass of cells from which erythrocytes and vessels originate. Keller laboratory (Choi et al. 1998) observed a clonal precursor, *in vitro*, that had the potential to differentiate into blood or endothelium, called blast colony-forming cell (BL-CFC) in 1998. This cell was thought to correspond to the *in vivo* hemangioblast. After these observations, the term “hemangioblast” was used to describe bipotent cell, instead of a population of cells, as described by Murray. Only 15 years later a low number of BL-CFCs was identified in the primitive streak of a mouse embryo at

E7.5 (Huber et al. 2004). A deeper analysis of the bipotency of the BL-CFC, identified a transient hemogenic endothelial stage preceding the differentiation to erythrocytes, suggesting that the hemangioblast does not specify into blood cells directly, but it requires an endothelial intermediate (Lancrin et al. 2009). In zebrafish, a clonal analysis identified a common progenitor for both lineages, without taking in account a model consisting of a transient hemogenic endothelial state, that may explain the presence of bipotent cells in the gastrula (Vogeli et al. 2006). *in vivo* clonal analysis confirmed the previous *in vitro* observations, reinforcing the idea that mesodermal cells differentiate in hemogenic endothelium prior to specify into primitive blood, in a linear pathway (Padron-Barthe et al. 2014). Recent single-cell transcriptomics revealed a group of seven transcription factors, namely Erg, Fli1, Tal1, Lyl1, Lmo2, Runx1, Cbfb and Gata2 to be co-expressed in HE, prior to the endothelial to hematopoietic transition downstream to the BL-CFC differentiation protocol. Specifically, they identified Erg and Fli1 to promote the endothelial cell fate and Runx1, together with Gata2, to induce the hematopoietic fate (Bergiers et al. 2018). Moreover, another model was suggested, angioblast could act in a cell non-autonomous manner to promote blood differentiation and erythrocyte proliferation in another population of cells (Parker and Stainier 1999).

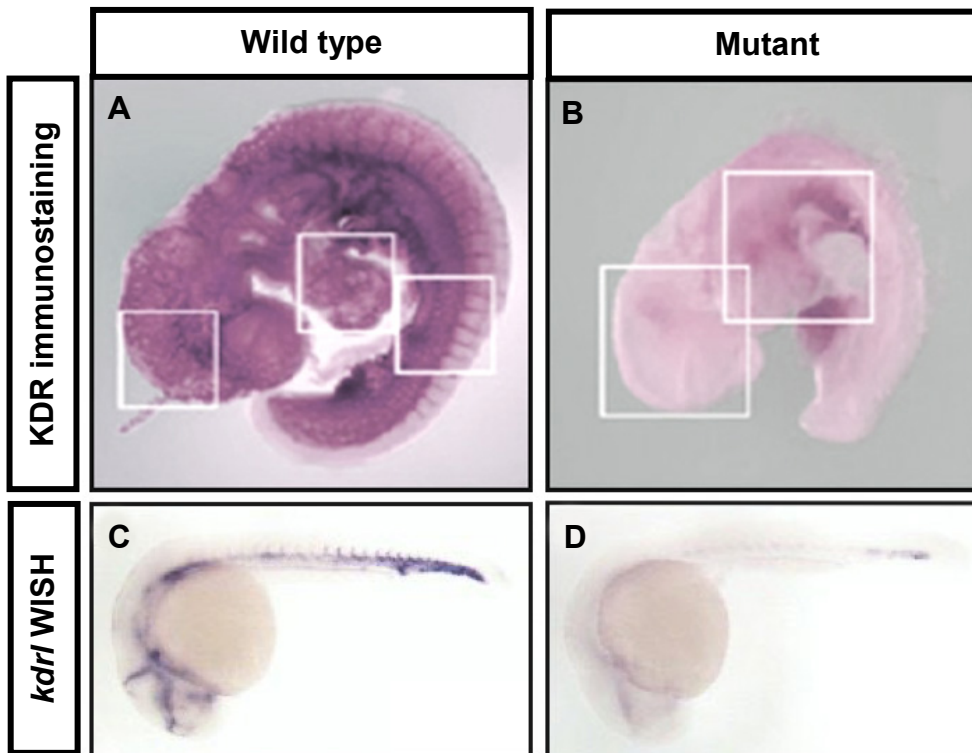


**Figure 4. Vertebrate avascular models**

In the top two panels the vasculature of mouse embryos is stained using anti-KDR antibody. In the wild type (WT) mice, vessels are detectable throughout the body at E9.5 (A), whereas in *Etv2* mutants at the same stage, ECs fail to specify and vessels are not formed (B) (Sumanas and Choi 2016).

Similarly, in WT zebrafish embryos a WISH for *kdr* marks the developing vessels at 24 hpf (C), while *npas4l* mutant lacks most of endothelial tissue and *kdr* transcript is detectable only in a small population of cells in the caudal region (D) (Habeck et al. 2002).

### 1.4.3 *cloche* mutant

In 1995 Stainier et al. discovered a spontaneous mutation in a population of zebrafish from an Indonesian fish farm. The gene was named *cloche* because of the

enlarged and bell-shaped heart of the mutants, due to the lack of endocardium (Stainier et al. 1995). Although the name *cloche* was given based on the heart phenotype, the mutant embryos show another striking phenotype: the absence of endothelial and hematopoietic tissues without exhibiting additional defects in other mesodermal-derived tissues. The zebrafish embryos can develop up to 5 dpf without a functional vasculature due to their limited size (Liao et al. 1997). Interestingly, the role of *cloche* in endothelial cell specification has been tested to be cell-autonomous; however, its role in blood development is less clear and it was reported to function, at least in part, in a cell non-autonomous manner (Parker and Stainier 1999). The presence of a gene controlling both blood and vasculature suggests the existence of bipotent hemangioblast cells, missing in *cloche* mutants. For more than two decades, *cloche* mutant has been used as an avascular model, to study the impact of vasculature on the development of other organs, such as the retina (Dhakal et al. 2015) and the liver (Field et al. 2003). Since the *cloche* locus is located in a telomeric region, the identification of the nature of this gene has required many efforts. Only recently, our laboratory described that *cloche* encodes for a bHLH-PAS transcription factor, and the gene is called *npas4l* due to its similarity, in terms of amino acid sequence, to the mammalian *Npas4*. By performing epistasis experiments, we confirmed that *Npas4l* acts at the top of the hemato-endothelial specification cascade. Interestingly, this gene was lost during evolution in the mammalian lineage, being present in the other vertebrates (Reischauer et al. 2016).

## **1.5 Endothelial cell specialization**

### **1.5.1 Morphological and functional heterogeneity of endothelial cells**

As previously mentioned, ECs consist of a heterogenous population. In the adult organism many types of specialized endothelia are present. Vessels are morphologically and functionally distinct and optimized to fulfill the requirements of a certain tissue in terms of nutrients and oxygen supply. Organ-specific signals can influence the behavior and the development of ECs, in order to acquire new features and to have specific functions, not only related to blood transport (Rocha and Adams 2009). For example, the endothelium of arteries and veins is continuous; on the contrary, at the level of the capillaries, the ECs can form a continuous, fenestrated or discontinuous monolayer. In organs involved in filtration and secretion, such as the kidney glomeruli, the endothelium is fenestrated and permeable. In the brain, on the contrary, it is necessary to protect the neurons from xenobiotics and pathogens. To perform this task, the blood brain barrier (BBB) limits the transfer of molecules into the brain, and the continuous endothelium located in this region guarantees a very low and selective permeability (Tse and Stan 2010). Specialized vascular niches are also involved in the formation of blood cellular components. Bone marrow ECs (BMECs) are a subset of ECs constituting the vasculature of bones that regulate hematopoietic stem cell (HSC) maintenance and white blood cell trafficking (Itkin et al. 2016). Another striking distinction that can be



observed among vascular plexi is the coverage of perivascular cells. Perivascular cells include pericytes and vascular smooth muscle cells. These cell types are recruited by the vessels, and confer specific function to the vessel they cover. Large vessels contain vascular smooth muscle cells that are fundamental to regulate vascular tone and blood pressure. Capillaries are nearly devoid of vascular smooth muscle cells, but are wrapped by a high number of pericytes (Potente and Makinen 2017). Pericytes contact the endothelium and modulate vessel stability and transendothelial transport. In the case of the BBB, pericytes play a crucial role in controlling and limiting endothelial transcytosis (Dore-Duffy and Cleary 2011; Dore-Duffy 2008). The high heterogeneity among mature endothelia is caused by a combination of a different exposure to organ-specific growth factors and the inherent transcriptional identity of ECs during development (Nolan et al. 2013).

### **1.5.2 Hematopoiesis**

Hematopoiesis in the embryo can be divided into two distinct waves: primitive and definitive. The HSC formation through an endothelial intermediate in the VDA is known as definitive hematopoiesis. Primitive hematopoiesis, instead, occurs earlier in the vertebrate embryos, at around E7 in mouse and from 2 somite stage in zebrafish. Blood progenitors are specified from the mesoderm, concomitantly with endothelial cell precursors, and form clusters including angioblasts and primitive erythrocytes in the blood islands (Paik and Zon 2010). The second wave of hematopoiesis is called definitive hematopoiesis and requires an endothelial

intermediate in the developing embryo. Definitive hematopoiesis in mouse starts around E10 and in zebrafish it occurs from 32 hpf.

In zebrafish the first site of HSC formation is the VDA, via a process that will be discussed in the next chapter. Next, HSCs colonize the caudal hematopoietic tissue (CHT) and the thymus, where they find a niche to proliferate. At 4 dpf HSCs populate the kidney where they increase in number (Figure 5). This area represents the most prominent site of hematopoiesis from larval stage onwards (Davidson and Zon 2004). Definitive hematopoiesis can occur in multiple sites of the murine embryos, it starts in the yolk sac and only later in the placenta (Gekas et al. 2005; Gekas, K, and H 2008) and in the aorta-gonad-mesonephros (AGM) region (Medvinsky and Dzierzak 1996), as discussed in the next chapter. Fetal liver is one of the major sites of definitive hematopoiesis during embryogenesis, from E11 to P0 (Sanchez et al. 1996).

Shortly before birth, definitive hematopoiesis takes place in the fetal bone marrow, which represents the most important site of hematopoiesis postnatally.

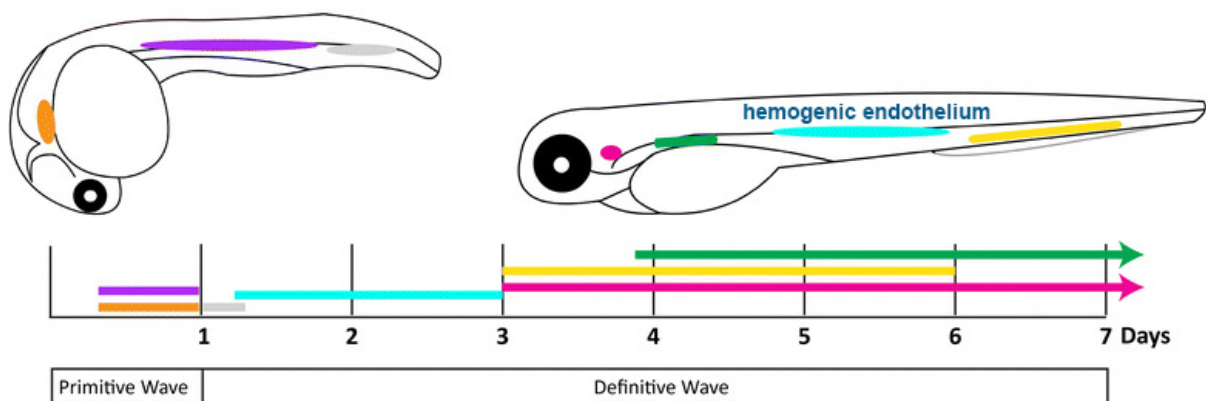


### **Figure 5. Hematopoiesis waves in zebrafish**

Primitive hematopoiesis starts in the LPM, from the anterior LPM (orange) monocytes are formed, while from the posterior LPM (purple) primitive erythrocytes arise. The so-called intermediate wave takes place in the posterior blood island (PBI) (grey). Definitive HSCs emerge from the VDA (cyan) from 36 hpf. Some HSCs colonize the CHT (yellow) and the thymus (magenta) where they proliferate and differentiate. HSCs populate the kidney (green) starting from 4 dpf until adulthood. (Rasighaemi et al. 2015)

### **1.5.3 Hemogenic endothelium and hematopoietic stem cell formation**

A fascinating example of specialized endothelium is the hemogenic endothelium (HE).

HE can be detected during development, and represents the most important site where definitive hematopoiesis occurs in the embryo. A subset of ECs in the ventral wall of the dorsal aorta (VDA) differentiates into HE and acquires the potential to become HSCs, emerging from the luminal layer of vessels into the circulation through a process called endothelial-to-hematopoietic transition (EHT). HE can be detected in mouse between E10-E11.5 in the AGM region and in zebrafish between 30 and 72 hpf in the VDA.

HSCs express surface markers such as CD31, CD41 and c-Kit and are multipotent cells that can give rise to lymphoid and myeloid lineage (Imanirad et al. 2014). Growth factors such as VEGF (Leung et al. 2013) and TGFB (Monteiro et al. 2016) have been shown to be involved in HE formation and subsequent HSC development.

Specifically, VEGF-A, through VEGFR2 can activate Notch signaling in ECs in the VDA, which leads to the direct induction of *Gata2* via *RBPJ*. Notch-dependent *Gata2b* induction was shown to be necessary for *runx1* expression in zebrafish and it is crucial for the emergence of HSCs, upstream of *Runx1* (Gritz and Hirschi 2016; Marcelo et al. 2013) and *c-Myb* (Zhang et al. 2011).

The transcriptional cascade upstream of HSC formation is evolutionary conserved. Loss-of-function models for *Notch1* exhibit a reduction in expression of HSC markers both in mouse (Marcelo et al. 2013; Zape and Zovein 2011) and in zebrafish (Konantz et al. 2016). *Gata2* function, moreover, has been studied in HSC formation not only during embryogenesis but also in the expansion of adult HSCs in the bone marrow (Ling et al. 2004). Accordingly, *Gata2* knockout leads to embryonic lethality (E10.5) due to impaired erythropoiesis and lack of HSC formation (Tsai et al. 1994).

*Runx1* has been described to be an essential master regulator of EHT and HSC formation, and its function is highly conserved in vertebrates (Swiers, de Bruijn, and Speck 2010). *runx1* is expressed in the VDA and the AGM region and act cell autonomously in the HSC emergence from the DA. RUNX1 has a dual role, being able to repress endothelial program, and to induce hematopoiesis, with sequential activation of CD41 and CD45 (Lancrin et al. 2009). *c-Myb* was described as a downstream effector of RUNX1. *c-Myb* mice mutants die *in utero* at E15.5 due to lack of hematopoiesis, resulting in defective erythroid and myeloid development (Mucenski et al. 1991). The conserved function of *c-Myb* (Soza-Ried et al. 2010) has been extended not only to HSCs development but also to HSCs maintenance and

HSC proliferation (Lieu and Reddy 2009). Zebrafish mutants for *c-Myb* show normal expression of *runx1* in the HE, but defective HSC extrusion leading to an accumulation of HSCs unable to egress from the VDA into the sub-aortic space (Zhang et al. 2011).

## **1.6 bHLH-PAS transcription factors**

### **1.6.1 Structure and regulation of bHLH-PAS family**

A plethora of key cellular processes including cell differentiation, cell cycle and stress response are controlled by gene networks downstream of bHLH transcriptional factors.

A basic helix-loop-helix (bHLH) is the structural domain that defines this family of proteins involved in gene regulation. This conserved architecture confers to the proteins the ability to bind the DNA upon dimerization with another bHLH transcription factor (Massari and Murre 2000). Subgroups were identified to further classify these transcription factors, based on the presence of additional domains involved in protein-protein dimerization. The three main sub-families of bHLH proteins are (1) those containing solely the bHLH domain, sufficient to induce the dimerization of the proteins, and those that exhibit a second dimerization domain, that can be (2) a leucine zipper module (Zip) or (3) the PER/ARNT/SIM (PAS) domain (Kewley, Whitelaw, and Chapman-Smith 2004). bHLH-PAS transcription factors generally present one bHLH domain, two PAS domains and a C-terminus end of variable length containing the transactivation domains (Fribourgh and Partch

2017). In order to form functional transcriptional complexes, bHLH-PAS proteins need to form heterodimers between class I and class II subunits (Figure 6). Class I proteins are either finely regulated at the transcriptional level, or present only in a certain tissue, or at the post-translational level, where specific environmental factors determine their stability. Class II proteins are expressed ubiquitously and do not exhibit major regulations at the protein level. Important members belonging to class I proteins are HIF-1 $\alpha$ , AHR, CLOCK, and NPAS regulated by oxygen level, xenobiotics, circadian rhythms or by a specific tempo-spatial expression, respectively. Example of class II proteins are ARNT, ARNT2, and BMAL1. The members of this family can have a preference to interact with a certain subset of class I proteins, for instance, BMAL1 is known to bind preferentially to CLOCK (Huang et al. 2012).

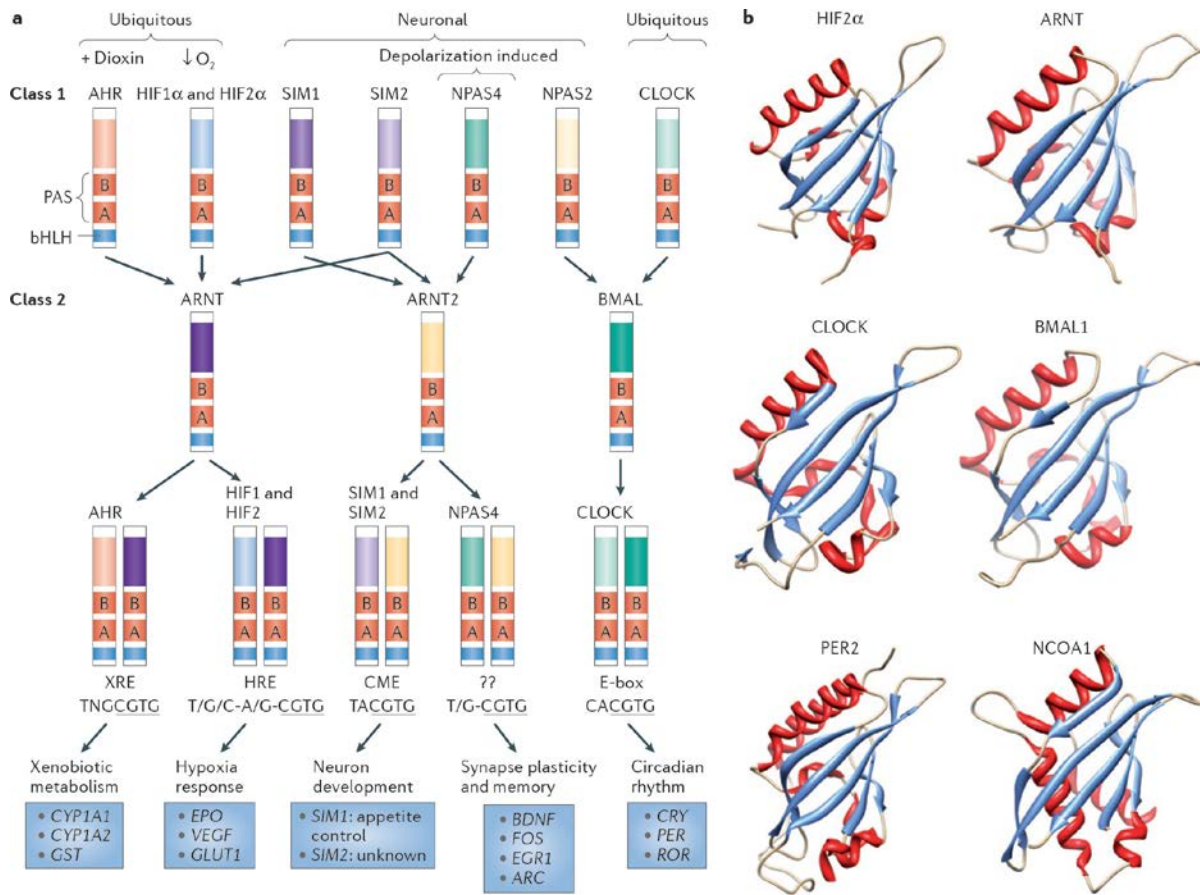


**Figure 6. Structure and function of bHLH-PAS transcription factors**

a) Depiction of Class 1 and Class 2 bHLH-PAS transcription factors. Class 1 proteins are finely regulated, whereas Class 2 members are more ubiquitous.

b) bHLH and PAS domains are involved in the specific heterodimerization between Class 1 and Class 2 protein. The quaternary structure obtained determines the binding between the transcriptional complex and the target DNA (Bersten et al. 2013).

### 1.6.2 Hypoxia inducible factors

Regulation of oxygen homeostasis is essential to all vertebrates throughout life. During development and diseases, organs and tissues are exposed to levels of oxygen that may drastically change in relatively short time. In hypoxic conditions, mitochondrial respiration is less efficient, resulting in a reduction of ATP synthesis.

ATP availability is fundamental in cellular metabolism, and it is indispensable to maintain essential cellular functions. Cancer and ischemia are medical conditions where hypoxia, influencing gene networks and cellular behavior, has been shown to have a detrimental effect at the whole-organism level.

HIF-1 $\alpha$  (hypoxia Inducible Factor 1  $\alpha$ ) and HIF-2 $\alpha$  are the main two transcription factors involved in regulating their target genes in response to a reduction of oxygen availability. HIFs activity is regulated by oxygen level via the oxygen dependent degradation domain (ODD). In normoxic conditions, HIF is constitutively transcribed and translated, but its lifespan is very short and it is readily degraded by the proteasome, via the ubiquitin system in an oxygen-dependent manner. When oxygen is available, prolyl hydroxylases (PHDs) hydroxylates two prolines in the ODD of HIF (Jaakkola et al. 2001; Hoffman et al. 2001; Dayan et al. 2009). These Hydroxyprolines are recognized by the von Hippel–Lindau tumor suppressor protein (VHL) that recruits a Cullin 2 (Cul2) E3 ubiquitin ligase that mediates the ubiquitination of HIFs, causing their degradation (Nguyen et al. 2015). During hypoxia, PHDs, without sufficient oxygen available, are not able to efficiently target HIFs. Consequently, HIF protein is quite stable and after translocating to the nucleus, it dimerizes with ARNT. The HIF/ARNT complex binds to the hypoxia response elements (HREs), interact with CBP/p300 and induce transcription of its target genes. The most important target genes of HIFs are involved in glycolysis (LDHA, PFK), erythropoiesis (EPO) and angiogenesis (VEGF)(Baltaziak et al. 2013; Lemus-Varela et al. 2010; Horiuchi et al. 2002; Tang et al. 2004). There are three proteins belonging to the HIF family, HIF-1 $\alpha$ , HIF-2 $\alpha$  and HIF-3 $\alpha$ . HIF-1 $\alpha$  and HIF-



2 $\alpha$  are very conserved and are known to induce a plethora of genes in response to hypoxia, HIF-3 $\alpha$  can act as a negative regulator of the other HIFs, but it was shown to exhibit also a transcriptional activity (Zhang et al. 2014; Gu et al. 1998; Hara et al. 2001). Interestingly both *Hif-1 $\alpha$*  and *Hif-2 $\alpha$*  mouse mutants were shown to die embryonically with severe vascular defects (Carmeliet et al. 1998; Ryan, Lo, and Johnson 1998) (Peng et al. 2000; Tian et al. 1998).

## 2. AIM OF THE STUDY

---

Sequential transcriptional waves direct the differentiation of ECs starting from pluripotent mesodermal cells. Subsequently, ECs specialize to acquire unique features, such as hematopoietic potential. At the top of the endothelial specification cascade lies *cloche*. Zebrafish *cloche* mutants show a striking phenotype: the lack of most endothelial and blood cells, thus suggesting that *cloche* is a key regulator of ECs and blood cell differentiation. Recently, our laboratory discovered that the *cloche* gene encodes a bHLH-PAS transcription factor named Npas4l. After this discovery, many questions arose, especially regarding its regulation and its molecular function. Understanding these processes would increase our knowledge of endothelial cell differentiation, and it would open the possibility to study the conservation of this mechanism across different species, with a potential impact in translational research. The goal of this thesis is to describe the subsequential molecular events that lead to endothelial cell specification and specialization in vertebrates.

- **Aim 1. Upstream regulators of *npas4l* and angioblast differentiation.**

After the characterization of the early spatiotemporal expression pattern of *npas4l*, I will perform a screening of compounds known to inhibit key protein involved in patterning the gastrulation to test which signaling pathways have an impact on *npas4l* regulation. Transcriptomic and *in silico* prediction analyses will be used to identify the signaling pathways and the transcription factors acting upstream of *npas4l*.

- **Aim 2. Identification and characterization of downstream targets of *npas4l*.**

I will identify the genes induced directly and indirectly by *Npas4l*. Epigenomic and transcriptomic approaches will be combined with chromatin immunoprecipitation to describe the genes acting downstream of *npas4l in vivo*. Zebrafish mutants will be generated to study the function of the target genes and I will describe a novel function for *tspan18b* in vascular development.

- **Aim 3. Identification of a functional ortholog of *npas4l* in mammals: role of HIFs in endothelial cell differentiation.**

*npas4l* was lost in the mammalian lineage during evolution. To study how conserved is endothelial cell specification across vertebrates, an *in vitro* assay in mouse cells will be described. To identify the functional mammalian ortholog of *npas4l* I will perform a knockdown of *Eomes* in P19 cells. To confirm these data, I will characterize the phenotype of mouse *Hif-1 $\alpha$*  mutant during gastrulation, prior to endothelial cell formation.

- **Aim 4. Role of Hifs in endothelial cell specialization.**

The function of *hif-1 $\alpha$*  and *hif-2 $\alpha$*  will be tested in zebrafish and by analyzing the phenotype of the mutants, I will discuss a role for these two bHLH-PAS transcription factors in HE specification and HSC formation.

### 3. MATERIAL AND METHODS

---

## 3.1 Materials

### 3.1.1 Antibiotics

Antibiotic	Working concentration
Ampicillin	100 µg/ml
Penicillin – Streptomycin	200 U/ml

### 3.1.2 Antibodies

Antibody	Supplier
Anti-DIG-AP, Fab fragments	Roche
Anti-HA tag – CHIP Grade	Abcam

### 3.1.3 Buffers

Buffers/Solutions	Composition
Egg water	3g Instant Ocean 0.75g Calcium sulfate dissolved in 10 liters of distilled water
Ginzburg Fish Ringer solution	55 mM NaCl, 1.8 mM KCl, 1.25 mM NaHCO <sub>3</sub>
Blocking Buffer	2mg/ml BSA 2% Sheep Serum Dissolved in PBST
Tris Alkaline buffer	100mM Tris HCl pH 9.5 100mM NaCl 0.1% Tween 20 Dissolved in distilled water
PBST	0.1% Tween 20 in PBS
RIPA	150 mM NaCl 1.0% IGEPAL CA-630 0.5% sodium deoxycholate 0.1% SDS 50 mM Tris pH 8.0
TBST	Tris-buffered saline 0.1% Tween 20
PBS	8g NaCl 0.2g KCl 1.44g Na <sub>2</sub> HPO <sub>4</sub> 0.24g KH <sub>2</sub> PO <sub>4</sub> dissolved in 900 ml of distilled water,

adjust pH 7.4, makeup volume to 1000 ml with distilled water.

### 3.1.4 Chemicals

<b>Chemical</b>	<b>Supplier</b>
Mineral oil	Sigma
SOC medium	ThermoFisher Scientific
LB agar	Roth
SB431542	Sigma
DIG RNA labeling mix	Roche
SKLB1002	Sigma
Bovine serum albumin (BSA)	Sigma
Chloroform	Merck
IWR1	Sigma
Citric acid	Sigma-Aldrich
PFA 4%	Sigma-Aldrich
DMH1	Sigma-Aldrich
DNA ladders	ThermoFisher Scientific
DAPT	Sigma-Aldrich
Ethanol	Roth
Methanol	Roth
Lipofectamine 3000	Invitrogen
Cyclopamine	Sigma-Aldrich
Gel loading dye	ThermoFisher Scientific
Protease Inhibitor	Roche
SAG	Sigma-Aldrich
FBS	Biochrom
Isopropanol	Roth
BCI	Sigma-Aldrich
RIPA buffer	Sigma-Aldrich
Methylene blue	Sigma-Aldrich
NBT/BCIP stock solution	Roche
Tricaine	Pharmaq
Phosphate-buffered saline (PBS)	Sigma-Aldrich
Dimethyloxalyglycine (DMOG)	Sigma-Aldrich
Dimethylsulfoxide (DMSO)	Sigma-Aldrich
SU5402	Sigma-Aldrich
Tween-20	Sigma-Aldrich
tRNA	Sigma-Aldrich
CutSmart buffer	NEB
Agarose, low gelling temperature	Sigma-Aldrich
Trizol	Ambion

<b>SYBR safe</b>	Invitrogen
<b>Phenol:chloroform:isoamyl alcohol (25:24:1)</b>	Sigma-Aldrich
<b>1-Phenyl-2-thiourea</b>	Sigma-Aldrich

### 3.1.5 Enzymes

<b>Enzyme</b>	<b>Supplier</b>
<b>DNase I</b>	Promega
<b>DNase I + RDD</b>	Qiagen
<b>Trypsine</b>	Gibco
<b>PrimeSTARMax DNA polymerase</b>	Takara
<b>T4 DNA ligase</b>	Takara
<b>Pronase</b>	Roche
<b>Proteinase K</b>	Roche
<b>Bsmbl</b>	NEB
<b>EcorI-HF</b>	NEB
<b>NotI-HF</b>	NEB
<b>XhoI</b>	NEB
<b>XbaI</b>	NEB
<b>HindIII</b>	NEB
<b>BamHI-HF</b>	NEB
<b>NotI-HF</b>	NEB
<b>BsaI</b>	NEB
<b>T7 RNA polymerase</b>	Promega
<b>RNasin ribonuclease inhibitor</b>	Promega
<b>Dynamo Flash SYR green qPCR kit</b>	ThermoFisher Scientific
<b>Nextera Tn5 transposase</b>	Illumina

### 3.1.6 Growth Media

<b>Media</b>	<b>Composition</b>
<b>SOC</b>	Tryptone 2% Yeast extract 0.5% NaCl 0.05% KCl 0.0186% dissolve in distilled water and adjust pH 7 and then add MgCl <sub>2</sub> 10 mM D-glucose 20 mM then autoclave.
<b>LB agar</b>	Roth



<b>DMEM high Glucose 1X 1995</b>	Gibco - Invitrogen
<b>LB medium</b>	Roth

### 3.1.7 Kits

<b>Kit</b>	<b>Supplier</b>	<b>Purpose</b>
<b>RNA clean and concentrator</b>	Zymo Research	RNA purification
<b>RNAeasy Micro kit</b>	QIAGEN	RNA extraction and purification
<b>mMESSAGE mMACHINE kit (T3)</b>	Ambion	<i>in vitro</i> mRNA synthesis
<b>MEGA short script T7 kit</b>	Ambion	<i>in vitro</i> gRNA synthesis
<b>mMESSAGE mMACHINE kit (Sp6)</b>	Ambion	<i>in vitro</i> mRNA synthesis
<b>mMESSAGE mMACHINE kit (Sp6)</b>	Ambion	<i>in vitro</i> mRNA synthesis
<b>Arcturus PicoPure RNA Isolation Kit</b>	ThermoFisher Scientific	RNA extraction and purification
<b>MAXIMA first strand cDNA</b>	ThermoFisher Scientific	cDNA synthesis
<b>GeneJET PCR purification kit</b>	ThermoFisher Scientific	DNA purification
<b>RNAeasy Mini kit</b>	Qiagen	RNA extraction and purification
<b>pGEM-T-easy vector kit</b>	Promega	TA cloning
<b>GeneJET plasmid miniprep kit</b>	ThermoFisher Scientific	Plasmid extraction
<b>QuantiTect Reverse Transcription Kit</b>	Qiagen	cDNA synthesis
<b>MinElute PCR purification kit</b>	Qiagen	DNA purification

### 3.1.8 Laboratory supplies

<b>Laboratory supply</b>	<b>Supplier</b>
<b>Bacterial culture tubes</b>	Sarstedt
<b>Nitrile gloves</b>	VWR
<b>Glass Beakers</b>	VWR
<b>Microcentrifuge tubes</b>	Sarstedt
<b>Falcons tubes</b>	Greiner
<b>Glass imaging dish</b>	MatTek

<b>PCR tubes</b>	Sarstedt
<b>Dyna Protein G Magnetic Beads</b>	Invitrogen
<b>Plastic petri dish</b>	Greiner
<b>6-Tube Magnetic Separation Rack</b>	NEB
<b>Forceps and scissors</b>	Dumont
<b>Glass bottles and flasks</b>	Duran
<b>15 ml Tenbroeck Tissue Grinder</b>	Wheaton
<b>Pipettes P2</b>	Gilson
<b>Pipettes P10</b>	Gilson
<b>Pipettes P20</b>	Gilson
<b>Pipettes P100</b>	Gilson
<b>Pipettes P200</b>	Gilson
<b>Pipettes P1000</b>	Gilson
<b>Pipette for higher volume pipetboy</b>	Integra

### 3.1.9 Microscopes

<b>Microscope</b>	<b>Supplier</b>
<b>Stereomicroscope Stemi 2000</b>	Zeiss
<b>Stereomicroscope SMZ18</b>	Nikon
<b>Primo Vert Micro</b>	Zeiss
<b>Stereomicroscope SMZ25</b>	Nikon
<b>Confocal microscope upright LSM700</b>	Zeiss
<b>Confocal microscope inverted LSM800</b>	Zeiss

### 3.1.10 Laboratory equipment

<b>Equipment</b>	<b>Supplier</b>
<b>NanoDrop 2000</b>	ThermoFisher Scientific
<b>HRMA machine – Eco Real-Time</b>	Illumina
<b>Injection micromanipulator</b>	World precision instruments
<b>Picospritzer III</b>	Parker
<b>PCR mastercycler Pro</b>	Eppendorf
<b>Nutator</b>	Edmund Buhler
<b>Dark reader transilluminator</b>	Clare chemical
<b>GasDocUnit</b>	Medres
<b>Sonicator SONOPULS</b>	Bendelin
<b>Electrophoresis power supply</b>	Bio Rad
<b>Thermomixer</b>	Eppendorf
<b>-80°C freezer</b>	Thermoscientific Hera Freeze hfu
<b>Weighing balance</b>	Sartorius

Needle puller	Sutter model p1000
Tissue homogenizer	Bullet Blender gold
Liquid Culture Bacterial shaker	Infors HAT
Bacterial incubator 37°C	Heraeus
Thermoblock	VWR
Microwave	Bosch
Biological hood – tissue culture	Herasafe KS
Hypoxia Chamber, C-Chamber, ProOX 110, ProCO2	Biospherix
Zebrafish tanks	Tecniplast
55 °C incubator Inculine	VWR
Zebrafish aqua culture system	Tecniplast
Zebrafish incubator	Lovibond and Panasonic

### 3.1.11 Morpholinos

Morpholino	Sequence
<i>hif-1aa</i>	TTTTCCCAGGTGCGACTGCCTCCAT
<i>hif-1ab</i>	ACCCTACAAAAGAAAGAAGGAGAGC
control	CCTCTTACCTCAGTTACAATTTATA
<i>hif-2aa</i>	ATGATGCTGAAGAACCTTGTCCTGC
<i>hif-2ab</i>	TCATCGCGCCGTTCTCGCGTAATTC

### 3.1.12 Primers

Oligonucleotide	Purpose
<i>npas4l</i> -ISH forward: <b>ACTCGGGCATCAGGAGGATC</b> <i>npas4l</i> -ISH reverse: <b>TAATACGACTCACTATAG GACACCAGCATACGACACAAC</b>	Cloning and amplification <i>npas4l</i> WISH probe
<i>dnajb5</i> -ISH forward: <b>CTGGACTCAGTTCGGCGTCAA</b> <i>dnajb5</i> -ISH reverse: <b>TAATACGACTCACTATAG CTGAAGTGGGCGTGTCTT</b>	Cloning and amplification <i>dnajb5</i> WISH probe
<i>tspan18b</i> forward: <b>ATTTAGGGAGATTGTGGCAGC</b> <i>tspan18b</i> reverse: <b>CCATGGCCAGGATGATGTA</b>	Identification of <i>tspan18b</i> mutant alleles
<i>npas4l</i> forward: <b>CGCAGGTTCCGTATCTCACT</b> <i>npas4l</i> reverse: <b>TGTGTGTGTTCCAGGTCCA</b>	For Identification of <i>npas4l</i> mutant alleles
<i>tspan18b</i> gRNA: <b>TAATACGACTCACTATAGGACGCCCGTGAAGAGAAG AGTTTTAGAGCTAGAAATAGCAAG</b>	<i>tspan18b</i> guide RNA

<b>gapdh forward: TACCATGTGACCAGCTTGAC</b> <b>gapdh reverse: AGAAACCTGCCAAGTATGATGAG</b>	qPCR primers
<b>npas4l forward: GTACGTTCTCAGACACATACAG</b> <b>npas4l reverse: CTACAGGATTGTGCTCTACAG</b>	qPCR primers
<b>Npas4 forward: TCTGAAAGTGTCTAATCTACC</b> <b>Npas4 reverse: GCCTGAATATCTCCAATTC</b>	qPCR primers
<b>rpl13 forward: AATTGTGGTGGTGAGGTG</b> <b>rpl13 reverse: GGTGGTGTTCATTCTCTTG</b>	qPCR primers
<b>Beta-actin forward: CTCTGGCTCCTAGCACCATGAAGA</b> <b>Beta-actin reverse: GTAAAACGCAGCTCAGTAACAGTCCG</b>	qPCR primers
<b>Etv2 forward: CTCGCTACTCCAAAATAAC</b> <b>Etv2 reverse: CATAATTCATTCCCGGCTTC</b>	qPCR primers
<b>Eomes forward: ACAACACACAGATGATAGTG</b> <b>Eomes reverse: TATGGTCGATCTTTAGCTGG</b>	qPCR primers
<b>Tal1 forward: CTAGGCAGTGGGTTCTTTGG</b> <b>Tal1 reverse: AGTTTCTTGTCTGGTGGGTG</b>	qPCR primers
<b>Constant oligo CRISPR/Cas9: AAAAGCACCGACTCGGTGCCACTTTTTCAAGTTGAT AACGGACTAGCCTTATTTAACTTGC TATTTCTAGCTCTAAAAC</b>	gRNA synthesis
<b>evi1 forward: CC gaattc gccacc ATGGCACTAGAGAAACAGGCCA</b> <b>evi1 reverse: CC ctcgag TCATACGTGACTGAGAGATTG</b>	Cloning in PcDNA3.1+
<b>npas4l forward: CC gaattc ATGAGCTGCGGAGACTCGG</b> <b>npas4l reverse (nostop): CC CTCGAG GATCAGTGTGTGTCATCAG</b>	Cloning in npas4l-HAtag-P2AtdTomato
<b>npas4b forward: CC gaattc ATGTTTTTCATCAGAAAGCAGA</b> <b>npas4b reverse: CC TCTAGA TTAAAACATGTGATCACCGGT</b>	cloning in pCS2+
<b>Hif-1α forward: CGATGACACAGAACTGAAG</b> <b>Hif-1α reverse: GAAGGTAAAGGAGACATTGC</b>	qPCR primers
<b>Epas1 forward: CCAAAGTCCAGAACTTG</b> <b>Epas1 reverse: TTCTTCTCGATCTCACTCAG</b>	qPCR primers
<b>hif2ab forward: TTTGTGCTGTATTGCAGGCTA,</b> <b>hif2ab reverse: CCATGAGTCTGTCTGCATCTG.</b>	For identification of <i>hif-2ab</i> mutant alleles
<b>runx1-ISH forward: GGACGCCAAATACGAACCT</b> <b>runx1-ISH reverse:</b>	For cloning and amplification

<b>TAATACGACTCACTATAG AGCCACTTGGTTCTTGAT GG</b>	<i>runx1</i> WISH probe
<b><i>cmyb</i>-ISH forward: GCTGCTAAAGTCAGCCCAAC <i>cmyb</i>-ISH reverse: TAATACGACTCACTATAG GTTTAATCGTGCCGACCA CT</b>	For cloning and amplification <i>cmyb</i> WISH probe
<b><i>notch1a</i> forward: AGCCCTTGTCATTATGGTGTG <i>notch1a</i> reverse: ACACAAGCGTCCGGTGTATC</b>	For identification of <i>notch1a</i> mutant alleles
<b><i>notch1b</i> forward: AGAACGGAGCAACTTGCA <i>notch1b</i> reverse: CCAACTTCCAGATCCTCTTGAC</b>	For identification of <i>notch1b</i> mutant alleles
<b>NICD forward: CATCGCGTCTCAGCCTCAC NICD reverse: CGGAATCGTTTATTGGTGTGCG</b>	For genotyping of <i>UAS:NICD</i> line
<b><i>etv2</i> forward: CGAGGTTCTGGTAGGTTTGGAG <i>etv2</i> reverse: GCACAAAGGTCATGTTCTCAC</b>	qPCR primers
<b>T7 primer: TAATACGACTCACTATAGGG</b>	For sequencing
<b>Sp6 primer: ATTTAGGTGACACTATAG</b>	For sequencing
<b><i>pCS2.0+</i> reverse sequencing : GTTTGTCCAAACTCATCAATG</b>	For sequencing insert
<b><i>Hif-3α</i> forward: GATTTTATCCATCCCTGTGAC <i>Hif-3α</i> reverse: CTTCTTCTTTGACAGGTTTCG</b>	qPCR primers
<b>M13 primer: GTAAAACGACGGCCAGT</b>	For sequencing
<b><i>Ahr</i> forward: CACATCCGCATGATTAAGAC <i>Ahr</i> reverse: TACTTCGCTTCTGTAAATGC</b>	qPCR primers
<b><i>Hif-1α</i> forward: CGCCTCTGGACTTGTCTCTT <i>Hif-1α</i> reverse: CCATCTGTGCCTTCATCTCA</b>	for identification of <i>Hif-1α</i> mutant alleles with PCR
<b><i>Epas-1</i> forward: GGTTAAGGAACCCAGGTGCT <i>Epas-1</i> reverse: GGGATTCTCCTTCCTCAGC</b>	for identification of <i>Epas-1</i> mutant alleles with PCR

### 3.1.13 Plasmids

Plasmid	Resistance	Source	Purpose
<b>pT7-gRNA vector</b>	Ampicillin	Addgene	Vector for gRNA cloning
<b>pGEM-T</b>	Ampicillin	Promega	Vector for sequencing cloning
<b><i>pCS2+</i></b>	Ampicillin	Addgene	Expression vector to clone CDS of genes
<b><i>pcDNA3.1+</i></b>	Ampicillin	Aggene	Expression vector to

			clone CDS of genes
<b>eomesa expression vector</b>	Ampicillin	Kimelman lab	Synthesize mRNA of <i>eomesa</i>
<b>pT3Ts-nlsCas9nls</b>	Ampicillin	Addgene	Expression vector for Cas9 mrRNA

### 3.1.14 Softwares

Software	Purpose
Primer3	Primer design
Adobe Photoshop, illustrator	Image formatting
GraphPad Prism	Statistical and data analysis
Zen	Image processing
IGV	Genome viewer
Microsoft Office	Writing, data analysis, image formatting
ApE	Sequence analysis
CLC sequence viewer	Sequence analysis
Jasper	Promoter analysis
GSEA	Data enrichment analysis
MEMESuite	<i>de novo</i> binding motif prediction

### 3.1.15 Zebrafish lines

Lines	Details	Publication
AB	Wild type	
<i>Tg(kdrl:EGFP)<sup>s843</sup></i>	Vascular-specific reporter	(Jin et al. 2005)
<i>Tg(-1.5hsp70l:GAL4)<sup>kca4</sup></i> <i>(5xUAS-E1b:6xMYC-notch1a)<sup>kca3</sup></i>	NICD overexpression globally with heat shock	(Scheer et al. 2001)
<i>Tg(cmyb:EGFP)<sup>z1169</sup></i>	HSCs	(North et al. 2007)
<i>Tg(kdrl:Ras-mCherry)<sup>s896Tg</sup></i>	Vascular-specific reporter	(Chi et al. 2008)

### 3.1.16 Mouse lines

Lines	Details	Publication
<i>Hif1a<sup>tm3Rsjo</sup></i>	Hif-1α flox allele	(Ryan et al. 2000)
<i>Epas1<sup>tm1MCS</sup></i>	Hif-2α flox allele	(Gruber et al. 2007)

### 3.1.17 Cell lines

Line	Details	Supplier
P19	Embryonal carcinoma	ATCC

## 3.2 Methods

### 3.2.1 Zebrafish maintenance

Zebrafish fish were put in the aqua culture system (Tecniplast) from 5 dpf on as described in “The zebrafish book. A guide for the laboratory use of zebrafish (*Danio rerio*), 4<sup>th</sup> edition, 2000, Westerfield M.” in a fish aqua culture system (Tecniplast). Zebrafish adults were kept at 28°C water temperature with a 14 hrs-10 hrs light-dark cycle. Fish tanks were organized in racks connected to a water recycling system, approximately 25 fish were kept in each tank. The water circulates in a closed circuit and UV lights are used to sterilize the water.

A maximum of 80 zebrafish embryos were kept in egg water in 90 mm Petri dish in a 28°C incubator. At around 24 hpf, PTU was added to the egg water to inhibit pigmentation, allowing an easier analysis at the microscope (Westerfield 1993).

### 3.2.2 Zebrafish breeding

Zebrafish are photoperiodic in their breeding, and produce embryos every morning, shortly after sunrise. After 4 PM I put into a breeding tank two female and one male. Males are longer, slimmer, and more yellow, females, instead, are plumper and more silvery. On the next morning, around 9.00 AM, I collected the eggs. When I needed to inject at one cell stage, I physically separated the males from the females with a plastic divider the day before the injection. On the next morning, at around 8.30, I removed the divider and waited approximately 20 minutes before to collect the eggs. The eggs were collected in a plastic 90 mm Petri dish and around 30 ml of egg water was added. In the afternoon all the eggs received new egg water and the dead eggs were removed (Westerfield 1993).

### **3.2.3 Preparation of injection needles**

Glass capillaries were put in the micropipette puller P1000, the two extremities of the capillary were pulled by a wire, and the center of the capillary was heated by a platinum filament. The tension induced by the pulling, on the heated glass, caused the glass to fuse in the center and to separate into two capillaries with a very thin extremity. This thin tip was later opened using forceps, in order to allow the injection mix to go through.

### **3.2.4 Microinjection**

Up to 5  $\mu$ l of the injection solution was loaded into the injection needle. In all the mixing solutions, a certain amount of phenol-red was added, in order to visualize the size of the drop. The size of the drop was measured using a glass micrometer. A drop of mineral oil was placed in the center of a micrometer and a drop was injected into the mineral oil. By changing the settings of the picospitzer, it was possible to obtain the correct size in order to inject 1 nl. For mRNA overexpression experiment, I injected into the yolk of embryos at 1-2 cell stage. For CRISPR/Cas9 mutagenesis, I injected into the cell of a zygote at 1 cell stage.

### **3.2.5 Quantitative real-time PCR**

Primers were designed in order to use as a template selectively the cDNA and not the genomic DNA. The amplicon size was between 80 bp and 200 bp, and the primers were designed in two different exons, or on an exon-exon junction. We tested the primers looking at the melt-curve of the amplicon; an isolated peak, without additional bumps, reflects the amplification of only one product, without aspecific amplifications. Moreover, the amplicon was cloned in pGEM-T and sent to sequence, in order to confirm the reliability of the amplified product. I have always performed three technical replicates, using biological triplicates. For each well, the amount of reagents mixed in the solution was as follows: 0.5  $\mu$ l of primer fw 10 mM, 0.5  $\mu$ l of primer rv 10 mM, 5  $\mu$ l of SYBR Green, 3  $\mu$ l of Water. Then, 1  $\mu$ l of cDNA, diluted 1:10 or 1:20 from the cDNA reaction mix was added in each well.



### **3.2.5 Drug treatment**

Drug treatment started from 50% epiboly, until tailbud stage.

AB embryos were collected from three different couples and dechorionated using pronase as described in the CHIP protocol. Individual embryos were put in a well of a 96 well plate, coated with 0.5 ml of 2% agarose, to avoid the embryos to stick to the plastic surface. The embryos were kept individually to avoid the formation of agglomerates of embryos in case of hydrophobic drugs. I tested several concentrations of the drugs used, in order to find the highest concentration that did not lead to gross morphological defects. 8 embryos for each condition were pooled together to extract the total RNA, to test the levels of *npas4l* expression.

### **3.2.7 Measurement of nucleic acid concentrations**

The concentration of nucleic acids was measured using the Nanodrop 2000. First of all, I measured the blank, using 1  $\mu$ l of the solution used to elute the nucleic acid. Then, after carefully cleaning the sensor, 1  $\mu$ l of the sample was placed on the sensor in order to measure its concentration, via its 260 nm absorption and its purity, via the 260/280 and 260/230 ratios.

### **3.2.8 DNA sequencing**

I sequenced amplicons and vectors using Seqlab (Göttingen) or GATC Biotech (Constance). In both cases a Sanger-sequencing technique was used, and I obtained sequences up to 1 kb.

### **3.2.9 TA cloning**

TA cloning was used to sequence amplicons amplified with the KAPA 2G polymerase mix (Kapa biosystem) or amplicons derived from the HRM analysis. The insert was ligated into the pGEM-T-easy vector following manufacturer's instructions. The reaction was assembled as follows:

50 ng of purified PCR  
product  
1  $\mu$ l of pGEM-T-easy vector

1  $\mu$ l pf T4 ligase  
5  $\mu$ l 2X ligation buffer  
up to 10  $\mu$ l of water

The ligation mix was kept at 16 °C for 1 hour or overnight at 4°C. After the ligation, I transformed the competent cells with the construct and the bacteria were plated on LBA plates containing IPTG and X-gal. White colonies indicated the successful integration.

### **3.2.10 DNA restriction digestion**

DNA digestion was performed mixing together the restriction enzyme or a combination of restriction enzymes with the buffer indicated, following NEB guidelines. In the tube I mixed: 1  $\mu$ g of DNA, 2  $\mu$ l of restriction enzyme (Units varied based on the enzyme used), 5  $\mu$ l of indicated buffer and water up to 50  $\mu$ l. The incubation time varied from 2 hours to overnight incubation, when possible.

### **3.2.11 DNA ligation**

Ligation of insert into the vector was performed using compatible 5' sticky ends using T4 DNA ligase and buffer (Takara) following manufacturer's instructions. The molar ratio insert:vector used was 3:1 or 5:1.

### **3.2.12 Plasmid DNA preparation**

Mini-prep DNA plasmid isolation was performed using the GeneJET plasmid miniprep kit (Thermo) , following manufacturer's instructions.

### **3.2.13 *in situ* hybridization: probe synthesis**

The probe was synthesized starting from a PCR product of the target gene starting from cDNA or a plasmid in which the CDS of the gene was cloned. I designed the primer using primer3, in order to obtain an amplicon of 800-1100 bp, and I added the T7 promoter sequence at the 5' end of the reverse primer.

After amplification and purification of the amplicon, I sent the amplicon to be sequenced using the T7 primer.

I synthesized the probe using the T7 transcriptase as follows:

Reagent	Amount for reaction
DNA	150 ng
10x T7 polymerase buffer	2.5 µl
10x DIG-RNA mix	2.5 µl
RNAsin (40 U/µl)	2.5 µl
T7 Transcriptase	2 µl
H2O	up to 25 µl

The solution was incubated at 37°C for 2 hours. I performed DNase treatment by incubating the mix with 1 µl of DNase I. After adding DNase I, the samples were incubated for 15 additional minutes at 37 °C. I purified the probe using RNA clean and concentrator kit following manufacturer's instructions. The RNA probe was eluted in 10 µl of RNase-free water and stored at -20°C.

### **3.2.14 *in situ* hybridization**

In situ hybridization was performed following the protocol of Thisse et al. (Thisse and Thisse 2014)

### **3.2.15 Mouse maintenance**

The animal experiments presented in this study were performed according to the German law for animal protection (Regierungspräsidium Darmstadt, Hesse, Germany). Animals were kept in a Specific-Pathogen-Free (SPF) facility, managed by a dedicated team of trained animal caretakers. The maintenance and administration of the mouse strains was done via the CAT system. Prior to sample harvesting, animals were anesthetized with CO<sub>2</sub>, and sacrificed by cervical dislocation. Animal were kept in Green Line IVC Sealsafe PLUS mouse cages (Tecniplast).

### **3.2.16 Chromatin Immunoprecipitation Sequencing (ChIP-seq)**

#### Sample preparation

I microinjected 3000 embryos with 25 pg of mRNA in each embryo at 1-2 cell stage: npas4l-3XHATAG-P2A-tdTomato

I collected the embryos at tailbud stage in 20 ml of E3 in a glass beaker - 500 embryos each beaker - and add 200  $\mu$ l of Pronase at 30 mg/ ml. I shook the beakers gently and I incubated the embryos at 28 °C. After around 3 minutes I washed the embryos with E3 medium three times. I gently pipetted in order to remove the chorion from the last embryos. I transfer the embryos into a 15 ml falcon tube and aspirated the supernatant E3.

I deyolked the embryos using 1 ml deyolking buffer (Ginzburg Fish Ringer without Ca<sup>2+</sup>) by pipetting the embryos using a 200  $\mu$ l tip . I shook the embryos for 5 minutes and I pelleted the cells at 300 g for 30 seconds, discarding the supernatant.

I then added 4.6 ml of E3 medium and 4 ml fresh 4% PFA and I incubated the embryos at room temperature for 15 minutes on a nutator mixer. I quench the formaldehyde with Glycine and I incubated the falcons for 5 minutes on a nutator mixer. I remove entirely the supernatant and rinse the embryos with ice-cold PBS. After removing the PBS I snap froze the samples in liquid nitrogen and stored them at -80 °C.

#### Pre-blocking and binding of antibody to magnetic beads

The following steps were performed following steps in a 5-6 °C cold room.

I mixed the magnetic beads and I washed 125ul of beads in a 1 ml fresh block solution (0.5% BSA in 1X PBS) in a 1.5 ml eppendorf tube.

I collected the beads by spinning at 3000 rpm for 5 min. I washed twice the magnetic beads in 1.5 ml block solution. I then Collected the beads with the magnetic stand and discard supernatant.

I resuspended the beads in 125ul of block solution and added 25ul of the anti-HA antibody.

I incubated the antibody at 4 °C overnight on a rotating platform.

I collect the beads with the magnetic stand, removing supernatant. I washed the beads in 2 ml block solution three times. And I resuspended the beads in 150 µl of block solution.

### Chromatin preparation

all lysis buffers in the following steps contained protease inhibitor

I resuspended the deyolked embryos stored in the -80°C with 2 ml cell lysis buffer (10 mM Tris–HCl pH 7.5, 10 mM NaCl, 0.5% IGEPAL. I transferred the samples to a tissue grinder to lyse the cells. I homogenized the embryos 3 times, every 5 minutes. I pelleted the nuclei spinning a 15 ml falcon containing the samples at 3500 rpm for 5 minutes at 4°C. After resuspending the nuclei in lysis buffer I pipetted up and down to disrupt the nuclei. I added 2 volumes of IP buffer (16.7 mM Tris–HCl, 167 mM NaCl, 1.2 mM EDTA, 0.01% SDS). I put the samples in a ice-water bath and sonicated them using the Bandelin SONOPULS ultrasonic homogenizer using the MS72 micro tip. The sonication was performed with 20% amplitude with 12x3 cycles of 10sec on, 50 sec off with 12 minutes on ice between each 12x cycles. After sonication I added 120ul 10% Triton X-100. We checked that the size of sonicated chromatin was around 250 bp, performing gel electrophoresis. After spinning at 14000 rpm for 10 minutes at 4°C, I separated the samples into five 1.5 ml tubes. I added 25ul of magnetic beads bound with anti-HA tag antibody in each tube and I incubated the samples overnight on a rotating platform at 4 °C.

### Washing, elution, and reversal of cross-linking

The following steps were performed following steps in a 5-6 °C cold room.

I collected the beads with the magnetic stand and I removed the supernatant. After adding RIPA buffer, I resuspended the beads and, I put the tubes in the magnetic

stand and I removed the supernatant. I performed this washing steps five times. The last time was done using TBS buffer, and after removing it, I resuspended the beads in 100uL of elution buffer (50mM Tris pH8.0, 10mM EDTA, and 1%SDS) twice (total volume 200uL) at 65° for 15 mins each time and reversed crosslinks overnight at 65° with shaking at 1000rpm. Then I added 200uL of TE buffer, RNaseA (final conc 0.2ug/mL) incubated at 37° for 2 hrs, I then treated with Proteinase K (0.2ug/mL final conc) and incubated at 55° for 2h. An equal amount (400uL) of phenol:chloroform:isoamyl alcohol (25:24:1) was added and aqueous phase extracted after centrifugation at 8000rpm for 5 mins. This was done twice. Aqueous phase was then added to a Qiagen MinElute PCR purification column and purified according to manufacturer's instructions (Bogdanovic et al. 2013).

The DNA obtained was then sent to sequencing.

### **3.2.17 Assay for Transposase-Accessible Chromatin with High-Throughput Sequencing (ATAC-Seq)**

We collected single embryos at 1-2 somite stage, we dechorionated the embryos using pronase similarly to the ChIP protocol. I homogenized the samples using a micro pestle. I centrifuged the samples at 500g for 10 minutes at 4°C, I removed the supernatant and I added to the pellet 50 µl of cold PBS. The samples were spun at 500g for 5 minutes at 4°C, I removed the supernatant and I added 50 µl of cold lysis buffer (10 mM Tris-HCl, 10 mM NaCl, 3 mM MgCl<sub>2</sub>, 0.1% NP-40.). After finger-vortexing the tubes, the samples were spun at 500g, 4 °C for 10 min I removed the supernatant and I added 25 µl of transposition mix (25 µl TD Buffer, 2.5 µl TDE1 (Nextera Tn5 Transposase) 22.5 µl Nuclease Free H<sub>2</sub>O). I resuspended the pellet in the transposition mix and I incubated the samples at 37°C for 15 minutes. I purified the DNA using the Qiagen MinElute Reaction Cleanup Kit according to manufacturer's instructions. The DNA obtained was then given to the sequencing facility (Doganlı et al. 2017)

### **3.2.18 RNA extraction and cDNA synthesis of zebrafish embryos for RT-qPCR.**

We pooled 10 to 20 embryos in a 1.5 microfuge tube, removing water. I added 900 µl of TRIzol reagent and we added 100 µl of 0.5 mm zirconium oxide beads to each tube. The samples were homogenized using the bullet blender tissue homogenizer. I incubate homogenized samples for 5 minutes at room temperature. I then added 200 µl of chloroform and I mixed the samples by inversion. After 2 minutes incubation at room temperature, the samples were centrifuged at 12,000g for 15 minutes at 4°C. I carefully transfer the upper aqueous phase to a new RNase-free tube. I added one volume of isopropanol and I inverted the samples, to precipitate the RNA. I incubated the samples for 10 minutes at room temperature. After spinning the samples at 12000g for 10 minutes at 4 degrees, a pellet was visible. I removed the supernatant without touching the pellet and I washed the pellet in 1 ml of 80% ethanol. I inverted the tubes and centrifuged the samples at 8000g for 5 minutes at 4°C. I then removed the ethanol and left the tubes open at room temperature, in order to dry the pellet. I then resuspended the embryos in 20 µl RNase-free water and the sample were incubated at 55°C for 15 minutes. The RNA obtained was then retrotranscribed using the Maxima First Strand cDNA Synthesis Kit with dsDNase (Thermoscientific), following manufacturer's instructions(Peterson and Freeman 2009).

### **3.2.19 Mouse Embryos dissection**

Embryos dissection was done following The FELASA guidelines and recommendations. I sacrificed pregnant mice by CO<sub>2</sub> using the GasDocUnit (Medres) attached to the Tecniplast green line cage I laid the animal on absorbent paper and soak it in 70% ethanol. I made a small lateral incision at the midline with regular surgical scissors, holding the skin the skin above and below the incision and pull the skin apart toward the head and tail to expose the abdomen. I removed the uterus I cut it along the mesometrium. The uteri were placed in ice cold PBS. I separated each embryo and, using forceps, I removed the muscle layer and the decidua. By removing the two apexes, I was able to remove the embryo using the

tips of forceps. The embryos were immediately transferred to the extraction buffer used in the Arcturus PicoPure RNA Isolation Kit (ThermoFisher Scientific) (Shea and Geijsen 2007).

### **3.2.20 Mouse Embryos RNA Isolation**

I used the reagents and the columns provided in the Arcturus PicoPure RNA Isolation Kit.

I added 100  $\mu$ l of Extraction buffer for each individual embryo. I incubated the embryos 30 minutes at 42°C. After conditioning the column according to manufacturer's instructions, I added 100  $\mu$ l of Ethanol 70% to the samples and I pipetted up and down. I load the samples into the preconditioned column. After spinning at 1250 rpm for 2 minutes, I added at the column 100  $\mu$ l of W1 buffer, and spun the samples at 11000 rpm 1 minute. In-column DNase treatment was performed by adding a mix of 5  $\mu$ l DNase I + 35  $\mu$ l RDD. After 15 minutes of incubation I spun the samples at 11000 RPM for 30 seconds, I then added 40  $\mu$ l of W1 buffer, spun again at 11000 RPM for 30 seconds and repeated with 100  $\mu$ l buffer W2.

I used 11  $\mu$ l of elution buffer Nuclease-free to the column and the samples were spun at 3800 rpm for 1 minute and at 11000 for 1 additional minute. The total RNA extracted was then reverse transcribed using the Quantitect Kit (Qiagen), according to manufacturer's instructions.

### **3.2.21 gRNA design**

The gRNA design was performed using CHOPCHOP online tool (<http://chopchop.cbu.uib.no>) targeting the coding sequence of the gene of interest.

### **3.2.22 gRNA assembly and synthesis.**

I mixed 5  $\mu$ l of the specific oligo and 5  $\mu$ l of the constant oligo (primers table in



materials section). I Annealed oligos together in the thermocycler, using the following cycles:

95C 5min

95C -> 85C -2C/sec

85C -> 25C -0.1C/sec

4C hold

I Added 0.5 µl of T4 polymerase (NEB), 2 µl of NEB buffer 2.1 and 2.5 µl of dNTPS 10 mM (NEB). the reaction was incubated for 20min at 12C.

I purified the template using the QIAquick nucleotide removal kit, eluting in 20 µl . To synthesize the gRNA I used 5 µl of template DNA and I added 4.0 µl of transcription buffer (Promega), 2 µl of DTT 100 µM, 05 µM of RNasin (RNase inhibitor, Promega), 6 µl of 100 mM rNTP-mix (Promega) , 0.5 µl of T7-RNA Polymerase (Promega) and 2 µl of Water RNase-free. I incubated the reaction at 37 °C for 3 hours, I added 2 µl of Turbo DNase (ThermoFisher Scientific) and incubated 15 additional minutes at 37°C. I purified the gRNA using the RNA clean and concentration kit (Zymo Research).

### **3.2.23 Heat shock treatments**

Heat shock treatment was performed using pre-heated water, kept at 37 °C, the embryos were quickly transferred to a dish containing warm water and kept at 37 °C for 60 minutes, afterwards the embryos were placed in the incubator at 28 °C and analyzed at different time points.

### **3.2.24 mRNA synthesis**

For the genes cloned in pCS2+, I linearized the vector using Not1-HF as described in the chapter 3.2.10, I purified the digested vector using the GeneJET PCR purification kit (Thermo Scientific), and I synthesized the mRNA using the mMESSAGING mMACHINE SP6 kit (Ambion). I then purified the mRNA using the RNA

clean and concentrator kit (Zymo Research). I tested the integrity of the mRNA, by running 1  $\mu$ l of purified mRNA on an agarose gel.

### 3.2.25 Mutant generation and alleles recovered

-*npas4l* allele  $\Delta 4$ :

```

Mut  CTCCGCGCGTCCAAGCGCTTCAGGTCCACCAA----GCATCTAAGGCGGGCGTGATCAGATGAACA
      |||
WT   CTCCGCGCGTCCAAGCGCTTCAGGTCCACCAAAGGAGCATCTAAGGCGGGCGTGATCAGATGAACA

```

-Npas4l Protein

```

Mut  MSCGDSGIRRILRASKRFRSTKHLRRGVIR*TVRYGTCERCCPSAQSTDSHTCTA*
WT   MSCGDSGIRRILRASKRFRSTKGASKARRDQMNSEIRNLRALLPISPEHRLSYLHS

```

-*tspan18b* allele ins16:

```

Mut  TTGTGGCAGCAAACCCTGTGGCAAATTGTGGCAGCAAACCCACGGGCGTCTACATCAT
      |||
WT   TTGTGGCAGCAAACCCT----C---TTCT-----CTTCACGGGCGTCTACATCAT

```

-Tspan18b protein

```

Mut  ANPVANCGSKPHGRLHHPGHRHAVPAGFPRLLSHTRKQVFAALFLHADPHYFGRAGGRHSRLHLPGASDQGILH*
WT   ANPLLFYGVYIILAMGGMLFLLGFLGCCGAIRENKLLLLFFMLILIIFLAELAAAAILAFIFREHLTREYFTKELKKH

```

## 4. RESULTS

---

## 4.1 Upstream regulators of *npas4l* and angioblast differentiation

### 4.1.1 Spatiotemporal expression analysis reveals an early induction of *npas4l* in the ventral mesoderm

*cloche* mutant was described by Prof. Didier Stainier in the early 90s (Stainier et al. 1995), but the discovery of the gene defective in the *cloche* mutant was reported by our group only in 2016 (Reischauer et al. 2016). Normally, taking advantage of Next Generation Sequencing, the identification of a mutation does not take so much time and effort, but the case of *cloche* was definitely peculiar, given its location in the telomeric region of chromosome 13. Importantly, the *npas4l* gene, mutated in *cloche* mutant, was not previously reported nor annotated in the available genomic resources. Telomeres usually contain multiple repetitions and the sequencing data are more challenging to assemble and align, therefore, for some specific regions, a deeper coverage is required in order to resolve such ambiguities (Treangen and Salzberg 2011). To identify *npas4l*, a RNA-sequencing (RNA-Seq) analysis of the *cloche* mutant was performed at tailbud stage, just before somitogenesis occurs. This stage was chosen because *npas4l* expression levels were thought to be high at tailbud stage, since one of the earliest angioblast markers, *etv2*, is detectable starting from the onset of somitogenesis and is nearly absent in *cloche* mutant. Once our group resolved the DNA sequence of the region including *npas4l*, I could investigate its expression dynamics during embryogenesis by qPCR. *npas4l* is

detectable during gastrulation, preceding the expression of other angioblast markers, such as *etv2* and *tal1*, which are detected only from 11 hpf. Importantly, the expression of *npas4l* increases during gastrulation, peaking at 80% epiboly and drastically decreases by 24 hpf (Figure 7A). To dig deeper into the early spatiotemporal expression of *npas4l*, I performed whole mount *in situ* hybridization (WISH) at early stages, from 40% epiboly to 80% epiboly (Figure 7B). This experiment indicates that *npas4l* is expressed in the ventral side of the embryo from 50% epiboly, although its expression seems broad and not defined in a certain subpopulation of cells. *npas4l* expression is then restricted and it appears stronger in intensity at 80% epiboly, concordantly to the qPCR data (Figure 7A). The ventral mesoderm of the embryo was previously described to give rise to endothelial and blood progenitors in zebrafish (Vogeli et al. 2006), and the restricted expression of *npas4l* in this population proves that EC progenitors are already specified during gastrulation. These data conclude that *npas4l* is the earliest marker for angioblasts known so far in zebrafish and endothelial cell precursors are specified during gastrulation in the ventral mesoderm.

#### **4.1.2 Drug screening assay indicates BMP and FGF/Erk signaling pathways to be involved in *npas4l* regulation**

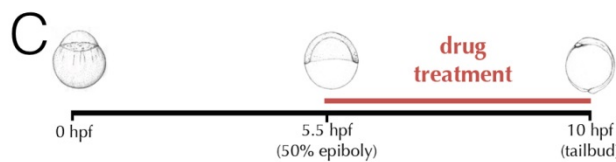
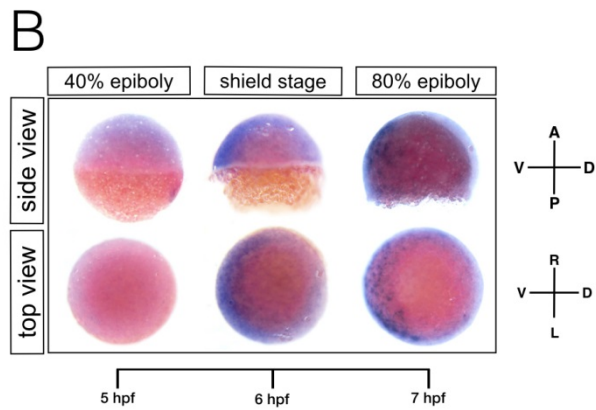
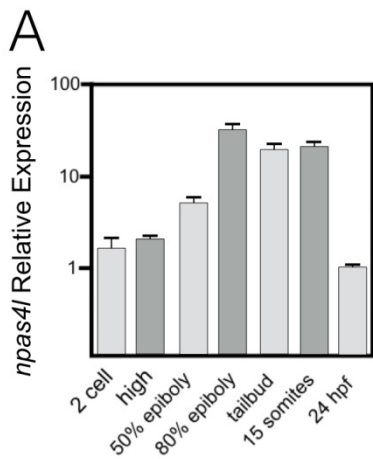
To understand the signaling pathways involved in *npas4l* regulation, I performed a drug screening assay, treating embryos during the time window spanning from 50% epiboly to tailbud stage (Figure 7C). I tested several compounds known to specifically inhibit or activate different pathways involved in cell fate determination

and gastrulation (Figure 7D). qPCR was used to precisely assess the level of *npas4l* mRNA after the drug treatment. After optimizing the ideal working concentration for each drug used, I identified few compounds that efficiently affected *npas4l* expression, but without influencing the expression level of the housekeeping gene *gapdh*. The compound that gave us the strongest results were DMH-1 and BCI (Figure 7E) that led to a reduction of *npas4l* expression level by 50% and 80%, respectively. WISH of *npas4l* after BCI treatment, confirmed the downregulation of *npas4l* in the LPM (Figure 7F).

DMH-1 is a BMPR1 inhibitor that has been broadly used to block BMP signaling (Hao et al. 2010). BCI inhibits DUSP6, which is a protein involved in blocking the effects of FGF/Erk pathway (Molina et al. 2009). BMP signaling is a well-known regulator of mesodermal patterning, as described in the introduction and the BMP family consists of many ligands binding to the BMP receptor 1. I wanted to understand the possible BMP ligands implicated in inducing *npas4l* expression. One of the candidates, due to its expression pattern was *bmp2b* (Shin et al. 2007). I took advantage of the *hsp70l:bpm2b* line Shin et al. developed to temporally induce *bmp2b* expression upon heatshock treatment. I performed the heatshock at 30% epiboly and I recovered a significant induction of *npas4l* at tailbud stage compared to the WT control (Figure 7G).

BCI is an activator of Erk signaling, which is the downstream effector of the tyrosine kinase receptor phosphorylation cascade. To understand what specific signaling could be involved in *npas4l* regulation, I analyzed previously published RNA-seq

datasets (Pauli et al. 2012), looking for the most expressed tyrosine kinase receptors from 50% epiboly to tailbud stage, and I found *fgfr* genes to be highly abundant during gastrulation. To test a specific role for Fgfr1 in *npas4l* regulation, I treated embryos using a potent inhibitor called SU5402 at the optimal concentration of 35  $\mu$ M and I confirmed that *npas4l* was upregulated by the blockage of FGF signaling (Figure 7G). Interestingly, FGF pathway has been previously reported to play a role in the cross-antagonism between cardiac and hemangioblast progenitors (Simoes, Peterkin, and Patient 2011) and FGF inhibition leads to an expansion of vascular precursors at the expense of cardiac precursors. Notably, *npas4l* mutant also exhibits an expansion of cardiac progenitors (Schoenebeck, Keegan, and Yelon 2007). Taken together, these data indicate that FGF negatively regulates *npas4l* expression, and this effect may play a role in the cardiac expansion at the expense of vascular progenitors previously observed upon SU5402 treatment. BMP signaling, however, is known to be involved in mesoderm specification and expansion, thus controlling *npas4l* in a more indirect way.



**D**

Drug	[ ]	Function
DMSO	0.5%	control
SU5402	35 $\mu$ M	FGF inhibitor
BCI	3.5 $\mu$ M	FGF activator
SB431542	10 $\mu$ M	TGF- $\beta$ inhibitor
DAPT	10 $\mu$ M	Notch inhibitor
DMH-1	10 $\mu$ M	BMP inhibitor
Cyclopamine	10 $\mu$ M	Hedgehog inhibitor
SAG	10 $\mu$ M	Hedgehog activator
SKLB1002	10 $\mu$ M	Vegfr2 inhibitor

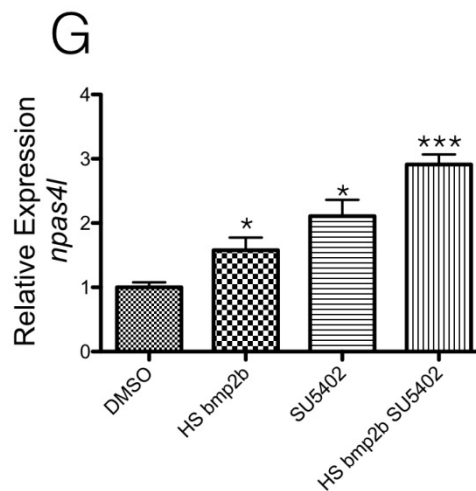
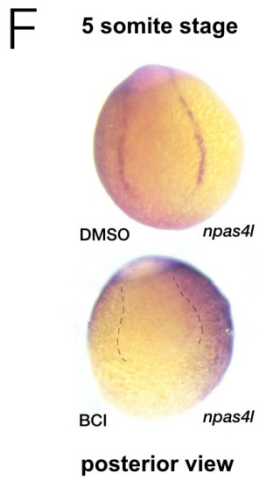
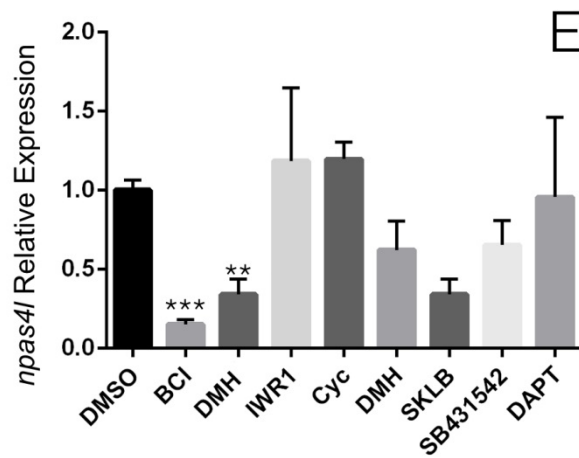




### **Figure 7. Early modulation of *npas4l* spatiotemporal expression**

A) Timecourse of *npas4l* expression measured using qPCR. The expression level is normalized to *npas4l* expression at 24 hpf. Error bars represent s.e.m. from three biological replicates. B) WISH for *npas4l* during gastrulation: 40 % epiboly, shield stage and 80% epiboly. The embryos are shown from top view (top panels) and side view (bottom panels). C) Schematic representation of the drug screening experiment. D) Table showing the compounds used in the screening along with their working concentrations. E) *npas4l* relative expression measured at tailbud stage after drug treatment. Error bars represent s.e.m. from three biological replicates. F) WISH for *npas4l* at 5-somite stage after BCI incubation. Posterior view. Outline in BCI-treated embryo delineate the presumptive PLPM region. G) *npas4l* relative expression measured at tailbud stage after FGF inhibition, using SU5402, or *bmp2b* overexpression. Error bars represent s.e.m. from three biological replicates.

### **4.1.3 *in silico* binding motif prediction combined with transcriptome analysis of BCI-treated embryos suggest a role for *eomesa* upstream of *npas4l***

After the identification of two signaling pathways modulating *npas4l* expression *in vivo*, I wanted to study the molecular link between BMP, FGF and *npas4l*. To understand the genes implicated downstream to FGF and BMP but upstream to *npas4l*, I decided to use a transcriptomic approach (Figure 8A), combined with the *in silico* analysis of *npas4l* promoter. Thanks to the sequence our group assembled and annotated surrounding the *npas4l* locus, I had the possibility to analyze *npas4l* promoter in detail (Figure 8C). Taking advantage of an available online tool called Jaspar (<http://jaspar.genereg.net>), I performed a prediction of transcription factor binding sites present in the promoter (Figure 8C). Moreover, I performed a

microarray analysis after BCI treatment, to identify the molecular players involved downstream to FGF in regulating *npas4l*. With Jaspar I have identified transcription factors with putative binding site within *npas4l* promoter. Then, I checked which of these transcription factors were downregulated or upregulated after *dusp6* inhibition. Interestingly, I found that one transcription factor was present in both datasets, Eomes. Therefore, Eomes represented the strongest candidate with a role in *npas4l* regulation *in vivo* (Figure 8B).

#### **4.1.4 eomesa can induce *npas4l* expression *in vivo***

To test whether the transcription factors I identified had a role in *npas4l* regulation, I performed an overexpression experiment. I cloned *eomesa* in pCS2.0+ plasmid, and I transcribed *in vitro* the mRNA of *eomesa*. Next, I injected 250 pg of *eomesa* at one cell stage and I extracted the total RNA of injected and uninjected embryos, followed by qPCR analysis to measure the expression level of *npas4l* at 4 hpf and germ-ring stage. Strikingly, I found that *eomesa* is a potent inducer of *npas4l* *in vivo* (Figure 8D). I was interested in understanding not only if the overall *npas4l* expression level was increased but I also wanted to analyze whether the spatial regulation of *npas4l* was maintained or perturbed after *eomesa* overexpression. To address this question, I performed WISH for *npas4l* on 50% epiboly embryos after the injection of 250 pg of *eomesa*. As shown in Figure 8E, the expression of *npas4l* is confined in the ventral side of the embryo in the WT embryos, but *eomesa* overexpression was sufficient to induce *npas4l* expression ectopically, indicating that *eomesa* is sufficient to promote *npas4l* expression in pluripotent cells. *eomesa* is

postranslationally regulated by TGFB and BMP signaling. It was shown that, in mouse, EOMES can bind to the promoter of different genes physically interacting with SMAD1 or SMAD2/3 (Faial et al. 2015). Although I showed that *eomesa* is a very potent inducer of *npas4l*, the zebrafish *eomesa* maternal zygote mutant exhibits a non-fully penetrant phenotype in mesodermal patterning, resulting in defects not only limited to vasculature and blood development, but also in other mesodermal-derived tissues, such as somites (Xu et al. 2014). Altogether my data suggest that *eomesa* is a regulator of *npas4l* expression, and angioblast specification in zebrafish.

#### **4.1.5 *Eomes* function is conserved in mammals and can lead to endothelial cell differentiation *in vitro***

P19 cells are a type of murine pluripotent cells that can give rise to different cell types, among others cardiomyocytes and ECs (Marikawa et al. 2009). To test whether *Eomes* can initiate the hematoendothelial specification cascade also in mammalian cells, despite *npas4l* not being present in mammalian genomes, I transfected the mouse *Eomes in vitro* in P19 cells. Surprisingly, *Eomes* could strongly induce *Etv2* and *Tal1*, two well-known angioblast markers conserved across vertebrates (Figure 8F). To confirm that EOMES acts upstream of *Etv2*, I performed a knockdown of *Eomes*, using a pool of silencing RNAs (siRNAs) targeting the mRNA of *Eomes* in multiple points and I recovered a significant reduction of *Etv2* transcript level compared to scrambled siRNA (Figure 8G). After establishing that *Eomes* acts upstream of *Etv2* not only in zebrafish, but also in a mammalian model, I

sought to determine the molecular link between EOMES and *Etv2* in mammals. Given that *npas4l* was lost during evolution in the mammalian lineage, it is likely that another protein took over Npas4l function, retaining the potential to drive the hematoendothelial specification cascade in mammals. This point will be discussed in the chapter 4.3.1 of this thesis.



## Figure 8 Role of *Eomes* in angioblast specification in vertebrates

A) Schematic representation of the experiment. B) Microarray results showing *eomesa* downregulation after BCI treatment. C) *npas4l* genomic locus, the predicted EOMES-binding site is highlighted in red. In yellow the TATAbox, in cyan the 5'UTR, in pink the first exon and in magenta the first intron. D) *npas4l* relative expression after *eomesa* overexpression at one cell stage. Error bars represent s.e.m. from three biological replicates. E) *npas4l* WISH in uninjected and injected embryos with *eomesa* mRNA. Animal and side view. F) *Tal1* and *Etv2* relative expression in P19 mouse cells after *Eomes* overexpression. Error bars represent s.e.m. from three biological replicates. G) Relative expression of *Etv2* and a selection of bHLH transcription factors following *Eomes* knockdown in P19 cells. Error bars represent s.e.m. from three biological replicates.

### 4.1.6 Proposed Model

In this part of my thesis, I propose that *npas4l* is an early expressed gene, whose expression is regulated by the interaction of multiple factors, specifically:

1) *npas4l* expression is restricted in the ventral mesoderm from 50% epiboly and its expression increases during gastrulation via the combination of FGF and BMP signaling pathways;

2) FGF ligands are enriched in the dorsal part of the embryo and FGF signaling pathway limits the expression of *npas4l*. Moreover, the expression of *eomesa* is reduced upon activation of FGF/Erk pathway. BMP ligands, specifically *bmp2b*, are expressed in the ventral part of the embryo and are positive regulators of *npas4l* expression.

3) I showed that *eomesa* is a potent inducer of *npas4l*, whose promoter contains Eomes binding sites. Interestingly, Eomes function is conserved in mammals and

this T-Box transcription factor is able to drive the endothelial specification program in multipotent cells *in vitro*.

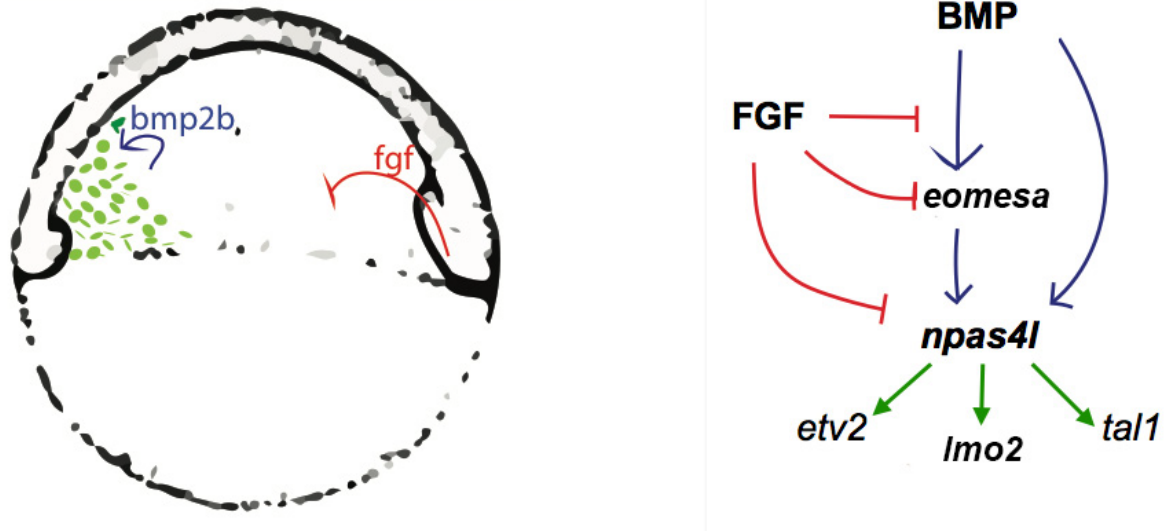


Figure 9. Model of *npas4l* regulation and early angioblast specification

See text for details

## 4.2 Identification and characterization of downstream targets of *npas4l*

### 4.2.1 *npas4l* overexpression followed by transcriptome analysis reveals its primary and secondary target genes

As I previously mentioned, after the discovery of the identification of the gene mutated in the *cloche* mutant, I was curious to test the effects of *npas4l* overexpression in zebrafish zygotes at the whole transcriptome level. I synthesized

the mRNA of *npas4l*. I injected at one-cell stage several concentrations of *npas4l* mRNA and I found that 25 pg was sufficient to strongly induce the EC specification program at 9 hpf, without severely affecting the embryo development. After *npas4l* mRNA injection, I harvested the embryos at 30% epiboly (4 hpf) and 95 % epiboly (9 hpf) (Figure 10A). I extracted the total RNA and I performed a microarray analysis. I expected to recover early induced genes at 30% epiboly, and the secondary targets at 90% epiboly, induced by the direct targets of Npas4l. As seen in Figure 10E, *npas4l* overexpression is sufficient to drive the whole endothelial specification program, and most of the known endothelial markers were upregulated more than 3-fold at 95% epiboly. Data enrichment analysis confirmed that mesodermal patterning and vasculogenesis processes were strongly induced upon *npas4l* overexpression (Figure 10B). Interestingly, only around 60 genes were upregulated both at 3-fold at 30% epiboly and 95% epiboly (Figure 10C). As expected, I found the angioblast markers *etv2*, *lmo2*, and *tal1* to be strongly induced by Npas4l at 30% epiboly, suggesting that these transcription factor may be direct targets of Npas4l. Moreover, known endothelial specific genes such as *kdrl*, *dll4*, *nrp1* and *tie1* are detectable at 95% epiboly but not at 30% epiboly, indicating that the combination of primary and secondary transcription factors downstream to *npas4l* are responsible for the induction of genes expressed in mature endothelium. As discussed in the introduction, *npas4l* mutant shows a striking phenotype, the lack of both vascular and hematopoietic tissue. After a careful analysis of the transcriptomic data generated, I observed most of endothelial markers being induced by *npas4l*, but important transcription factors involved in primitive and

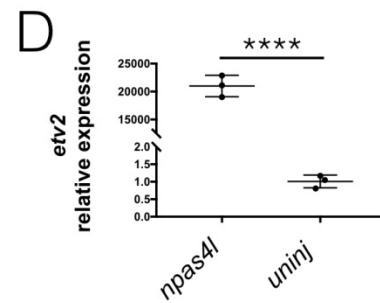
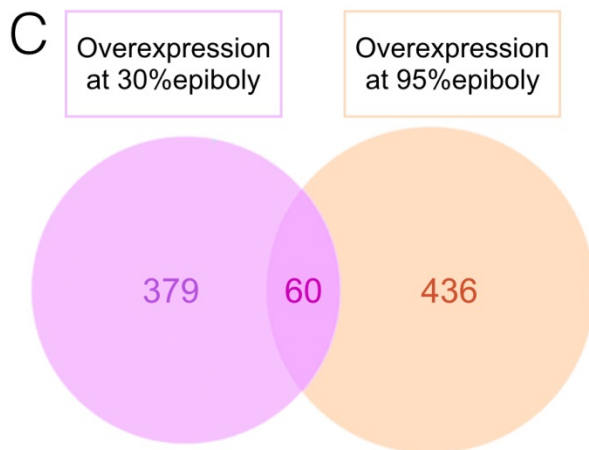
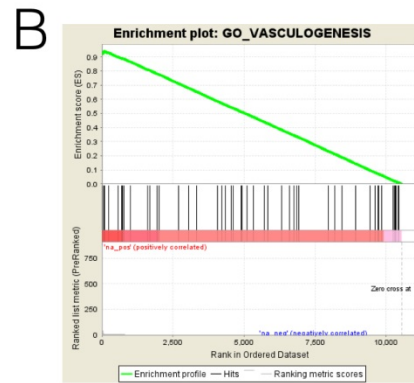
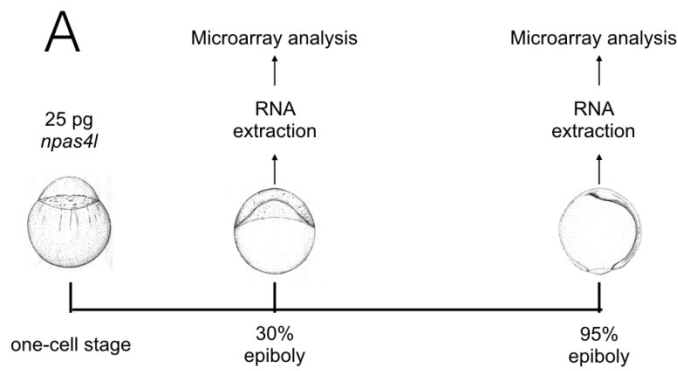


definitive hematopoiesis were not affected (Figure 10E). Surprisingly, these data indicate that *npas4l* is sufficient and necessary to promote vascular specification, but it is not sufficient to induce blood development.

Interestingly, we found *dnajb5* to be induced at 30% and 95% epiboly after *npas4l* overexpression. We performed a WISH for *dnajb5* at 5-somite stage and we recovered its expression in the LPM, suggesting a role for this gene in angioblast function (Figure 10F).

*npas4l* is a paralog of *npas4a* and *npas4b*, transcription factors with a role in neurogenesis and neuronal function. The high level of *npas4l* caused the induction of neuronal genes, probably due to aspecific effects. To better understand the real targets of *npas4l* I took advantage of complementary strategies, as discussed in the next chapter. To test whether the other *npas4* genes were able to induce *npas4l*-related targets, we overexpressed both *npas4a* and *npas4b* and we could detect a significant induction of *etv2* of around 1.5 and 1500 folds, respectively. Importantly, *npas4l* overexpression leads to an induction of *etv2* up to 20000 folds (Figure 10D).

Altogether, I have found that *npas4l* promotes transcription factors expressed during early angioblast specification, such as *etv2*, *tal1* and *lmo2*, already 4 hours after its overexpression. These three transcription factors, downstream and in combination to *npas4l*, are responsible for the expression of endothelial-specific genes, such as *kdrl*, *nrp1b* and *dll4*, that are induced by *npas4l* overexpression specifically at 9 hpf.



**E**

Gene name	<i>npas4l</i> injected 30% epiboly	<i>npas4l</i> injected 95% epiboly
<i>etv2</i>	805.05	768.84
<i>tal1</i>	640.72	747.37
<i>lmo2</i>	220.80	89.29
<i>fam169aa</i>	213.04	15.78
<i>dnajb5</i>	205.31	114.97
<i>sox7</i>	38.11	41.15
<i>pcdh2g28</i>	19.36	3.49
<i>pcdh2g20</i>	19.15	3.60
<i>egfl7</i>	18.50	863.39
<i>klhl4</i>	8.52	20.86
<i>sox7</i>	7.04	36.77
<i>kdrl</i>	0.29	6.49
<i>dll4</i>	1.20	3.15
<i>nrp1b</i>	1.01	3.07
<i>gata1a</i>	0.96	0.88
<i>gfi1aa</i>	1.09	1.49
<i>runx1</i>	0.92	1.49

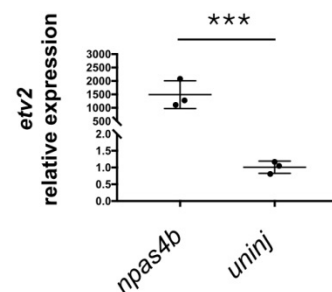
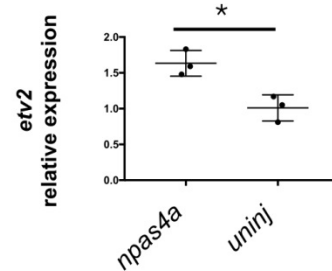


### **Figure 10. Endothelial cell specification induced by *npas4l* overexpression**

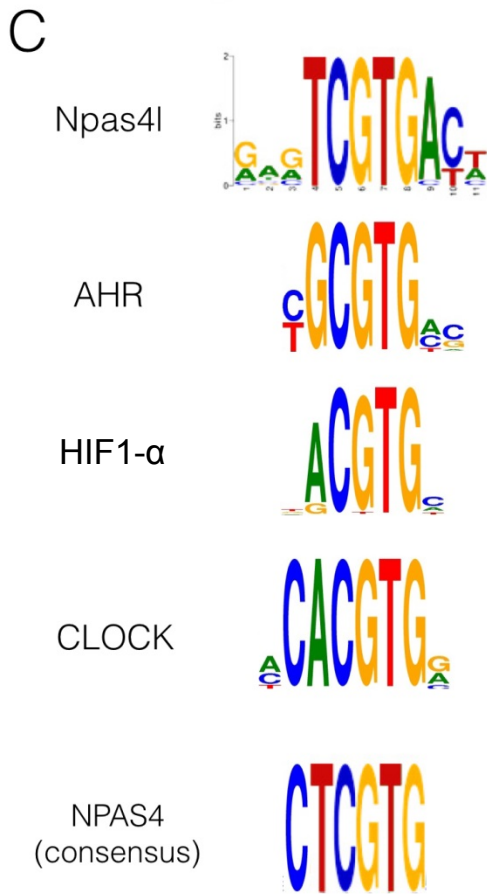
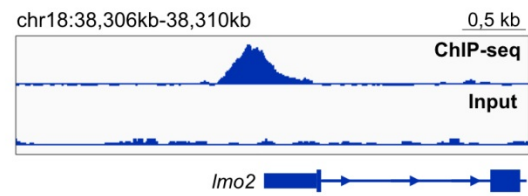
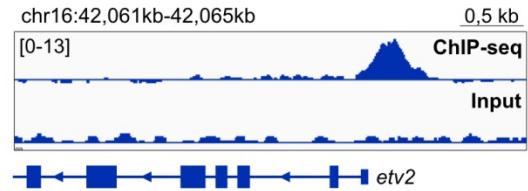
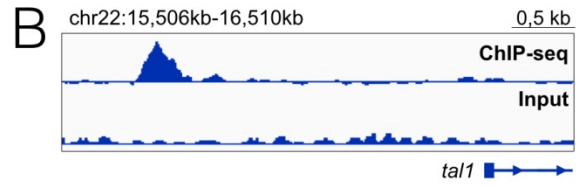
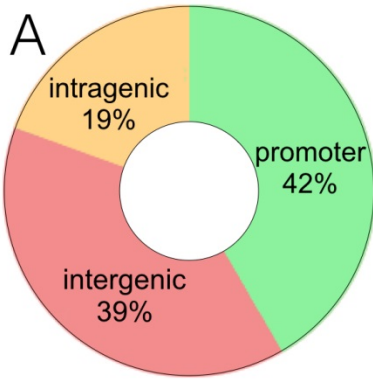
A) Schematic representation of the microarray experiment. B) Gene enrichment analysis performed on upregulated genes, using GSEA. C) Venn diagram highlighting the genes upregulated more than 3-fold after *npas4l* overexpression at 30% and at 50% epiboly. D) Comparison of *Etv2* relative expression after *npas4a*, *npas4b* or *npas4l* overexpression. Error bars represent s.e.m. from three biological replicates. E) Table showing the most upregulated genes at 30% epiboly in green, endothelial markers, in red, markers involved in primitive hematopoiesis F) WISH for *dnajb5* at 5-somite stage.

### **4.2.2 Chromatin immunoprecipitation sequencing identifies direct targets of Npas4l**

Chromatin immunoprecipitation (ChIP) is a technique that allows the pulldown of a protein of interest together with the DNA bound to it. In the case of a transcription factor, it is possible to sequence the DNA purified after the pulldown, in order to understand which regulatory regions are bound by the transcription factor at the genome-wide level. This approach is the golden standard to reveal the loci targeted by the transcription factor of interest, and, combined with a functional assay, it is possible to understand its direct target genes. *npas4l* was very recently identified and, therefore, no antibody against Npas4l is commercially available. To solve this issue, I generated a tagged version of Npas4l and I tried to rescue *npas4l* mutant phenotype with a myc-tagged, a flag-tagged and a HA-tagged version of Npas4l at C and at the N terminus. Unfortunately, these experiments were inconclusive. Transcription factors need to interact with many partners in order to drive the transcription of the target genes, and an additional peptide fused to the protein may result in a loss of the function, due to steric effects. Next, I tried to insert a flexible

linker between the protein and the HA-tag and I was able to efficiently rescue the mutant. Then, I injected around 3000 embryos and I performed the ChIP experiment as described in the material and methods section. The sequencing results indicated that Npas4l binds to the proximal promoter of approximately 15 genes (Figure 11D). In Figure 11, it is possible to visualize Npas4l occupancy at selected target sites. Importantly, *tal1*, *etv2* and *lmo2* are direct targets of Npas4l (Figure 11B) further confirming the direct relationship between these genes and *npas4l*. These data indicate that Npas4l has the ability to act as a master regulator gene, directing the expression of all the key transcription factors reported to have a role in angioblast differentiation. In addition, I performed a *de novo* binding motif identification of Npas4l using the MEME tool (<http://meme-suite.org>). I compared the identified motif with the reported binding motif of other bHLH-PAS transcription factors, such as AHR, HIF-1 $\alpha$  and CLOCK, and I observed that these proteins show a highly similar core motif: CGTG (Figure 11C). Npas4l binding sites are homogeneously distributed in the genome and in Figure 11A it is depicted a pie chart showing the proportion of regions bound by Npas4l, relative to their genomic localization. 42% of the peaks were found in promoter regions, within 10kb from the transcription starting site (TSS) of the gene, 19% in introns and 39% in intergenic regions. The intergenic regions may represent long-distance enhancers, but, unfortunately, a three-dimensional architecture of the zebrafish genome at this stage has not been developed yet and the functional role of these regions is not known. Npas4l binds regions of DNA in close proximity to some TSSs. However, transcription factors could regulate also more distal genes. Therefore, I considered all the genes within 50 kb from a Npas4l

binding site to be potentially regulated by this bHLH-PAS transcription factor. Next, I combined the list of the genes recovered with the genes functionally induced by Npas4l, as indicated by the overexpression experiment described in the chapter 4.2.1. I identified 10 genes: *tspan18b*, *si:ch211-237l4.6*, *rippy2*, *pycard*, *si:dkey-121a11*, *abi1a*, *egfl7*, *etv2*, *tal1* and *lmo2*. This list includes the genes whose promoter is in the surroundings of Npas4l binding sites and that are actively induced by Npas4l. Importantly, this data confirms that Npas4l directly regulates genes known to play a role in EC differentiation, such as *egfl7*, *etv2*, *tal1* and *lmo2*. Importantly, the role of the other genes has not yet been investigated in zebrafish vascular development.



**D**

gene name	gene function
<i>zic2b</i>	transcription factor
<i>si:ch73-364h19.1</i>	transmembrane
<i>gata2a</i>	transcription factor
<i>rippy2</i>	transcription factor
<i>vamp2</i>	vesicle formation
<i>gata3</i>	TF (missense)
<i>etv2</i>	transcription factor
<i>fli1b</i>	transcription factor
<i>tspan18b</i>	membrane protein
<i>lmo2</i>	transcription factor
<i>gtf3c2</i>	POL III complex
<i>egfl7</i>	ECM protein
<i>tal1</i>	transcription factor
<i>tal1</i>	transcription factor
<i>pimr63/pimr64</i>	Ser Thr Kinase

### Figure 11. Chromatin immunoprecipitation reveals Npas4l direct targets

A) Pie chart showing the proportion of regions bound by Npas4l relative to their genomic localization. B) Integrative Genomics Viewer (IGV) visualization of Npas4l occupancy at selected target sites: *tal1*, *etv2* and *lmo2* loci. C) *de novo* binding motif identification of Npas4l and comparison with previous reported binding motifs of other bHLH-PAS transcription factors. D) Table showing the genes whose proximal promoter is bound by Npas4l, with a peak within 2kb from their TSS.

### 4.2.3 Chromatin accessibility analysis in *npas4l* mutant does not suggest that Npas4l can act as a pioneer factor

To further characterize the molecular function of Npas4l, I wanted to investigate whether Npas4l acts as a pioneer factor. Pioneer transcription factors are known to bind to closed regions of the genome, and via the recruitment of chromatin remodelers they have the ability to make the chromatin more accessible (Iwafuchi-Doi and Zaret 2016). To address this question, I planned to perform an ATAC-seq experiment on single embryos. The available *npas4l* mutants are not suitable for such experiment for several reasons. The s5 allele shows a single nucleotide substitution (Reischauer et al. 2016), which makes the genotyping excessively laborious. In contrast, the m39 allele it is easy to genotype, but the big deletion may cause other defects that not necessarily are related to *npas4l* loss-of-function (Reischauer et al. 2016). Therefore, I generated a new allele, *npas4l*<sup>bn59</sup> using CRISPR/Cas9 technology by targeting exon 2, which encodes the bHLH domain, and I recovered a delta4 mutation, that leads to a premature stop codon after a 8 amino acid-long missense segment. *npas4l*<sup>bn59/bn59</sup> embryos exhibit a similarly strong phenotype compared to the previous published *npas4l* mutants, with the

advantage to be easy to genotype. I incrossed *TgBAC(etv2:EGFP)<sup>ci1Tg</sup>;npas4l<sup>+/-</sup>* and subsequently I sorted single embryos at 2-somite stage, when I could distinguish the mutants from the siblings by the absence or presence, respectively, of *TgBAC(etv2:EGFP)<sup>ci1Tg</sup>* expression in the LPM (Figure 12D). I performed ATAC assay as described in the methods and I genotyped each individual embryo using HRMA. Next, the purified DNA was sent to sequence and the results of the analysis are shown in Figure 12E. From the ATAC-sequencing analysis, endothelial genes, like *tie2* and *kdrl*, appeared to show reduced chromatin accessibility in *npas4l* mutant (Figure 12F). Interestingly, I then combined the ATAC-sequencing results with the ones from the ChIP-seq experiment, and I noticed that the chromatin accessible regions occupied by Npas4l are not changed in the mutant in the loci of interest, such as *etv2* (Figure 12G). *Imo2* is the only gene that exhibits less accessible chromatin surrounding the TSS which is also a direct target of Npas4l, but the chromatin sites do not overlap with the DNA sequence bound by Npas4l (Figure 12E). This data indicate that the differential accessibility of the promoters of endothelial genes, such as *tie2* and *kdrl*, may not be directly due to Npas4l. Our data, moreover, suggest that Npas4l binds to regions of the genome that are accessible prior to its expression, at dome stage (Chen et al. 2017), indicating that some other factors, expressed even earlier than *npas4l*, may be responsible for regulating the epigenetic state of the promoter of the direct target genes of Npas4l.

#### **4.2.4 Early transcriptome analysis of *npas4l* mutants reveals the reduction of early hematopoietic and endothelial markers**



A reported transcriptomic analysis of *cloche* mutants with the aim to identify new genes involved in vascular development has been reported 13 years ago (Qian et al. 2005). The generation of a new *cloche* mutant using CRISPR/Cas9 technology, as explained in the previous chapter, made possible to analyze the differentially expressed genes in these embryos with an unprecedented resolution. Moreover, by taking advantage of a reliable and efficient genotyping method, it is possible to discern mutants from siblings. Therefore, I selected 10 *TgBAC(etv2:EGFP)<sup>ci1Tg</sup>;npas4l<sup>-/-</sup>* embryos and 10 siblings embryos based on the vascular phenotype at 6-somite stage, and I processed them for RNA-sequencing (RNA-seq) (Figure 12A). In table 1 I show the most downregulated genes in the *npas4l* mutant, and as expected *tal1*, *etv2*, *egfl7* and *lmo2* are among the top downregulated genes. In figure 12 C it is possible to see the differences between the expression levels of the selected genes in WT and in mutant embryos. Notably, in contrast with the overexpression experiment, I detected some hematopoietic genes to be downregulated, as *gfi1aa* and *gata1a*. Interestingly, *fli1* was not downregulated in the mutant, as previously reported, and concordantly with our CHIP data its expression does not seem to be directly regulated by *npas4l*. As shown in Figure 12B, 7 genes are present in both the list of the most downregulated in the mutant and the list of the most upregulated genes after *npas4l* overexpression, this group of seven genes includes *tal1*, *etv2*, *egfl7*, *sox7* and *lmo2*, thus further supporting a model where these genes act as downstream effectors of *npas4l* in EC specification. I analyzed the RNA-Seq dataset focusing my attention on transcription factors, and I found that *morc3b* was almost 4-fold downregulated in the *npas4l* mutant,

suggesting a novel role for this gene in hematopoiesis or EC specification in zebrafish. Intriguingly, *Morc3* has been recently described to play a role in mouse hematopoietic stem cell development (Jadhav et al. 2016). Furthermore, I found that *per1* was strongly upregulated in *npas4l* mutants when compared with WT siblings. Interestingly, Per1 is a PAS-containing protein without DNA binding domain that negatively regulates Clock, and its function has been associated with circadian rhythms (Husse et al. 2012). Altogether, these data provide a transcriptomic overview of *npas4l* mutant as early as 6-somite stage, a critical stage for angioblast formation. The analysis performed on the dataset highlights the early-expressed genes that are differentially expressed after the knockout of *npas4l*. These genes may play a role in primitive blood cells formation and maintenance as well as angioblast differentiation and function.

GENE NAME	+/?	+/?	-/-	-/-	AVERAGE +/?	AVERAGE -/-	FOLD CHANGE	FUNCTION
<b><i>tal1</i></b>	166	163	13	8	164.5	10.5	-15.67	Transcription Factor
<i>gfi1aa</i>	73	92	12	10	82.5	11	-7.50	Transcription Factor
<b><i>lmo2</i></b>	210	211	61	33	210.5	47	-4.48	Transcription Factor
<i>morc3b</i>	103	84	20	29	93.5	24.5	-3.82	Transcription Factor
<b><i>egfl7</i></b>	44	42	15	16	43	15.5	-2.77	ECM Associated Protein
<i>si:ch211-93</i>	76	66	34	21	71	27.5	-2.58	Transmembrane Protein
<i>tpd521l</i>	65	80	31	24	72.5	27.5	-2.64	Cell Cycle Protein
<i>chmp5a</i>	82	48	29	21	65	25	-2.60	Multivesicular Bodies
<b><i>etv2</i></b>	294	244	127	86	269	106.5	-2.53	Transcription Factor
<i>pudp</i>	32	30	9	18	31	13.5	-2.30	rRNA Phosphatase
<i>ripk2</i>	37	31	11	18	34	14.5	-2.34	STT Kinase, immune response
<b><i>sox7</i></b>	51	59	24	21	55	22.5	-2.44	Transcription Factor
<i>gata1a</i>	14	20	3	11	17	7	-2.43	Transcription factor

**Table 1. Genes downregulated in *npas4l* mutant at 6-somite stage**

The genes in bold are also induced by *npas4l* at 95% epiboly. Importantly, hematopoietic genes such as *gata1a* and *gfi1aa* are downregulated in the mutant but are not induced by *npas4l* overexpression.

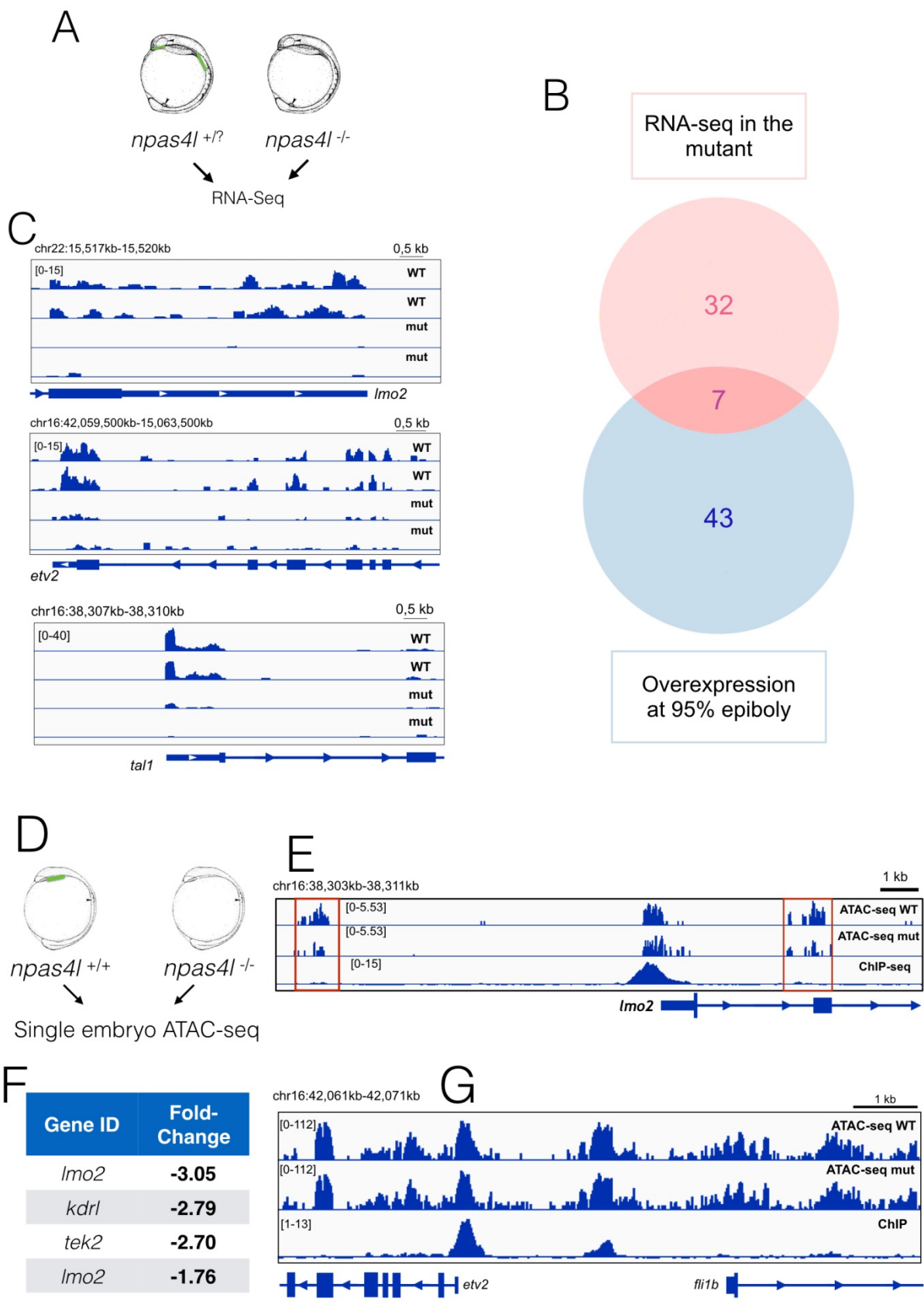


## Figure 12. Transcriptomic and epigenomic analysis of *npas4l* mutant

A) Schematic representation of the RNA-seq experiment performed in WT/heterozygous and mutant embryos. B) Venn diagram highlighting the genes downregulated in the *npas4l* mutant more than 2-fold and the top 50 genes induced by *npas4l* overexpression at 95% epiboly. C) IGV visualization of selected direct targets of Npas4l, showing significant reduction in expression level in *npas4l* mutant. D) Schematic representation of the ATAC-seq experiment performed in WT and mutant embryos. E) IGV visualization of accessible chromatin in WT and in mutant embryos at 1-somite stage, combined with the ChIP-seq results at the *etv2* locus. F) Table showing endothelial markers whose regulatory regions are differentially accessible in the mutant, compared to the wild type G) IGV visualization of accessible chromatin in WT and in mutant embryos at 1-somite stage, combined with the ChIP-seq results at the *lmo2* locus.

### 4.2.5 Combined analysis of different datasets reveals the downstream targets of *npas4l*

The data presented in the previous chapters derive from complementary strategies and different approaches. In order to have a reliable list of Npas4l targets, I combined the data from all datasets I generated. The Venn diagram in Figure 13A shows the combinatorial analysis of the 4 different datasets. For the RNA-seq I considered the genes downregulated more than 2-fold; for the ChIP I took into account all the genes that have the transcriptional starting site within 100 Kb from a Npas4l-binding site; for the microarray, given the high number of upregulated genes, I used a cutoff of 3-fold upregulation after *npas4l* overexpression at both 30% and 95% epiboly. We identified 4 protein-coding genes, namely *tal1*, *etv2*, *lmo2*, and *egfl7* that are present in all the datasets. Three of them - *tal1*, *etv2*, *lmo2* - are transcription factors specifically expressed in angioblasts, with a conserved function

across vertebrates. Importantly, the transcription factor *sox7* does not show *Npas4l* binding sites in its promoter, suggesting that its regulation, although tightly linked to *npas4l*, because it is induced by *Npas4l* and also downregulated in the *npas4l* mutant, is probably directly controlled by *etv2*, *tal1* or *lmo2*. Similarly, *cdh5*, *morc3b*, *tpd52l1*, and *nkx2.3* are induced by *npas4l* overexpression only at 95% epiboly but not at 30%, and are downregulated in the mutant, indicating that are regulated by a transcriptional wave secondary to *Npas4l*. Among the genes with a *Npas4l*-binding site within 100kb from their TSS, 6 genes - *rippy2*, *pycard*, *si:dkey-121a11*, *abi1a*, *tspan18b* and *si:ch211-237l4.6* - are induced by *Npas4l*, but they are not downregulated in the *npas4l* mutant at 6-somite stage, suggesting that probably, *npas4l* is not strictly necessary for the expression of these genes. Specifically, *tspan18b* and *si:ch211-237l4.6* were induced by *npas4l* overexpression at 95% epiboly, and the other 4 were upregulated at 30% epiboly. Moreover, *pard6b* was downregulated in the mutant and *Npas4l* binds in proximity of its TSS, indicating that *Npas4l* is not sufficient alone to induce *pard6b*, but another transcription factor could cooperate with *Npas4l* for promoting *pard6b* expression.

Taken together, the combined analysis of the datasets reveals the genes likely to be regulated, directly or indirectly, by *npas4l* during zebrafish embryonic development.

#### **4.2.6 Generation of mutants using CRISPR/Cas9 technology targeting the identified candidate genes downstream of *npas4l***

The genes downstream to *npas4l* like *etv2*, *tal1*, *sox7* and *lmo2*, when mutated exhibit a vascular phenotype in zebrafish (Craig et al. 2015; Schumacher et al. 2013; Hermkens et al. 2015). I wanted to study the function of other genes identified to be regulated by *Npas4l*, to possibly identify novel regulators of cardiovascular development and, to do so, I used CRISPR/Cas9 technology to generate zebrafish mutants. Among others, I generated a new allele for *tspan18b* using CRISPR/Cas9 by targeting exon 4 and I recovered a 16-nucleotide insertion that leads to a premature stop codon after a 74 amino acid-long missense segment. As seen in Figure 13B, *Tg(fli1a:EGFP) tspan18* mutants exhibit vascular defects at 36 hpf, when compared with the *Tg(fli1a:EGFP)* WT siblings. The defective sprouting angiogenesis in the mutants results in partial ISVs that do not fuse completely to form a continuous DLAV. The phenotype of this mutant indicates that *tspan18b* is a novel gene with a function in zebrafish vascular development, thus suggesting that the datasets developed in this thesis represent a valuable resource available for further studies.



**Figure 13. Combined analysis of the datasets reveals *tspan18b* ad a novel endothelial gene**

A) Venn diagram illustrating the cross-analysis of the different datasets used to identify the genes downstream of *Npas4l*. B) Maximal intensity projections of confocal Z-stacks of *Tg(fli1a:EGFP)* WT siblings and *tspan18b*<sup>-/-</sup> embryos at 24 hpf.

#### **4.2.7 Proposed Model**

In this second part of my thesis, the results indicate that *Npas4l* can directly regulate the most important factors involved in EC specification, initiating a transcriptional cascade leading to the establishment of a pool of functional ECs that will organize into a vascular network.

Specifically:

- 1) *Npas4l* is necessary and sufficient to drive EC specification as a whole, inducing most of endothelial markers.
- 2) *Npas4l* directly binds the promoter of early regulators of EC specification in vertebrates, such as *etv2*, *tal1* and *lmo2*.
- 3) Combined analysis of several datasets helped in identifying genes with a novel role in vascular development.



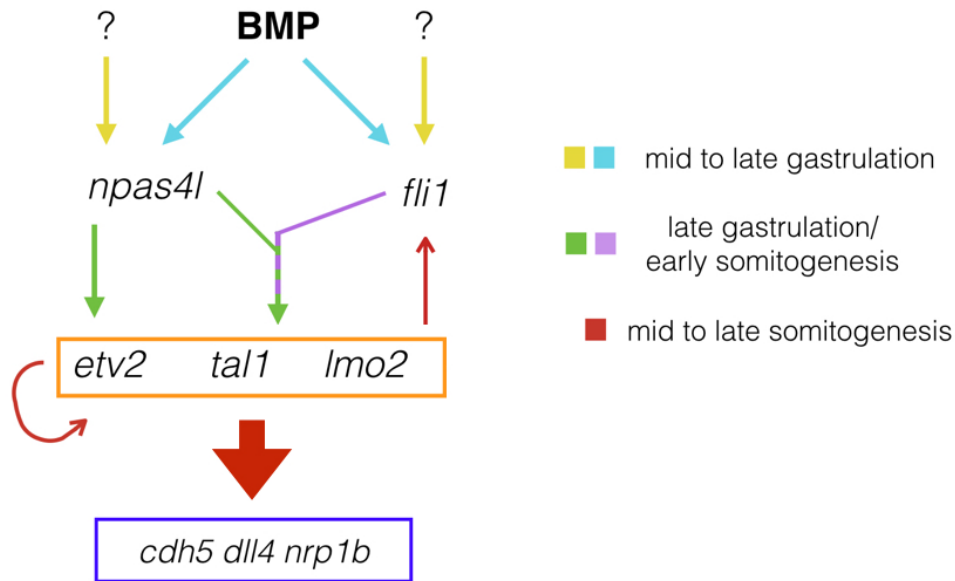


**Figure 14. Model of angioblast and endothelial cell specification.**

*Npas4l* directly regulate the triad of transcription factors expressed in angioblast *etv2*, *tal1* and *lmo2*, which in turn activate the EC specification program that causes the expression of *cdh5*, *dll4*, *nrp1b*. Interestingly, *fli1a* and *fli1b* expression levels do not change in *npas4l* mutant at 6 somites, and *fli1* genes are not induced early upon *npas4l* overexpression, but only at 95% epiboly. Other reports (Liu et al. 2008) have shown that *fli1* can induce *etv2*, *tal1* and *lmo2* only in presence of *npas4l*, suggesting that it may act in parallel to *npas4l*.

## 4.3 Identification of a functional ortholog of *npas4l* in mammals: role of HIFs in endothelial cell differentiation

### 4.3.1 *in vitro* identification of *npas4l*-homolog genes downstream of *Eomes*

In the chapter 4.1.5 I showed that *Eomes* is sufficient and necessary for *Etv2* and *Tal1* expression in mouse P19 cells. In zebrafish I showed that *Eomesa* can induce

*npas4l* expression and Npas4l acts directly upstream of *etv2*. In mammals, however, *npas4l* is not present in the genome; therefore, another transcription factor with similar function may have taken over the role of *npas4l* during evolution. To test this hypothesis, I performed a knockdown of *Eomes* using siRNA in P19 cells, followed by qPCR analysis to measure the mRNA level of other bHLH-PAS transcription factors expressed in P19 cells. As shown in Figure 8G, *Hif-1α* was the only one downregulated after *Eomes* knockdown, suggesting that this T-box transcription factor may indeed act upstream of *Hif-1α* in mouse, thus leading to the expression of *Etv2*.

#### **4.3.2 Role of *Hif-1α* and *Hif-2α* in mouse *Etv2* regulation and endothelial cell specification**

HIF-1α was shown to physically bind the promoter of *Etv2* *in vitro* (Tsang et al. 2017). Interestingly, I showed that, in zebrafish, Npas4l interacts with the promoter of *etv2* *in vivo*. To test the role of HIF-1α in mammalian EC specification *in vivo*, I took advantage of a genetic loss-of-function model of *Hif-1α*. After dissecting the embryos at E6.5, I performed single embryo RNA extraction followed by qPCR analysis to assess the expression level of *Etv2*. As shown in Figure 15, I could detect a reduction of *Etv2* in *Hif-1α* mutants, indicating that *Hif-1α* is, at least in part, responsible for *Etv2* regulation and subsequent EC specification in mouse. The direct link between *Hif-1α* and *Etv2* (Tsang et al. 2017), together with the sequence similarity between murine HIF-1α and the zebrafish homolog Npas4l, suggest that, during evolution, HIF-1α took over Npas4l function.

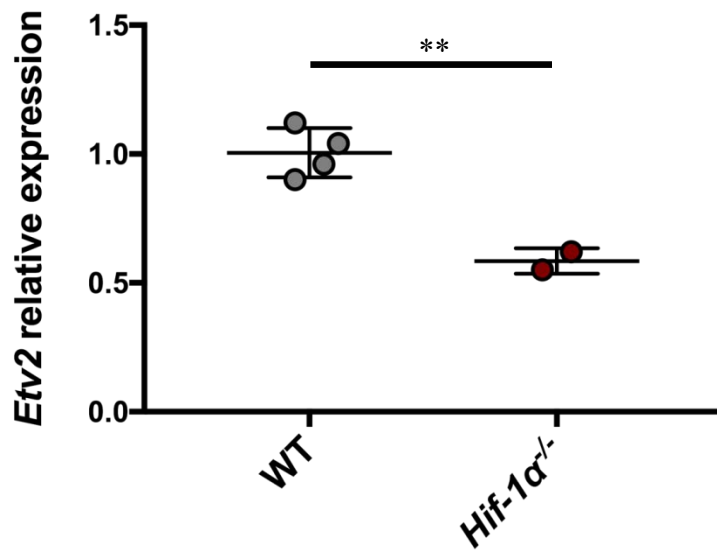


**Figure 15. Hif-1 $\alpha$  mouse mutants exhibit lower expression of *Etv2***

qPCR analysis of *npas4l* expression in E6.5 WT and *Hif-1 $\alpha$*  mutant mouse embryos, normalized to WT siblings. Error bars represent s.e.m. from three biological replicates.

## 4.4 Role of Hifs in endothelial cell specialization in zebrafish

This research was originally published in *Blood* Journal. Gerri\* and Marass\* et al., Hif-1 $\alpha$  and Hif-2 $\alpha$  regulate HE and HSC formation in zebrafish *Blood* Jan 2018; 131:963-973, © the American Society of Hematology (\*Joint first author.) doi: <https://doi.org/10.1182/blood-2017-07-797795>

<http://www.bloodjournal.org/content/early/2018/01/16/blood-2017-07-797795?sso>

### 4.4.1 Vasculogenesis and angiogenesis are not affected in *hif-1 $\alpha$* and *hif-2 $\alpha$* mutants

To test the role of *hif-1 $\alpha$*  and its paralog *hif-2 $\alpha$*  in zebrafish vascular development, I analyzed the phenotype of *hif-1aa;hif1-ab* double mutants (*hif-1 $\alpha$*  mutants or *hif-1 $\alpha$ <sup>-/-</sup>*) and *hif-2aa;hif2-ab* double mutants (*hif-2 $\alpha$*  mutants or *hif-2 $\alpha$ <sup>-/-</sup>*), carrying *kdrl:EGFP* transgene, which allowed me to observe the vasculature using a confocal microscope. As shown in Figure 16A vasculogenesis and angiogenesis were not affected in *hif-1 $\alpha$ <sup>-/-</sup>* nor in *hif-2 $\alpha$ <sup>-/-</sup>*. The DA, the PCV and the ISVs were not impaired in the *hif* zebrafish embryos, in contrast to what observed in the mouse *Hif-1 $\alpha$*  mutants that show very severe defects in embryo vascular development (Ryan, Lo, and Johnson 1998).

(Certain lines in this section 4.4.1 have been quoted verbatim from Gerri\* and Marass\* et al., *Blood* Jan 2018; 131:963-973, \*Joint first author).

#### **4.4.2 *hif-1α* and *hif-2α* mutants show reduced expression of HSC markers**

I explored the involvement of *hif-1α* and *hif-2α* in definitive hematopoiesis, a process that occurs through the EHT process in the VDA starting from 32 hpf, as described in the introduction. I first performed WISH for *runx1* and *cmyb*, markers of HSCs, at 36 hpf. In *hif-1α* mutants as well as in *hif-2α* mutants the signal was severely reduced compared to WT siblings, suggesting a defects in HSC differentiation (Figure 16B,C). Given the recent studies investigating the phenotypic difference between mutants and morphants (Kok et al. 2015), I wanted to understand whether morpholino (MO) could give similar results in terms of HSCs emergence, when compared to the phenotype of *hif-1α* and *hif-2α* mutants. I co-injected MOs targeting *hif-1aa* together with *hif-1ab* as well as *hif-2aa* together with *hif-2ab* and I could recover a similar phenotype after *runx1* and *cmyb* WISH as observed in *hif-1α*<sup>-/-</sup> or in *hif-2α*<sup>-/-</sup>. Indeed, the morphants showed a severe reduction of HSC markers expression compared to the embryos injected with control MO (Figure 17C). (Certain lines in this section 4.4.2 have been quoted verbatim from Gerri\* and Marass\* et al., *Blood* Jan 2018; 131:963-973, \*Joint first author).

#### **4.4.3 Hypoxia induces hemogenic endothelial specification and hematopoietic stem cell formation**

Previous studies showed that mimicking hypoxia with chemicals like DMOG, a pan-hydroxylase inhibitor, promotes HSC formation in zebrafish (Harris et al. 2013). As a

pan-hydroxylase inhibitor, DMOG has effects on biological processes independently of Hif (Elks et al. 2015). Moreover, DMOG effects do not strictly relate to the changes in O<sub>2</sub> tension. Therefore, to better understand the effect that hypoxia may have on HE specification and EHT, WT embryos were exposed to hypoxia for 8 hours using a hypoxia chamber set at 3% O<sub>2</sub>, and WISH was performed to evaluate the expression levels of *runx1* and *cmyb* (Figure 16E). WT embryos showed a strong induction of *runx1* and *cmyb* expression after hypoxia treatment compared with siblings developed in normoxia. To test whether hypoxia exposure affects vasculogenesis and DA formation, I performed confocal imaging using the *Tg(kdrl:EGFP)* line. I could not detect any major abnormalities in the axial vasculature of the embryos developed in hypoxic condition (Figure 16A). Taken together, these data suggest that hypoxia is a potent inducer of HE specification, promoting *runx1* and *cmyb* expression, leading to an increased in HSC formation. (Certain lines in this section 4.4.1 have been quoted verbatim from Gerri\* and Marass\* et al., *Blood* Jan 2018; 131:963-973, \*Joint first author).

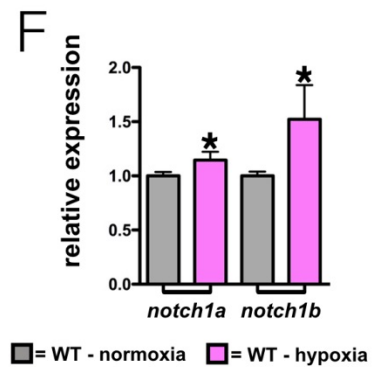
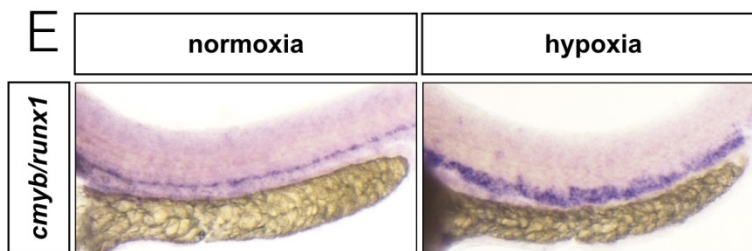
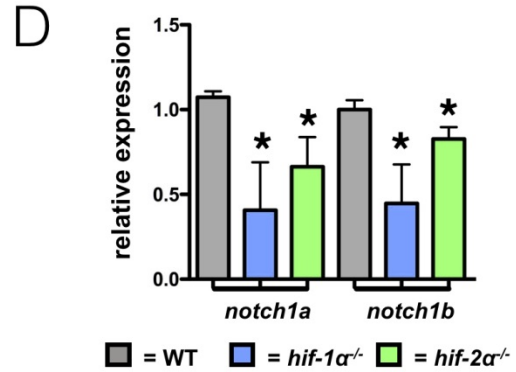
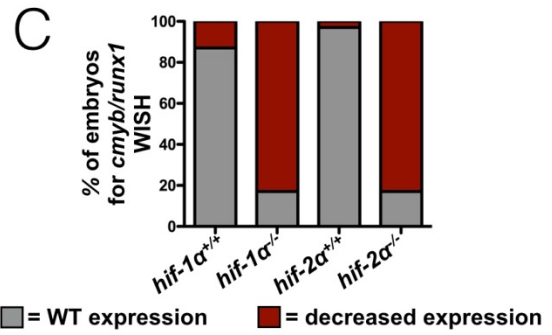
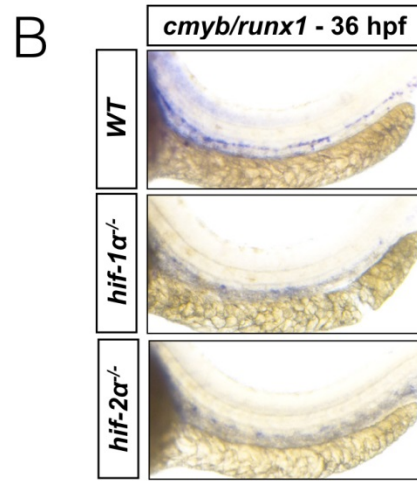
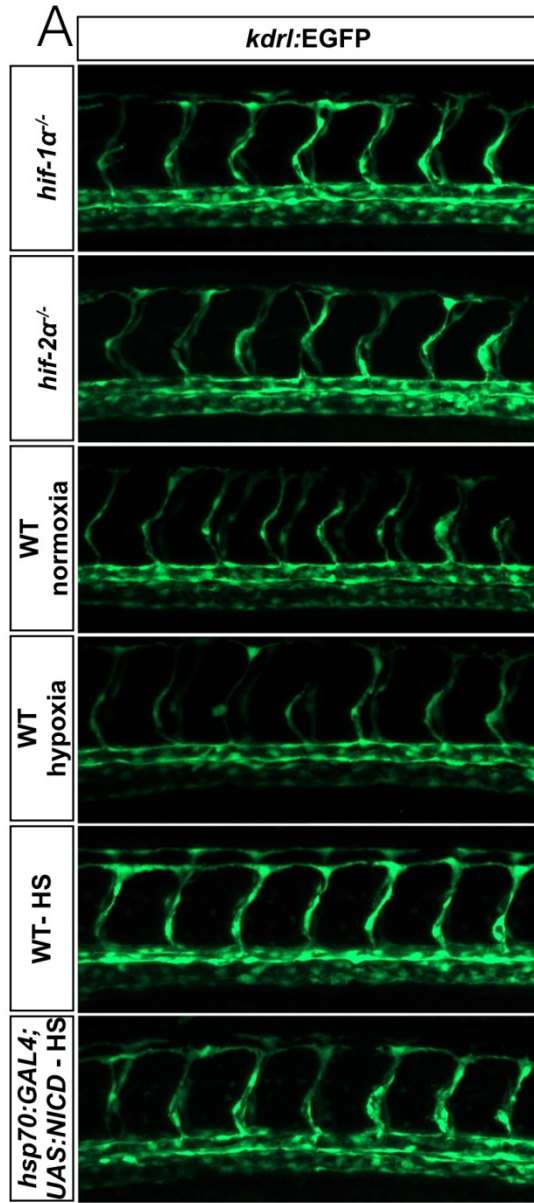


**Figure 16. *hif-1α* and *hif-2α* regulates HSC development in zebrafish**

A) Maximal intensity projections of confocal Z-stacks of zebrafish mutant and transgenic embryos treated in different conditions carrying *Tg(kdrl:EGFP)* reporter at 36 hpf. B) WISH for *cmyb/runx1* in WT, *hif-1α<sup>-/-</sup>* and *hif-2α<sup>-/-</sup>* embryos at 36 hpf C) Quantification of *cmyb/runx1* WISH results, showing the percentages of embryos with WT and decreased expression in the genotypes listed. D) qPCR analysis of *notch1* receptors genes at 36 hpf in WT, *hif-1α<sup>-/-</sup>* and *hif-2α<sup>-/-</sup>* embryos. E) WISH for *cmyb/runx1* in WT embryos after normoxia and hypoxia exposure. F) qPCR analysis of *notch1* receptors genes at 36 hpf after normoxia and hypoxia exposure. (Certain lines have been quoted verbatim from Gerri\* and Marass\* et al., Blood Jan 2018; 131:963-973, \*Joint first author)..

**4.4.4 Defects in hemogenic endothelial specification in *hif-1α* and *hif-2α* morphants**

To further investigate the role of hypoxia transcription factors during HSC formation, I used a reporter line *Tg(kdrl:Hsa.HRAS-mCherry)<sup>s896</sup>;Tg(cmyb:EGFP)<sup>zf169</sup>*, hereafter *Tg(kdrl:mCherry);(cmyb:EGFP)*. In this transgenic line, HSCs express EGFP, and ECs express mCherry. In the VDA it is possible to detect double positive cells described as the HE. The hemogenic endothelial cells (HECs) are a subset of specialized ECs in the VDA that temporally express both markers (Bertrand et al. 2010). These ECs extrude from the VDA, entering the intervascular region and into the PCV as HSCs (Anderson et al. 2015). To test whether *hif-1α* and the *hif-2α* play a role in HE differentiation, HSC proliferation or HSC emergence from the VDA and EHT I analyzed the dynamics of double positive cells in *hif-1α* and *hif-2α* morphants. I performed time-lapse live imaging of morphants carrying



*Tg(kdrl:mCherry);(cmyb:EGFP)* transgenes and I observed that *hif-1 $\alpha$*  and *hif-2 $\alpha$*  morphants exhibit a reduced number of double-positive cells in the VDA (Figure 17A) compared with control MO-injected embryos, as confirmed by quantification (Figure 17B). The time-lapse imaging (Figure 17A,B), together with the *runx1/cmyb* WISH data (Figure 16B), indicate that both Hif-1 $\alpha$  and Hif-2 $\alpha$  play a fundamental role in EC specialization and HE specification, upstream of HSC emergence.

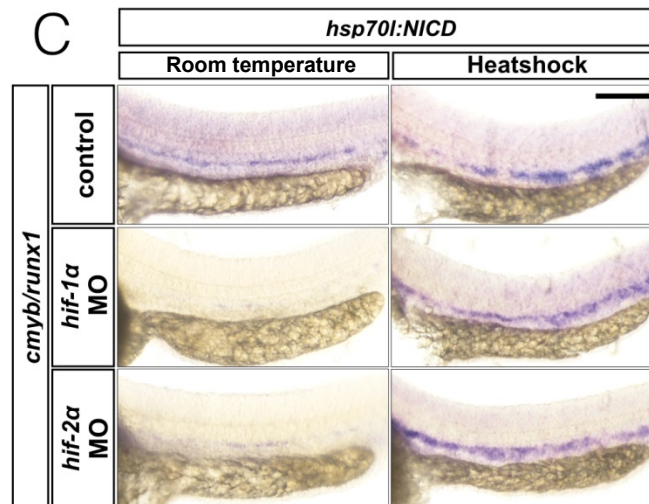
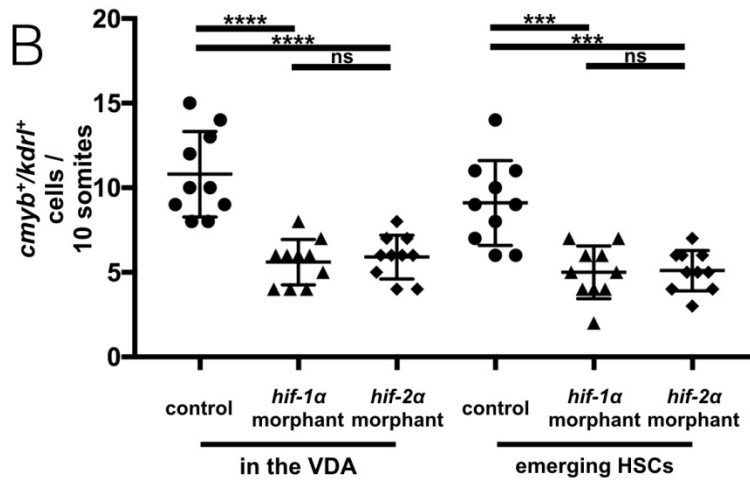
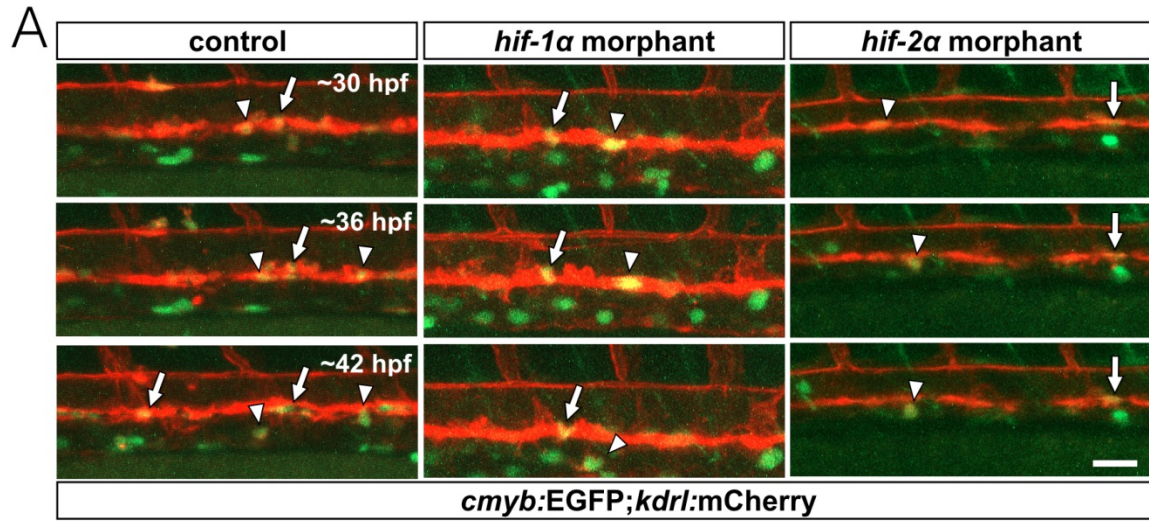


### Figure 17. Hypoxia inducible factors regulate hemogenic endothelial specification

A) Maximal intensity projections of time-lapse confocal images of 36 hpf *Tg(cmyb:EGFP);Tg(kdrl:mCherry)* control, *hif-1α* and *hif-2α* morphants. Arrows point to *cmyb:EGFP+;kdrl:mCherry+* cells in the VDA, and arrowheads point to *cmyb:EGFP+;kdrl:mCherry+* emerging HSCs. Scale bar, 50 μm. B) Quantification of *cmyb:EGFP+;kdrl:mCherry+* cells in the VDA and emerging HSCs in a 10-somite-long trunk region in control, *hif-1α* and *hif-2α* morphants (lateral views). n=10 embryos from 3 different clutches. D) WISH for *cmyb/runx1* expression in 36 hpf *Tg(hsp70l:GAL4;UAS:NICD)* embryos injected with control, *hif-1α* or *hif-2α* MOs kept at 28 °C or after heat shock; lateral views. Scale bar, 100μm.

#### 4.4.5 Notch signaling acts downstream of Hif pathway in HSC development

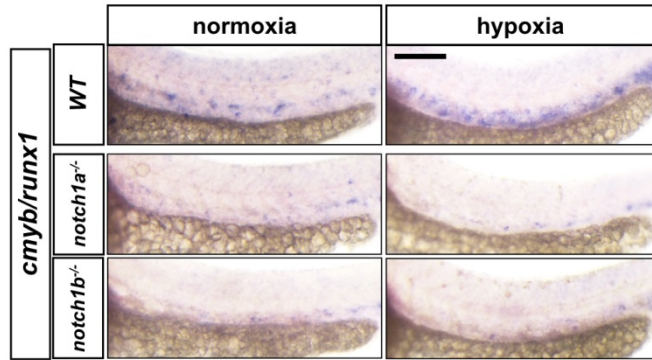
As described in the introduction, Notch1 signaling together with Gata2b are essential for EHT and HSC formation (Butko, Pouget, and Traver 2016). To investigate the genetic hierarchy between Notch and Hif, I performed a series of experiments combining loss-of-function and gain-of-function models for these two pathways. First, I wanted to test if hypoxia could have a direct effect on *notch1a*, *notch1b*, and *gata2b* regulation and found that they were strongly induced after hypoxia exposure compared with sibling embryos kept in normoxic conditions (Figure 16F). I also tested whether *notch1a*, *notch1b*, and *gata2b* mRNA levels were reduced in *hif-1α* and *hif-2α* mutants. *notch1a*, *notch1b*, and *gata2b* were significantly reduced in the mutants, when compared with WT siblings (Figure 16D). These data indicate that Notch is regulated by *hif-1α* and *hif-2α* in zebrafish. To test the relationship of these two pathways in HSC formation, we analyzed *notch1a* and *notch1b* mutants. First, I

performed WISH for *cmyb*, *runx1* and *gata2b* to assess HSC formation in *notch1a* and *notch1b* mutants, recapitulating the reported phenotype of *notch1a* and *notch1b* morphants (Ma and Jiang 2007). The level of EHT and HSC markers was drastically reduced in *notch1a* and *notch1b* mutants when compared with WT siblings (Figure 18A). To test whether hypoxia, through Hifs, requires Notch signaling to promote HSC formation, I exposed to normoxia or hypoxia embryos resulting from *notch1a*<sup>-/-</sup> or *notch1b*<sup>-/-</sup> incrosses and analyzed *runx1/cmyb* expression levels by WISH. WT sibling embryos exposed to hypoxia exhibited an increase in *runx1/cmyb* expression but *notch1*<sup>+/-</sup> or *notch1b*<sup>+/-</sup> embryos did not (Figure 18A). These data show that hypoxia does not promote *runx1* or *cmyb* expression in *notch1a* or *notch1b* mutants and does not rescue the EHT defects seen in the *notch1* loss-of-function models. Taken together, our results indicate that Hif and Notch are part of the same pathway during EHT and HSC formation. To further investigate the molecular hierarchy between Hif and Notch, we tested whether activation of Notch signaling could rescue the defects seen in Hif loss-of-function models. Therefore, I took advantage of a line carrying a transgene to induce the *notch1a* intracellular domain (NICD) in a temporally controlled manner. I used the *Tg(-1.5hsp70l:GAL4)<sup>kca4</sup>*; *(5xUAS-E1b:6xMYC-notch1a)<sup>kca3</sup>* line, hereafter, *Tg(hsp70: GAL4;UAS:NICD)*, to induce NICD expression upon heat shock treatment. To investigate whether NICD overexpression could affect the vascular network, I analyzed *Tg(kdrl:EGFP)* expression in *Tg(hsp70:GAL4;UAS:NICD)* embryos and I did not detect vascular abnormalities after heat shock (Figure 16A). Next, to test whether NICD overexpression could rescue the phenotype of *hif-1α* or *hif-2α* morphants, we

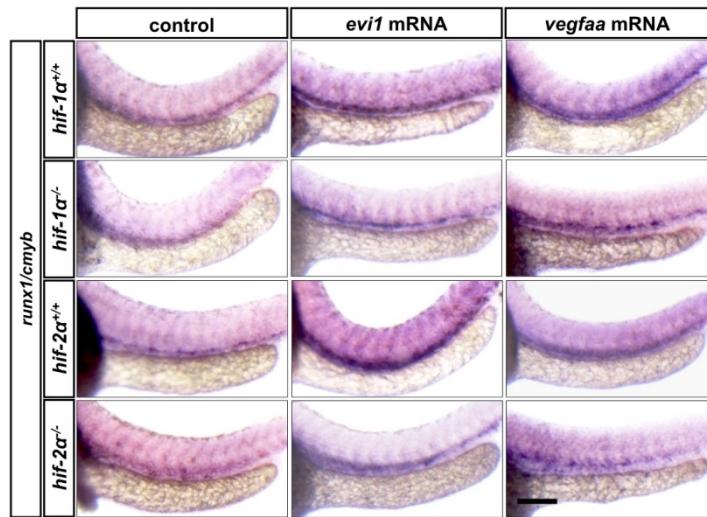
injected the MO in *Tg(hsp70:GAL4;UAS:NICD)* embryos. In *Tg(hsp70:GAL4;UAS:NICD)* embryos, after injection of *hif-1α* or *hif-2α* MOs, we could recover a significant increase of *runx1/cmyb* expression after heat shock and NICD overexpression, rescuing the defects observed in *hif-1α* and *hif-2α* morphants (Figure 17C).

To further understand the molecular link between Hif and Notch signaling, we tested whether the overexpression of *evi1* or *vegfaa* was able to rescue the EHT phenotype observed in *hif-1α* or *hif-2α* mutants. As previously described (Konantz et al. 2016) the overexpression of these genes leads to an increase of *notch1b* expression levels in HE during EHT. The injection of *evi1* or *vegfaa* mRNA in *hif-1α<sup>-/-</sup>* and *hif-2α<sup>-/-</sup>* rescued the HSC phenotype (Figure 18B), as highlighted by the quantification (Figure 18C), suggesting that *evi1* and *vegfaa* function downstream or in parallel to the Hif pathway during HE specification and HSC formation. Taken together, our observations suggest that Notch signaling functions downstream of hypoxia and the Hif pathway during EHT.

**A**



**B**



**C**

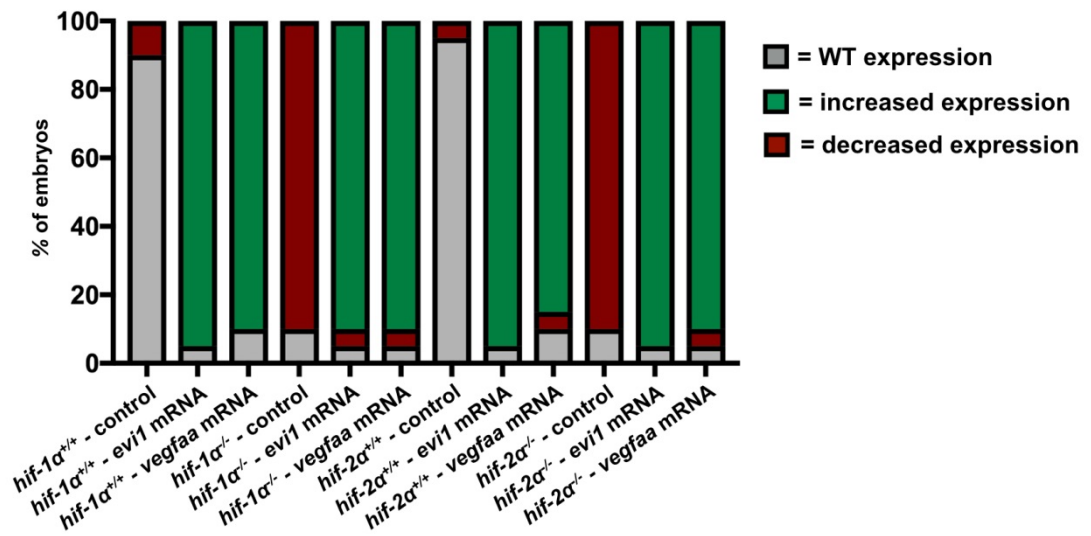


**Figure 18. Hifs act upstream of Notch signaling in HSC development in zebrafish.**

A) WISH for *cmyb/runx1* expression in 36 hpf WT, *notch1a*<sup>-/-</sup> and *notch1b*<sup>-/-</sup> embryos in normoxia and after hypoxia exposure. Scale bar, 100 um. B) WISH for *cmyb/runx1* expression in 36 hpf control WT siblings, *hif-1α*<sup>-/-</sup> and *hif-2α*<sup>-/-</sup> embryos in three different conditions: uninjected and injected with *evi1* or *vegfaa* mRNA; lateral views. Scale bar, 100 um. C) Quantification of *cmyb/runx1* WISH results, showing the percentages of embryos with WT, increased or decreased expression in each condition.

#### **4.4.6 Proposed model**

In the last part of this thesis, I showed that Hifs in zebrafish are involved in definitive hematopoiesis.

1) *hif-1α* and *hif-2α* in zebrafish have a role in EC specialization, specifically in HE specification. The defects seen in HE specification leads to a severe reduction of HSC formation detected in *hif-1α* and *hif-2α* mutants.

2) Hypoxia is a potent inducer of HE and HSC formation, acting via Hifs upstream of Notch1 signaling. *notch1a* and *notch1b* mutants show defect in EHT and the genes are regulated in normoxia and in hypoxia by Hif-1α and Hif-2α.

3) Promoting Notch1 signaling leads to a significant induction of HSC formation and overexpressing NICD could rescue *hif-1α* and *hif-2α* mutant phenotypes.

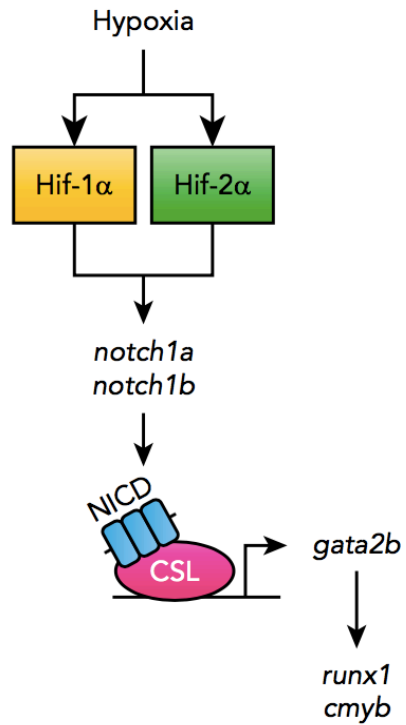


**Figure 19. Model of the HE specification driven by Hifs.**

EC specialization can be promoted by Hifs upstream of Notch1 signaling. Hypoxia is a potent inducer of HE specification and HSC formation.



## 5. DISCUSSION

---

## 5. Discussion

### 5.1 Upstream regulators of *npas4l* and angioblast differentiation

ECs are specialized epithelial cells constituting the luminal side of vessels. The first functional vessels observable in zebrafish are the axial vessels: the dorsal aorta and the cardinal vein. These two vessels are formed at around 18hpf, via a process called vasculogenesis. The precursors of ECs, before to mature and to assemble in a tube-like structure, are called angioblasts. During somitogenesis the progenitors of ECs express high levels of *etv2*, *tal1* and *lmo2*, transcription factors that have been shown to play a role in angioblast differentiation in zebrafish and in mouse (Lee et al. 2008; Craig et al. 2015). Angioblasts migrate from the LPM, where also cardiomyocyte progenitors are found. FGF pathway was shown to play a role in the competition between progenitors of ECs and progenitors of cardiomyocytes; specifically, FGF signaling promotes differentiation and proliferation of cardiomyocytes precursors at the expense of angioblasts (Simoës, Peterkin, and Patient 2011). Nevertheless, the molecular link between FGF and the balance between these two populations has yet to be identified. Recently *npas4l*, a transcription factor involved in angioblast specification was identified, but the regulation of *npas4l* has not been explored. Moreover, *npas4l* mutants exhibit an expansion of cardiomyocytes precursors, and lack angioblasts (Schoenebeck, Keegan, and Yelon 2007), suggesting that *npas4l* may be responsible, at least in part, to coordinate the equilibrium between cardiomyocytes and ECs.

Here I show that FGF signaling is a negative regulator of *npas4l* expression. This observation may explain the data observed by Simões et al. . I described that upon FGFR1 inhibition, *npas4l* expression level increases, and the inhibition of FGF signaling during somitogenesis may lead to a similar effect, thus causing an increment of angioblasts. I confirmed the link between FGF and *npas4l* by activating FGF signaling, using BCI, a *dusp6* inhibitor (Molina et al. 2009) that recently was shown to play a positive role in cardiomyocyte proliferation during heart regeneration (Missinato et al. 2018). Moreover, I showed that *npas4l* expression is enriched in the ventral side of the embryo, and FGF components were shown to be enriched in the dorsal part of the embryo (Furthauer et al. 2004), probably limiting *npas4l* expression to the ventral mesoderm.

BMP signaling is known to promote and to maintain mesoderm specification upstream of transcription factors such as Smad1/5 and Bra (Sharma et al. 2017; Faial et al. 2015). In zebrafish it was shown that by overexpressing a dominant negative version of BMP receptor, it is possible to severely impair hematopoiesis and endothelial cell specification (Pyati, Webb, and Kimelman 2005). Interestingly, this effect could be detected only when the dominant negative receptor was induced during gastrulation, but not during somitogenesis, suggesting that BMP is acting on a transcription factor expressed during an earlier stage, and my data indicate that this effect may be due, at least in part, to a reduction of *npas4l* expression. Previous studies suggested that BMP signaling has a role in regulating *Etv2* expression in mouse, thus promoting angioblast specification in mouse (Lee et al. 2008), and my

results confirm the conserved function of BMP in promoting angioblast differentiation. Moreover, the BMP ligands and receptors, in contrast to FGF components, are enriched in the ventral part of the embryo, the region where *npas4l* is expressed, as I showed by WISH experiments.

Importantly, the identification of *eomesa* as one of the upstream regulators of *npas4l* fits with the *Eomes* mouse mutant phenotype that exhibits a strong reduction in the expression of *Etv2* downstream targets (Costello et al. 2011). EOMES is known for its pleiotropic effect, having a role in endoderm development as well as mesoderm patterning. Interestingly, the specificity of EOMES for certain targets seems to be regulated by the balance between BMP and TGF- $\beta$  that coordinate EOMES in promoting mesodermal and endodermal genes, respectively (Faial et al. 2015).

The conserved function of *Eomes*, promoting EC differentiation in zebrafish and in mouse, may help in finding the missing link between the T-box transcription factor and angioblast specification in mammals. Studies aimed in identifying the molecular cues upstream of *Etv2*, in absence of a mammalian *Npas4l*, would increase our understanding of this fundamental developmental process and will improve the available protocols of EC differentiation for therapeutic purposes.

## 5.2 Identification and characterization of downstream targets of *npas4l*

The bHLH-PAS transcription factor Npas4l was only recently identified, but the *npas4l* mutant was previously described to lack most of hematopoietic and endothelial tissues (Stainier et al. 1995). Although it is considered the master regulator of endothelial cell specification and hematopoiesis, little is known about its direct and indirect targets. The function of *npas4l* is cell autonomous in angioblast, but the cell autonomy relative to hematopoiesis is less clear (Parker and Stainier 1999), suggesting that the regulation of these two cell types by Npas4l follows distinct pathways. As mentioned in the introduction, there are two types of angioblasts, one population is already committed to form the DA and the other one to the PCV (Kohli et al. 2013), but whether *npas4l* is sufficient to induce both populations is not known.

Here, I show that *npas4l* is sufficient to drive endothelial specification as a whole, as seen by transcriptome analysis at 95% epiboly. The transcriptional cascade initiated by *npas4l* is highlighted by the data showing that Npas4l has the potential to induce *tal1*, *etv2* and *lmo2* before the onset of gastrulation, suggesting that these three transcription factors are direct downstream targets of Npas4l. The endothelial markers seen at 95% epiboly are likely a result of a combinatorial effect of *tal1*, *etv2* and *lmo2*. In fact we can see a strong overlap between the genes upregulated after *npas4l* and *etv2* overexpression (Wong et al. 2009). I showed, using ChIP-seq, that the three transcription factors are indeed direct targets of Npas4l. Although data

regarding Etv2 ChIP are not available, we speculate that *etv2*, *lmo2* and *tal1* are linked by a positive feedback loop, and are directly responsible for the expression of the endothelial markers detected at 95%, downstream to *Npas4l*. The strong phenotype observed in *npas4l* is likely due to the fact that this bHLH-PAS protein acts as a master regulator gene, directly promoting three transcription factors with overlapping functions. The zebrafish single mutants for *etv2*, *tal1* and *lmo2* do not show a phenotype as severe as *npas4l* loss-of-function model (Schumacher et al. 2013; Craig et al. 2015; Weiss et al. 2012) but I speculate that the triple mutant will phenocopy *cloche* mutant. Another transcription factor with a role in endothelial cell specification is *fli1*. Previous reports showed that *fli1* expression is not affected early on in *cloche* mutant (Brown et al. 2000), and it was speculated to act upstream of *npas4l*. However, *fli1* is expressed temporally after *npas4l*, thus this hypothesis is unlikely. On the other hand, *fli1* is not induced early on by *npas4l* and the mutant does not show reduction of *fli1a* nor *fli1b* expression at 6 somite stage. Taken together, these data suggest that the physiological *fli1* expression is independent of *npas4l* and these two transcription factors may act in parallel, but *fli1* does not have the ability to compensate for the lack of *npas4l* in physiological or in an overexpression scenario (Liu et al. 2008).

*npas4l* mutant lacks hematopoietic and endothelial tissues. Notably, I could not detect blood markers to be directly regulated by *npas4l*, suggesting that this transcription factor is necessary for blood development, but not sufficient. This observation may be fundamental in understanding how primitive blood is formed in zebrafish embryo. As I mentioned in the introduction, one of the model for primitive

hematopoiesis describe the hemangioblast as a bipotent progenitor and *npas4l* as the main responsible for the transition from mesodermal cells to hemangioblasts. If this model was correct the most likely scenario would be to see both endothelial and blood markers being induced by *npas4l* overexpression. Probably *npas4l* expression has to be transitory in order for blood markers to appear, and in an overexpression scenario this condition can be achieved only later during development. A model where *npas4l* expression is actively downregulated in cells primed to become blood would fit the HE hypothesis during gastrulation, as suggested by Torres lab. (Padron-Barthe et al. 2014), and a persistent expression of *npas4l* would maintain the endothelial identity of the hypothetical HE. Interestingly, considering the previous observations performed by Parker and Stainier (Parker and Stainier 1999), angioblasts themselves could be responsible to induce another population of precursors of blood cells, expressing low or no levels of *npas4l*, in a cell non-autonomous fashion. If the latter model was the prominent mechanism of primitive hematopoiesis, it would be of great interest to identify the proteins, such as ligands or receptors that could influence cell-fate determination of surrounding cells, acting downstream of Npas4l.

The identification of *tspan18b* as a novel regulator of angiogenesis confirms the reliability of our data, and our combined analysis will be hopefully used in the future to identify new molecular players involved in hematopoiesis or endothelial cell specification and function, not only in zebrafish, but also in higher vertebrates.

### **5.3 Identification of a functional ortholog of *npas4l* in mammals: role of HIFs in endothelial cell differentiation**

*npas4l* is the master regulator of endothelial specification in zebrafish, but this gene was lost during evolution in mammals (Reischauer et al. 2016). Importantly, vessels and ECs are morphologically and functionally similar across vertebrates, and it is puzzling how mammals evolved another mechanism to promote the transition from multipotent mesodermal cells to *Etv2*-positive angioblasts, without *npas4l*. *Etv2*, as described in the introduction, is conserved in all vertebrates, and in human, mouse and zebrafish, it was shown to play a role in endothelial cell differentiation (Craig et al. 2015; Lee et al. 2008; Cheng et al. 2017). To know how *Etv2* is regulated in mammals would have an enormous impact in the generation of ECs starting from differentiated cells (Ginsberg et al. 2012).

To address this question, we took advantage of an assay I designed. As aforementioned, *eomesa* has the ability to induce *npas4l* *in vivo*. Importantly, its mammalian counterpart *Eomes* has a role in endothelial cell differentiation, *in vivo* (Costello et al. 2011) and *in vitro* (Figure 8 F,G).

Knockdown of *Eomes* led to *Etv2* downregulation *in vitro*, and, importantly, of *Hif-1 $\alpha$* . Moreover, in human stem cells, ChIP-seq experiments show that *Eomes* can bind to *Hif-1 $\alpha$*  locus (Tsankov et al. 2015). *Eomes* may indeed act upstream of *Hif-1 $\alpha$* , but it is not known if the phenotype exhibited by *Eomes* mutant is related to *Hif-1 $\alpha$*  function. Interestingly, it was recently found that *Hif-1 $\alpha$*  can bind the promoter of *Etv2* in embryonic stem cells (Tsang et al. 2017), similarly to what I showed for *Npas4l*.



Moreover Hypoxia, via *Hif-1 $\alpha$* , is sufficient to induce endothelial cell specification *in vitro* (Tsang et al. 2017). Our *in vivo* data suggest indeed that HIF-1 $\alpha$ , analogously to Npas4l, is responsible to promote *Etv2* expression during early stages of development suggesting that, during evolution, *Hif-1 $\alpha$*  acquired new features and took over *npas4l* function. The HIFs are structurally similar to Npas4l, but, in contrast with Npas4l, are conserved across all vertebrates, despite strong differences in terms of oxygen availability during embryogenesis. Zebrafish *npas4l* mutant, although it lacks blood vessels, develops until 5 dpf, acquiring oxygen from the environment through diffusion. Interestingly most organs, including a beating heart, are formed even in absence of the vasculature (Stainier et al. 1995). Mouse *Etv2* and *Vegf-a* mutants, however, die *in utero* at around E9.5 (Lee et al. 2008; Ferrara et al. 1996). This striking difference between zebrafish and mouse embryonic development is likely due to the different environment of the growing embryos. Development is external in non-mammalian vertebrates; in contrast, mammals develop inside the body of the mother, making the oxygen supply via blood vessels a necessary condition to sustain the embryo's growth in the first stages of development. This major difference in terms of oxygen availability played a crucial role in evolution, and during this process *Hif-1 $\alpha$*  may have acquired new features. The divergence of *Hif-1 $\alpha$*  function is emphasized by the differences between the mouse *Hif-1 $\alpha$*  mutant, that show defects in early vascular development (Ryan, Lo, and Johnson 1998) and the zebrafish *hif-1 $\alpha$*  mutant, that exhibits impaired endothelial cell specialization and HSCs formation, with normal vasculogenesis and angiogenesis (Figure 16 A,B).

## 5.4 Role of Hifs in endothelial cell specialization in zebrafish

The differentiation of many cell types from induced or native pluripotent stem cells has been obtained *in vitro* by promoting the expression of transcription factors or by treating multipotent cells with growth factors (Harding et al. 2017). Importantly, many morphogens used to induce cell specification *in vitro* were first identified studying embryonic development. In the case of HSCs, many groups have tried to optimize protocols to produce reliable and graftable HSCs *in vitro* but have not yet reported long-term engraftments in mouse adults. Rafii laboratory described a method to directly reprogram adult ECs to HSCs, by overexpressing transcription factors such as *Etv2* and *Fli1*, in combination with angiocrine signals (Lis et al. 2017). To better understand all the players involved in physiological hematopoiesis and how intrinsic and extrinsic factors are orchestrated during HE differentiation and HSCs extrusion could have a significant impact on the generation of therapy-grade HSCs. Here, using a genetic *in vivo* model in zebrafish, I describe a role of the Hif pathway acting upstream of Notch signaling during EHT.

Importantly, my work highlights a major difference in terms of Hif function during mouse and zebrafish development. I found that the role of Hifs is related to ECs in both species: in mouse they are instrumental for endothelial cell specification or proliferation but in zebrafish Hifs are mainly responsible for EC specialization, inducing HE specification. Moreover, with this work, I compared previous report on the effect DMOG, a compound used to induce Hif-1 $\alpha$  stability with actual hypoxia,

lowering the O<sub>2</sub> concentration of the environment to 3%, avoiding possible aspecific effects of DMOG. Interestingly, a recent study showed that, in mouse, aortic hemogenic ECs (HECs) are indeed hypoxic before to extrude and become HSCs (Imanirad et al. 2014).

The Hif-1 $\alpha$  pathway has been suggested to regulate HSC formation, taking advantage of morphant phenotypes (Harris et al. 2013). Recently, with the rise of CRISPR/Cas9 technology to induce loss-of-function mutation, the scientific community observed discrepancies between morphants and mutants phenotypes (Kok et al. 2015). Although MO is a very useful tool to study gene function, it is pivotal to validate the morphant phenotypes before to use it as reliable representation of a loss-of-function model. Here, I showed that *hif-1 $\alpha$*  and *hif-2 $\alpha$*  morphants phenocopy *hif-1 $\alpha$*  and *hif-2 $\alpha$*  mutants. Importantly, by using time-lapse confocal microscopy, I described that a diminished number of HECs in the VDA is the cause of the HSC defects in *hif-1 $\alpha$ <sup>-/-</sup>* and *hif-2 $\alpha$ <sup>-/-</sup>*.

HIF is known to interact with several signaling pathways, including TGF $\beta$ , VEGF and Notch (Mukherjee et al. 2011; McMahon et al. 2006; Lin et al. 2004). Here, my results suggest that Hif and Notch are part of the same pathway during HSC formation. Specifically, NICD, as well as *evi1* and *vegfaa* could rescue the HSC defects observed in *hif-1 $\alpha$*  and *hif-2 $\alpha$*  mutants, suggesting that Hif functions upstream of Notch signaling. Previous reports showed that the link between Notch and Hif pathways is context specific, especially in development processes such as vasculogenesis, angiogenesis and arterial specification (Kume 2010).

My study describes the relationship between Hif and Notch pathway during HE specification. These observations will help in understanding better the importance of the microenvironment and the vascular niche in the formation of HSCs, with a possible impact in the optimization of protocols aimed to produce reliable HSCs *in vitro* for therapeutic purposes.

# 6. CONCLUSIONS

---

After the recent identification of the master regulator of endothelial cell specification in zebrafish, I investigated the molecular mechanisms involved in *npas4l* function, analyzing its upstream regulators as well as its downstream targets. In order to identify the mammalian functional ortholog of *npas4l*, I studied the role of Hifs in both mouse and zebrafish embryonic development.

### **AIM1. Upstream regulators of *npas4l* and angioblast differentiation**

I reported the signaling pathways and the transcription factors involved in *npas4l* regulation during gastrulation. Specifically, BMP signaling, active in the ventral region of the embryo, promotes *npas4l* expression, in contrast, FGF pathway limits *npas4l* expression. In addition, FGF-Erk signaling negatively regulates *eomesa* expression, a transcription factor able to potently induce *npas4l* transcription. Importantly, by using an *in vitro* assay, I confirmed that *Eomes* acts upstream of angioblast markers such as *Tal1* and *Etv2* also in mammalian cells.

### **AIM2. Identification and characterization of downstream targets of *npas4l***

Using complementary approaches such as transcriptome analyses, epigenome analyses and chromatin immunoprecipitation I identified direct as well as secondary targets of Npas4l. Specifically, microarray and RNA-Seq were used to study the differential expression of genes downstream to *npas4l* in loss-of-function as well as gain-of-function models. Chromatin immunoprecipitation, followed by sequencing, was used to identify the binding motif of Npas4l and its direct targets, whose

promoter physically interacts with Npas4l protein. A combined analysis revealed *tspan18b* to be a potential novel gene with a role in vascular development. Taking advantage of CRISPR/Cas9 technology, I found that *tspan18b* is involved in angiogenesis.

### **AIM3. Identification of a functional ortholog of *npas4l* in mammals: role of HIFs in endothelial cell differentiation**

I reported that *Eomesa* has the potential to induce *npas4l* in zebrafish and I found that murine *Eomes* acts upstream of *Hif-1 $\alpha$*  and *Etv2* in mammalian cells. Previous reports demonstrated that HIF-1 $\alpha$  binds to *Etv2* promoter in embryonic stem cells. In order to test *Hif-1 $\alpha$*  function *in vivo*, I used a genetic loss-of-function model for *Hif-1 $\alpha$*  and I found a significant reduction of *Etv2* expression in *Hif-1 $\alpha$*  mutant embryos. Since the angioblast marker *etv2* is absent in zebrafish *npas4l* mutant, these data suggest that HIF-1 $\alpha$  acquired some novel features during evolution of mammals and took over Npas4l function in the mammalian lineage.

### **AIM4. Role of Hifs in endothelial cell specialization in zebrafish**

I analyzed the phenotype of *hif-1 $\alpha$*  and *hif-2 $\alpha$*  mutants in zebrafish, without observing defects in angioblast differentiation and early vasculature patterning formation, in strong contrast with the phenotype observed in mouse mutants. I recovered a significant reduction of HSC markers in the ventral wall of the dorsal aorta in *hif-1 $\alpha$*  and *hif-2 $\alpha$*  mutants. Using timelapse live imaging, I observed a reduction in the hemogenic endothelial population, a type of specialized ECs that will give rise to

HSCs. Importantly, hypoxia could induce the emergence of HSCs, via Hif-1 $\alpha$  and Hif-2 $\alpha$ , upstream of Notch signaling. These observations indicate that, in zebrafish, Hif-1 $\alpha$  and Hif-2 $\alpha$  are involved in endothelial cell specialization and heterogeneity, but not in endothelial cell differentiation.



# I. Zusammenfassung

---

## Einleitung

Das Herz-Kreislauf-System ist eines der ersten Gewebe, das sich im Wirbeltierembryo entwickelt und ist essentiell für die Beseitigung von Abfallprodukten und die Lieferung von Sauerstoff und Nährstoffen für die wachsende Organe. Gefäße bestehen aus 3 Schichten: Tunica Intima, Tunica Media und Tunica Adventitia. Die innerste Schicht, die Tunica Intima, wird von Endothelzellen (ECs) gebildet, einer bestimmten Art von Epithel, das die luminaire Seite von Gefäßen auskleidet.

Das Herz-Kreislauf-System besteht aus einem Netzwerk von Gefäßen, durch das das Blut in einem geschlossenen Kreislauf fließt, der durch das Herz angetrieben wird. Das Endothelium ist an einer Fülle von biologischen Prozessen, wie der Kontrolle der Vasokonstriktion und Vasodilatation und Modulieren der Gefäßpermeabilität und Homeostase.

Um zu verstehen, wie Gefäße funktionieren, ist es wichtig, zunächst die molekularen Mechanismen zu verstehen, die der Differenzierung, Spezialisierung und dem Wachstum von Endothelzellen zugrunde liegen.

Der erste Schritt der vaskulären Entwicklung wird Vaskulogenese genannt. Dieser Term beschreibt die Neubildung von Gefäßen. Der Prozess beginnt damit, dass sich mesodermale Zellen an der ventralen Seite des Embryos zu Angioblasten spezifizieren, den Vorläufern von Endothelzellen. Die Angioblasten migrieren im anterior lateral plate Mesoderm in Richtung der Mittellinie, wo sie zur dorsalen Aorta und die Kardinalvene verschmelzen. In späteren Stadien kommt es auch zur Gefäßbildung durch Angiogenese. Während dieses Ereignisses sprießen

Endothelzellen von bereits existierenden Gefäßen um ein komplexes Gefäßnetzwerk zu bilden. In vielen vaskulären Nischen durchlaufen die Endothelzellen einen Differenzierungsprozess, der die morphologische und funktionelle Heterogenität des Endothelium definiert. Das hämogene Endothel stellt ein spezialisiertes Endothel mit einzigartigen Eigenschaften dar. Eine Untergruppe von Endothelzellen in der ventralen Wand der dorsalen Aorta spezifizieren sich zu hämogenen Endothelzellen, die aus der luminalen Schicht der Blutgefäße austreten und als hämatopoetische Stammzellen (HSC) in den Kreislauf gelangen.

Während der Embryogenese erfolgt die Hämatopoese in zwei verschiedenen Wellen, der primitiven und der definitiven. In Bezug auf das primitive Blut wurden viele Modelle in der Literatur beschrieben, die dessen Entwicklung zu erklären versuchen, z.B. die Anwesenheit eines bipotenten Vorläufers für Endothelzellen und Erythrozyten oder einer endothelial-zu-hämatopoetischen Transdifferenzierung während der frühen Embryogenese. In der definitiven Welle werden HSCs aus dem Hämogenen Endothel in der ventralen Wand der dorsalen Aorta gebildet.

Viele Fragen bezüglich der transkriptionellen Wellen upstream der Angioblast Spezifikation sind noch offen. Die Identität von *cloche*, einem Gen, das für die Differenzierung von Endothelzellen im Zebrafisch notwendig ist, wurde erst kürzlich von unserer Gruppe entdeckt. Nur sehr wenig ist über seine vorgeschalteten Regulatoren oder seine molekularen Wirkungsmechanismen bekannt.

In dieser Arbeit werde ich die Akteure beschreiben, die an der Regulation der Expression von *npas4l* beteiligt sind, sowie seine direkten und indirekten

Downstream-Effektoren. Darüber hinaus, angesichts der Tatsache, dass *npas4l* im Säugetiergenom nicht vorhanden ist, werde ich ein Modell vorschlagen, dass Hif1-a als sein funktionelles Homolog in Säugetieren beschreibt. Ich werde den Phänotyp der Hif - Maus - Mutante und die Zebrafisch - Hif – Mutante vergleichen, und zwar in Hinblick auf die Bedeutung von Hypoxie- induzierbaren Faktoren für die Spezialisierung endothelialer Zellen während HSC Entwicklung in Zebrafisch und für die Spezifikation von Endothelzellen in der Maus.

### **Upstream-Regulatoren der Differenzierung von *npas4l* und Angioblasten**

Zunächst habe ich die spatiotemporale Expression von *npas4l* während der frühen Embryogenese untersucht. Die Expression von *npas4l* erhöht sich während der Gastrulation, und nimmt 24 hpf drastisch ab. Ich fand *npas4l* mRNA in der ventralen Seite der Embryo bereits bei 50% Epibolie. *npas4l* Expression ist auf wenige Zellen im ventralen Mesoderm begrenzt und erscheint stärker bei 80% Epibolie, übereinstimmend mit dem qPCR Daten. Andere gut beschriebene Angioblastenmarker erscheinen nach der Gastrulation, zu Beginn der Somitogenese, was *npas4l* dem frühesten bisher bekannten Marker für endotheliale Vorläuferzellen macht.

Um zu verstehen, welche Signalwege in der *npas4l* - Regulation involviert sind, habe ich einen Wirkstoff screening-Assay durchgeführt , bei dem Embryonen während eines bestimmten Zeitfensters behandelt werden, von 50% epibolisch zu tailbud.

Dieses Experiment legte nahe, dass der FGF-Signalweg ein negativer Regulator von *npas4l* ist, und BMP ein positiver Regulator. Darüber hinaus induzierte ich die Überexpression von *bmp2b* selektiv zu Beginn der Gastrulation, wobei ich eine signifikante Zunahme der *npas4l* Expression feststellte. Um die Transkriptionsfaktoren zu identifizieren, die in der *npas4l* Regulierung involviert sind, führte ich ein Transkriptomik Experiment, durch, in Kombination mit einer in silico Analyse des *npas4l* Promotors. Ich identifizierte *eomesa* als einen möglichen Regulator von *npas4l* in vivo. Interessanterweise war eine Überexpression von *eomesa* ausreichend um *npas4l* ektopisch zu induzieren. Schließlich, um die Funktion von *eomes* in Mauszellen zu testen, führte ich Knockdown- und Überexpressionsexperimente durch und ich fand, dass der T-Box Transkriptionsfaktor upstream von *Etv2* und *Tal1* wirkt. Diese Daten deuten darauf hin, dass es einen konservierten Pathway für die Angioblastendifferenzierung zwischen Zebrafisch und Maus gibt, auch in Abwesenheit von *npas4l*.

### **Identifizierung und Charakterisierung von Downstream targets von *npas4l***

Um die Downstream - Effektoren von *npas4l* zu identifizieren, haben wir eine Serie von komplementären Experimenten durchgeführt, einschließlich Transkriptom - und Epigenomanalysen von gain of function and loss of function Modellen von *npas4l*.

Zunächst überexprimierte ich *npas4l* im Einzellstadium und sammelte Embryonen bei 30% und 95% Epibolie, mit dem Ziel, direkte Ziele zu identifizieren, die wahrscheinlich bei 30% Epibolie induziert werden, und sekundäre Ziele, die durch *npas4l* nachgeschaltete Effektoren bei 95% Epibolie induziert werden.

Ich konnte bestätigen, dass die Überexpression von *npas4l* ausreicht, um Endothelzellspezifikation als Ganzes generell bei 95% Epiboly zu induzieren. Allerdings kam es nicht zur Induktion von primitiven hämatopoetischen Marker wie *runx1*, *gfi1aa* und *gata1a*. Als nächstes führte ich ein ChIPSeq durch um die direkte Beziehung zwischen *npas4l* und seinen potentiellen direkten/primären Targetgenen zu bestätigen.

Ich konnte das Bindungsmotiv von Npas4l mit einer de-novo Vorhersage-Software extrapolieren und stellte fest, dass es den Promotor von *etv2*, *tal1* und *lmo2* physikalisch bindet. *etv2*, *tal1* und *lmo2* hatte ich zuvor als Transkriptionsfaktoren identifiziert, die durch *npas4l*-Überexpression bei 30% Epibolie induziert wurden. Als dritten Ansatz analysierte ich das Transkriptionsprofil der *npas4l* Mutante im 6-Somit-Stadium und bestätigte die Notwendigkeit dieses Transkriptionsfaktors für die Initiierung von endothelialen und hämatopoetischen Programmen. Tatsächlich waren *etv2*, *tal1* und *lmo2* in dieser Mutante herunterreguliert. Dies bestätigt ein Modell, in dem *npas4l* diese konservierten Transkriptionsfaktoren direkt reguliert, und dadurch die Angioblastendifferenzierung fördert.

Ich kombinierte die Datensätze in einer Kreuzanalyse und identifizierte potentielle bisher unbekannte Zielgene, die an der Endothelzellefunktion beteiligt sind. Um diese Hypothese zu testen, generierte ich eine Mutante für einen der vielversprechenden Kandidaten, *tspan18b*. Mutante *tspan18b* Embryonen für zeigten Defekte in der Angiogenese bei 48 hpf. Die kombinierte Analyse der generierten Datensätze stellt eine Plattform dar, die helfen kann potentielle bisher unbekannte coding und non-

coding Gene in der Entwicklung des vaskulären Systems der Vertebraten zu identifizieren.

### **Identifizierung eines funktionellen Orthologs von *npas4l* in Säugetieren: Rolle von HIFs in der Endothelzeldifferenzierung**

Im ersten Ziel dieser Arbeit habe ich beschrieben, dass *Eomes* ausreichend und notwendig für die *Etv2*- und *Tal1*-Expression in pluripotenten Mauszellen ist. Darüber hinaus habe ich gezeigt, dass *eomesa* im Zebrafisch die Expression von *npas4l* induzieren kann und dass *npas4l* *etv2* und *tal1* direkt reguliert. Da das Säugetiergenom kein Ortholog von *npas4l* mit einer bekannten Rolle in der Angioblast Spezifikation aufweist, stellte ich die Hypothese auf, dass ein anderer Transkriptionsfaktor die Rolle von *npas4l* während der Evolution übernommen hat. Um diese Hypothese zu testen, verwendete ich ein Funktionsverlustmodell für *Eomes* und ich fand heraus, dass HIF1- $\alpha$ , ein Transkriptionsfaktor, der zu der gleichen Proteinfamilie wie *npas4l* gehört, nach einem Knockdown von *Eomes* in Säugetierzellen deutlich herunterreguliert ist. Um die Funktion von Hif1-a in vivo zu untersuchen, verwendete ich ein Funktionsverlustmodell für *Hif1- $\alpha$* , bei denen ich eine signifikante Reduktion von *Etv2* in *Hif1- $\alpha$*  mutierte Embryonen im Vergleich zu WT-Geschwistern beobachtete. Diese Daten deuten darauf hin, dass während der Evolution *npas4l* in der Säugetierlinie verloren ging und HIF1- $\alpha$  neue Funktionen übernahm, in dem es die Funktion von *Npas4l* - Funktion ersetzte, und dadurch die Differenzierung von Endothelzellen zu fördern.

## Die Rolle von Hifs bei der Endothelzell-Spezialisierung im Zebrafisch

Um die Rolle von *hif-1α* und seinem Paralog *hif-2α* in der vaskulären Entwicklung von Zebrafischen zu testen, analysierte ich den Phänotyp von *hif-1aa;hif1-ab* Doppelmutanten (*hif-1α<sup>-/-</sup>*) and *hif-2aa;hif2-ab* Doppelmutanten (*hif-2α<sup>-/-</sup>*). Interessanterweise weisen Embryonen, denen *hif-1α* or *hif-2α* fehlt, keine Defekte in Vaskulogenese und Angiogenese auf, im Gegensatz zu dem in dem in den Hif1-a-mutanten Mäusen observierten Phänotyp. Ich habe gezeigt, dass *hif-1α* und *hif-2α* eine Rolle in der Endothelzell-Spezialisierung im Zebrafisch spielen, speziell in der Spezifikation des hämogenen Endothels. Ich habe die Rolle von *hif-1α* und *hif-2α* Mutanten in der definitiven Hämatopoese und fand heraus, dass die HSC – Marker *runx1* und *cmyb* in den Mutanten im Vergleich zu den WT-Geschwistern signifikant herunterreguliert. Mit Hilfe von Time lapse imaging von *hif-1α* und *hif-2α* morphants konnte eine signifikante Reduktion von hämogenen Endothelzellen in der VDA festgestellt werden, die notwendig für die Bildung von HSCs sind. Um den molekularen Link zwischen Hifs und definitiver Hämatopoese zu untersuchen, kombinierte ich gain of function und loss of function Modelle, und konnte zeigen, dass *hif-1α* und *hif-2α* upstream von *notch1*, *vegfaa*, und *evi1* wirken, Gene, die schon für Ihre Rolle in der Entwicklung von HSCs bekannt waren.



## II. English Summary

---

# **Role of *npas4l* and Hif pathway in endothelial cell specification and specialization in vertebrates**

## **Introduction**

The cardiovascular system is one of the first tissues to develop in the vertebrate embryo and it is critical for the removal of waste products and the delivery of oxygen and nutrients to the growing and mature organs. Vessels are constituted by three layers: *tunica intima*, *tunica media* and *tunica adventitia*. The most inner layer, the *tunica intima*, is formed by ECs (ECs), a specific type of epithelium covering the luminal side of vessels.

The cardiovascular system consists of a network of vessels where blood flows in a closed circuit, pumped by the heart. Endothelium is involved in a plethora of biological processes such as controlling vasoconstriction and vasodilatation, modulating vessel permeability and hemostasis.

To understand how vessels are formed, it is critical to understand the molecular mechanisms underlying endothelial cell differentiation, specialization and growth.

The first step of vascular development is called vasculogenesis, the process of *de novo* vessel formation. Initially, mesodermal cells in the ventral side of the embryo specify into angioblasts, the precursors of ECs. Angioblasts migrate from the lateral plate mesoderm towards the midline, where they coalesce to form the dorsal aorta and cardinal vein. At later stages, vessels form also via the angiogenic process. During this event, ECs sprout from pre-existing vessels, forming a complex vascular network.

In many vascular niches, the ECs undergo a differentiation process, that define the morphological and functional heterogeneity of the endothelium. The HE represents a specialized endothelium with unique features. A subset of ECs in the ventral wall of the dorsal aorta specify to become HECs, that extrude from the luminal layer of blood vessels and enter the circulation as HSCs (HSCs).

During embryogenesis, hematopoiesis occurs in two different waves, primitive and definitive. Regarding the primitive blood, many models were described in the literature to explain its development, e.g. the presence of a bipotent progenitor for ECs and erythrocytes or an endothelial-to-hematopoietic transition during early embryogenesis. In the definitive wave, HSCs are formed from the HE in the ventral wall of the dorsal aorta.

Many questions are still open regarding the transcriptional waves upstream of angioblast specification. The identity of *cloche*, a gene necessary for endothelial cell differentiation in zebrafish was only recently discovered by our group, and very little is known about its upstream regulators or its molecular mechanism of action. In my thesis, I will describe the players involved in regulating *npas4l* expression and its direct and indirect downstream effectors. Moreover, as *npas4l* is not present in the mammalian genome, I will propose a model for Hif1- $\alpha$  as its possible functional homolog in mammals. I will compare the phenotype of *Hif* mouse mutant and zebrafish *hif* mutant, focusing on the importance of hypoxia inducible factors in endothelial cell specialization during HSC development in zebrafish and in endothelial cell specification in mouse.

## Upstream regulators of *npas4l* and angioblast differentiation

At first instance, I investigated the spatiotemporal expression of *npas4l* during early embryogenesis. The expression of *npas4l* increases during gastrulation, and drastically decreases by 24 hpf. I detected *npas4l* mRNA in the ventral side of the embryo as early as 50% epiboly. *npas4l* expression is restricted to few cells in the ventral mesoderm and appears stronger at 80% epiboly, concordantly to the qPCR data. Other well-described angioblast markers appear after the end of the gastrulation stage, at the onset of somitogenesis, thus making *npas4l* the earliest marker for endothelial cell precursors known so far. To understand the signaling pathways involved in *npas4l* regulation, I performed a drug screening assay, treating embryos during a specific time window, from 50% epiboly to tailbud. This experiment suggested that FGF signaling is a negative regulator of *npas4l* and BMP a positive one. Moreover, I induced the overexpression of *bmp2b* selectively at the onset of gastrulation, detecting a significant increase in *npas4l* expression. In order to understand the transcription factors implicated in *npas4l* regulation, I performed a transcriptomic experiment, combined with the *in silico* analysis of *npas4l* promoter. I found *eomesa* to be a possible candidate to regulate *npas4l* *in vivo*. Interestingly, when overexpressed, *eomesa* was sufficient to ectopically induce *npas4l* expression. Finally, to test *Eomes* function in mouse cells, I performed knockdown and overexpression experiments and I found that the T-box transcription factor acts upstream of *Etv2* and *Tal1*. These data suggest the existence of a conserved pathway for angioblast differentiation between zebrafish and mouse, even in absence of *npas4l*.

## Identification and characterization of downstream targets of *npas4l*

In order to identify the downstream effectors of *npas4l*, we performed a series of complementary experiments, including transcriptomic and epigenomic analyses of gain-of-function and loss-of-function models for *npas4l*. Firstly, I overexpressed *npas4l* at one cell stage and I collected the embryos at 30% and 95% epiboly, with the aim to identify direct targets, likely induced at 30% epiboly, and secondary targets, induced by downstream effectors of *npas4l* at 95% epiboly. I confirmed that *npas4l* overexpression is sufficient to induce endothelial cell specification at 95% epiboly as a whole, but I did not detect the induction of primitive hematopoietic markers, such as *runx1*, *gfi1aa* and *gata1*. Next, I performed a ChIP-Seq experiment to confirm the direct relation between *npas4l* and the putative primary targets identified. I could extrapolate the binding motif of Npas4l using a *de novo* prediction software and found that it physically binds the promoter of *etv2*, *tal1* and *lmo2*, three transcription factors induced by *npas4l* overexpression at 30% epiboly. As third approach, I analysed the transcriptomic profile of *npas4l* mutant at 6-somite stage and confirmed the necessity of this transcription factor to initiate endothelial and hematopoietic programs. Importantly, *etv2*, *tal1* and *lmo2* were downregulated, reinforcing a model where *npas4l* directly regulates these conserved transcription factors, promoting angioblast differentiation. I combined the datasets together performing a cross-analysis of the results obtained and I identified putative novel target genes involved in endothelial cell function. To test this hypothesis, I generated a mutant for one of the most promising candidate, *tspan18b*. Mutant embryos for *tspan18b* exhibited defects in angiogenesis at 48 hpf. The combined

analysis of the generated datasets represents a resource that potentially includes novel coding and non-coding genes involved in vertebrate vascular development.

### **Identification of a functional ortholog of *npas4l* in mammals: role of HIFs in endothelial cell differentiation**

In the first aim of this thesis, I described that *Eomes* is sufficient and necessary for *Etv2* and *Tal1* expression in mouse pluripotent cells. In addition, I demonstrated that in zebrafish *eomesa* can induce *npas4l* expression and that Npas4l directly regulates *etv2* and *tal1*. Since the mammalian genome does not have an ortholog of *npas4l* with a known function in angioblast specification, I hypothesized that another transcription factor may have substitute the role of *npas4l* during evolution. To test this hypothesis, I used a loss-of-function model for *Eomes* and I found HIF1- $\alpha$ , a transcription factor belonging to the same protein family of *npas4l*, to be significantly downregulated after *Eomes* knockdown in mammalian cells. In order to study the function of *Hif1- $\alpha$*  *in vivo*, I used a genetic loss-of-function model of *Hif1- $\alpha$*  and I detected a significant reduction of *Etv2* in *Hif1- $\alpha$*  mutant embryos, when compared with WT siblings. These data suggest that, during evolution, *npas4l* was lost in the mammalian lineage and HIF1- $\alpha$  acquired new features, replacing Npas4l function, to promote endothelial cell differentiation in mammals.

### **Role of Hifs in endothelial cell specialization in zebrafish**

To test the role of *hif-1 $\alpha$*  and its paralog *hif-2 $\alpha$*  in zebrafish vascular development, I analysed the phenotype of *hif-1aa;hif1-ab* double mutants (*hif-1 $\alpha$* <sup>-/-</sup>) and *hif-2aa;hif2-ab* double mutants (*hif-2 $\alpha$* <sup>-/-</sup>). Interestingly, embryos lacking *hif-1 $\alpha$*  or *hif-2 $\alpha$*  do not

exhibit defects in vasculogenesis and angiogenesis, in contrast with the phenotype observed in mouse *Hif1- $\alpha$*  mutants. I demonstrated that *hif-1 $\alpha$*  and *hif-2 $\alpha$*  have a role in endothelial cell specialization in zebrafish, specifically in HE specification. I explored the role of *hif-1 $\alpha$*  and *hif-2 $\alpha$*  in definitive hematopoiesis and found that the HSCs markers, *runx1* and *cmyb*, were significantly downregulated in the mutants, when compared with the WT siblings. Time lapse imaging of *hif-1 $\alpha$*  and *hif-2 $\alpha$*  morphants revealed a significant reduction of HECs in the VDA, necessary for the formation of HSCs. To investigate the molecular link between Hifs and definitive hematopoiesis I combined gain-of-function and loss-of-function models, and showed that *hif-1 $\alpha$*  and *hif-2 $\alpha$*  act upstream of *notch1*, *vegfaa* and *evi1*, genes known to play a pivotal role in HSCs development.

### III. REFERENCES

---



- Aird, W. C. 2011. 'Discovery of the cardiovascular system: from Galen to William Harvey', *J Thromb Haemost*, 9 Suppl 1: 118-29.
- Anderson, H., T. C. Patch, P. N. Reddy, E. J. Hagedorn, P. G. Kim, K. A. Soltis, M. J. Chen, O. J. Tamplin, M. Frye, G. A. MacLean, K. Hubner, D. E. Bauer, J. P. Kanki, G. Vogin, N. C. Huston, M. Nguyen, Y. Fujiwara, B. H. Paw, D. Vestweber, L. I. Zon, S. H. Orkin, G. Q. Daley, and D. I. Shah. 2015. 'Hematopoietic stem cells develop in the absence of endothelial cadherin 5 expression', *Blood*, 126: 2811-20.
- Arnold, S. J., U. K. Hofmann, E. K. Bikoff, and E. J. Robertson. 2008. 'Pivotal roles for eomesodermin during axis formation, epithelium-to-mesenchyme transition and endoderm specification in the mouse', *Development*, 135: 501-11.
- Baltaziak, M., A. Wincewicz, L. Kanczuga-Koda, J. M. Lotowska, M. Koda, U. Sulkowska, M. Baltaziak, M. Podbielski, M. E. Sobaniec-Lotowska, and S. Sulkowski. 2013. 'The relationships between hypoxia-dependent markers: HIF-1alpha, EPO and EPOR in colorectal cancer', *Folia Histochem Cytobiol*, 51: 320-5.
- Bergiers, I., T. Andrews, O. Vargel Bolukbasi, A. Buness, E. Janosz, N. Lopez-Angueta, K. Ganter, K. Kosim, C. Celen, G. Itir Percin, P. Collier, B. Baying, V. Benes, M. Hemberg, and C. Lancrin. 2018. 'Single-cell transcriptomics reveals a new dynamical function of transcription factors during embryonic hematopoiesis', *Elife*, 7.
- Bersten, D. C., A. E. Sullivan, D. J. Peet, and M. L. Whitelaw. 2013. 'bHLH-PAS proteins in cancer', *Nat Rev Cancer*, 13: 827-41.
- Bertrand, J. Y., N. C. Chi, B. Santoso, S. Teng, D. Y. Stainier, and D. Traver. 2010. 'Haematopoietic stem cells derive directly from aortic endothelium during development', *Nature*, 464: 108-11.
- Blanco, R., and H. Gerhardt. 2013. 'VEGF and Notch in tip and stalk cell selection', *Cold Spring Harb Perspect Med*, 3: a006569.
- Bogdanovic, O., A. Fernandez-Minan, J. J. Tena, E. de la Calle-Mustienes, and J. L. Gomez-Skarmeta. 2013. 'The developmental epigenomics toolbox: ChIP-seq and MethylCap-seq profiling of early zebrafish embryos', *Methods*, 62: 207-15.
- Boylan, Michael. 2015. *The origins of ancient Greek science : blood, a philosophical study* (Routledge: New York).
- Brown, L. A., A. R. Rodaway, T. F. Schilling, T. Jowett, P. W. Ingham, R. K. Patient, and A. D. Sharrocks. 2000. 'Insights into early vasculogenesis revealed by expression of the ETS-domain transcription factor Fli-1 in wild-type and mutant zebrafish embryos', *Mech Dev*, 90: 237-52.
- Butko, E., C. Pouget, and D. Traver. 2016. 'Complex regulation of HSC emergence by the Notch signaling pathway', *Dev Biol*, 409: 129-38.
- Carmeliet, P., Y. Dor, J. M. Herbert, D. Fukumura, K. Brusselmans, M. Dewerchin, M. Neeman, F. Bono, R. Abramovitch, P. Maxwell, C. J. Koch, P. Ratcliffe, L. Moons, R. K. Jain, D. Collen, and E. Keshert. 1998. 'Role of HIF-1alpha in hypoxia-mediated apoptosis, cell proliferation and tumour angiogenesis', *Nature*, 394: 485-90.
- Catita, J., M. Lopez-Luppo, D. Ramos, V. Nacher, M. Navarro, A. Carretero, A. Sanchez-Chardi, L. Mendes-Jorge, A. Rodriguez-Baeza, and J. Ruberte. 2015. 'Imaging of cellular aging in human retinal blood vessels', *Exp Eye Res*, 135: 14-25.
- Chen, Y., S. Zeng, R. Hu, X. Wang, W. Huang, J. Liu, L. Wang, G. Liu, Y. Cao, and Y. Zhang. 2017. 'Using local chromatin structure to improve CRISPR/Cas9 efficiency in zebrafish', *PLoS One*, 12: e0182528.
- Cheng, Z., S. K. Verma, D. W. Losordo, and R. Kishore. 2017. 'Reprogrammed Human Endothelial Cells: A Novel Cell Source for Regenerative Vascular Medicine', *Circ Res*, 120: 756-58.

- Chi, N. C., R. M. Shaw, S. De Val, G. Kang, L. Y. Jan, B. L. Black, and D. Y. Stainier. 2008. 'Foxn4 directly regulates tbx2b expression and atrioventricular canal formation', *Genes Dev*, 22: 734-9.
- Choi, K., M. Kennedy, A. Kazarov, J. C. Papadimitriou, and G. Keller. 1998. 'A common precursor for hematopoietic and endothelial cells', *Development*, 125: 725-32.
- Ciruna, B., and J. Rossant. 2001. 'FGF signaling regulates mesoderm cell fate specification and morphogenetic movement at the primitive streak', *Dev Cell*, 1: 37-49.
- Costello, I., I. M. Pimeisl, S. Drager, E. K. Bikoff, E. J. Robertson, and S. J. Arnold. 2011. 'The T-box transcription factor Eomesodermin acts upstream of Mesp1 to specify cardiac mesoderm during mouse gastrulation', *Nat Cell Biol*, 13: 1084-91.
- Craig, M. P., V. Grajevskaja, H. K. Liao, J. Balciuniene, S. C. Ekker, J. S. Park, J. J. Essner, D. Balciunas, and S. Sumanas. 2015. 'Etv2 and fli1b function together as key regulators of vasculogenesis and angiogenesis', *Arterioscler Thromb Vasc Biol*, 35: 865-76.
- Davidson, A. J., and L. I. Zon. 2004. 'The 'definitive' (and 'primitive') guide to zebrafish hematopoiesis', *Oncogene*, 23: 7233-46.
- Dayan, F., M. Monticelli, J. Pouyssegur, and E. Pecou. 2009. 'Gene regulation in response to graded hypoxia: the non-redundant roles of the oxygen sensors PHD and FIH in the HIF pathway', *J Theor Biol*, 259: 304-16.
- Dhakal, S., C. B. Stevens, M. Sebbagh, O. Weiss, R. A. Frey, S. Adamson, E. A. Shelden, A. Inbal, and D. L. Stenkamp. 2015. 'Abnormal retinal development in Cloche mutant zebrafish', *Dev Dyn*, 244: 1439-55.
- Doganli, C., M. Sandoval, S. Thomas, and D. Hart. 2017. 'Assay for Transposase-Accessible Chromatin with High-Throughput Sequencing (ATAC-Seq) Protocol for Zebrafish Embryos', *Methods Mol Biol*, 1507: 59-66.
- Dore-Duffy, P. 2008. 'Pericytes: pluripotent cells of the blood brain barrier', *Curr Pharm Des*, 14: 1581-93.
- Dore-Duffy, P., and K. Cleary. 2011. 'Morphology and properties of pericytes', *Methods Mol Biol*, 686: 49-68.
- Elks, P. M., S. A. Renshaw, A. H. Meijer, S. R. Walmsley, and F. J. van Eeden. 2015. 'Exploring the HIFs, buts and maybes of hypoxia signalling in disease: lessons from zebrafish models', *Dis Model Mech*, 8: 1349-60.
- Ellertsdottir, E., A. Lenard, Y. Blum, A. Krudewig, L. Herwig, M. Affolter, and H. G. Belting. 2010. 'Vascular morphogenesis in the zebrafish embryo', *Dev Biol*, 341: 56-65.
- Faial, T., A. S. Bernardo, S. Mendjan, E. Diamanti, D. Ortmann, G. E. Gentsch, V. L. Mascetti, M. W. Trotter, J. C. Smith, and R. A. Pedersen. 2015. 'Brachyury and SMAD signalling collaboratively orchestrate distinct mesoderm and endoderm gene regulatory networks in differentiating human embryonic stem cells', *Development*, 142: 2121-35.
- Faure, S., P. de Santa Barbara, D. J. Roberts, and M. Whitman. 2002. 'Endogenous patterns of BMP signaling during early chick development', *Dev Biol*, 244: 44-65.
- Ferrara, N., K. Carver-Moore, H. Chen, M. Dowd, L. Lu, K. S. O'Shea, L. Powell-Braxton, K. J. Hillan, and M. W. Moore. 1996. 'Heterozygous embryonic lethality induced by targeted inactivation of the VEGF gene', *Nature*, 380: 439-42.
- Ferrara, N., H. P. Gerber, and J. LeCouter. 2003. 'The biology of VEGF and its receptors', *Nat Med*, 9: 669-76.
- Field, H. A., E. A. Ober, T. Roeser, and D. Y. Stainier. 2003. 'Formation of the digestive system in zebrafish. I. Liver morphogenesis', *Dev Biol*, 253: 279-90.
- Fish, J. E., and J. D. Wythe. 2015. 'The molecular regulation of arteriovenous specification and maintenance', *Dev Dyn*, 244: 391-409.

- Fribourgh, J. L., and C. L. Partch. 2017. 'Assembly and function of bHLH-PAS complexes', *Proc Natl Acad Sci U S A*, 114: 5330-32.
- Furthauer, M., J. Van Celst, C. Thisse, and B. Thisse. 2004. 'Fgf signalling controls the dorsoventral patterning of the zebrafish embryo', *Development*, 131: 2853-64.
- Gekas, C., F. Dieterlen-Lievre, S. H. Orkin, and H. K. Mikkola. 2005. 'The placenta is a niche for hematopoietic stem cells', *Dev Cell*, 8: 365-75.
- Gekas, C., E. Rhodes K, and K. A. Mikkola H. 2008. 'Isolation and analysis of hematopoietic stem cells from the placenta', *J Vis Exp*.
- Ginsberg, M., D. James, B. S. Ding, D. Nolan, F. Geng, J. M. Butler, W. Schachterle, V. R. Pulijaal, S. Mathew, S. T. Chasen, J. Xiang, Z. Rosenwaks, K. Shido, O. Elemento, S. Y. Rabbany, and S. Rafii. 2012. 'Efficient direct reprogramming of mature amniotic cells into endothelial cells by ETS factors and TGFbeta suppression', *Cell*, 151: 559-75.
- Goldie, L. C., M. K. Nix, and K. K. Hirschi. 2008. 'Embryonic vasculogenesis and hematopoietic specification', *Organogenesis*, 4: 257-63.
- Gritz, E., and K. K. Hirschi. 2016. 'Specification and function of hemogenic endothelium during embryogenesis', *Cell Mol Life Sci*, 73: 1547-67.
- Gruber, M., C. J. Hu, R. S. Johnson, E. J. Brown, B. Keith, and M. C. Simon. 2007. 'Acute postnatal ablation of Hif-2alpha results in anemia', *Proc Natl Acad Sci U S A*, 104: 2301-6.
- Gu, Y. Z., S. M. Moran, J. B. Hogenesch, L. Wartman, and C. A. Bradfield. 1998. 'Molecular characterization and chromosomal localization of a third alpha-class hypoxia inducible factor subunit, HIF3alpha', *Gene Expr*, 7: 205-13.
- Gutierrez-Lovera, C., A. J. Vazquez-Rios, J. Guerra-Varela, L. Sanchez, and M. de la Fuente. 2017. 'The Potential of Zebrafish as a Model Organism for Improving the Translation of Genetic Anticancer Nanomedicines', *Genes (Basel)*, 8.
- Habeck, H., J. Odenthal, B. Walderich, H. Maischein, S. Schulte-Merker, and consortium Tübingen screen. 2002. 'Analysis of a zebrafish VEGF receptor mutant reveals specific disruption of angiogenesis', *Curr Biol*, 12: 1405-12.
- Hao, J., J. N. Ho, J. A. Lewis, K. A. Karim, R. N. Daniels, P. R. Gentry, C. R. Hopkins, C. W. Lindsley, and C. C. Hong. 2010. 'In vivo structure-activity relationship study of dorsomorphin analogues identifies selective VEGF and BMP inhibitors', *ACS Chem Biol*, 5: 245-53.
- Hara, S., J. Hamada, C. Kobayashi, Y. Kondo, and N. Imura. 2001. 'Expression and characterization of hypoxia-inducible factor (HIF)-3alpha in human kidney: suppression of HIF-mediated gene expression by HIF-3alpha', *Biochem Biophys Res Commun*, 287: 808-13.
- Harding, A., E. Cortez-Toledo, N. L. Magner, J. R. Beegle, D. P. Coleal-Bergum, D. Hao, A. Wang, J. A. Nolta, and P. Zhou. 2017. 'Highly Efficient Differentiation of Endothelial Cells from Pluripotent Stem Cells Requires the MAPK and the PI3K Pathways', *Stem Cells*, 35: 909-19.
- Harris, J. M., V. Esain, G. M. Frechette, L. J. Harris, A. G. Cox, M. Cortes, M. K. Garnaas, K. J. Carroll, C. C. Cutting, T. Khan, P. M. Elks, S. A. Renshaw, B. C. Dickinson, C. J. Chang, M. P. Murphy, B. H. Paw, M. G. Vander Heiden, W. Goessling, and T. E. North. 2013. 'Glucose metabolism impacts the spatiotemporal onset and magnitude of HSC induction in vivo', *Blood*, 121: 2483-93.
- Harvey, William, Zacharias Sylvius, Jacobus de Back, and William Harvey. 1653. *The anatomical exercises of Dr. William Harvey, professor of physick and physician to the Kings Majesty, concerning the motion of the heart and blood* (Printed by Francis Leach for Richard Lowndes ... London).

- Hermkens, D. M., A. van Impel, A. Urasaki, J. Bussmann, H. J. Duckers, and S. Schulte-Merker. 2015. 'Sox7 controls arterial specification in conjunction with hey2 and efnb2 function', *Development*, 142: 1695-704.
- Hoffman, M. A., M. Ohh, H. Yang, J. M. Klco, M. Ivan, and W. G. Kaelin, Jr. 2001. 'von Hippel-Lindau protein mutants linked to type 2C VHL disease preserve the ability to downregulate HIF', *Hum Mol Genet*, 10: 1019-27.
- Hogan, B. M., R. Herpers, M. Witte, H. Helotera, K. Alitalo, H. J. Duckers, and S. Schulte-Merker. 2009. 'Vegfc/Flt4 signalling is suppressed by Dll4 in developing zebrafish intersegmental arteries', *Development*, 136: 4001-9.
- Horiuchi, A., T. Imai, M. Shimizu, K. Oka, C. Wang, T. Nikaido, and I. Konishi. 2002. 'Hypoxia-induced changes in the expression of VEGF, HIF-1 alpha and cell cycle-related molecules in ovarian cancer cells', *Anticancer Res*, 22: 2697-702.
- Huang, N., Y. Chelliah, Y. Shan, C. A. Taylor, S. H. Yoo, C. Partch, C. B. Green, H. Zhang, and J. S. Takahashi. 2012. 'Crystal structure of the heterodimeric CLOCK:BMAL1 transcriptional activator complex', *Science*, 337: 189-94.
- Huber, T. L., V. Kouskoff, H. J. Fehling, J. Palis, and G. Keller. 2004. 'Haemangioblast commitment is initiated in the primitive streak of the mouse embryo', *Nature*, 432: 625-30.
- Hughes, S., and T. Chang-Ling. 2000. 'Roles of endothelial cell migration and apoptosis in vascular remodeling during development of the central nervous system', *Microcirculation*, 7: 317-33.
- Husse, J., S. C. Hintze, G. Eichele, H. Lehnert, and H. Oster. 2012. 'Circadian clock genes Per1 and Per2 regulate the response of metabolism-associated transcripts to sleep disruption', *PLoS One*, 7: e52983.
- Imanirad, P., P. Solaimani Kartalaei, M. Crisan, C. Vink, T. Yamada-Inagawa, E. de Pater, D. Kurek, P. Kaimakis, R. van der Linden, N. Speck, and E. Dzierzak. 2014. 'HIF1alpha is a regulator of hematopoietic progenitor and stem cell development in hypoxic sites of the mouse embryo', *Stem Cell Res*, 12: 24-35.
- Isogai, S., N. D. Lawson, S. Torrealday, M. Horiguchi, and B. M. Weinstein. 2003. 'Angiogenic network formation in the developing vertebrate trunk', *Development*, 130: 5281-90.
- Itkin, T., S. Gur-Cohen, J. A. Spencer, A. Schajnovitz, S. K. Ramasamy, A. P. Kusumbe, G. Ledergor, Y. Jung, I. Milo, M. G. Poulos, A. Kalinkovich, A. Ludin, O. Kollet, G. Shakhar, J. M. Butler, S. Rafii, R. H. Adams, D. T. Scadden, C. P. Lin, and T. Lapidot. 2016. 'Distinct bone marrow blood vessels differentially regulate haematopoiesis', *Nature*, 532: 323-8.
- Iwafuchi-Doi, M., and K. S. Zaret. 2016. 'Cell fate control by pioneer transcription factors', *Development*, 143: 1833-7.
- Jaakkola, P., D. R. Mole, Y. M. Tian, M. I. Wilson, J. Gielbert, S. J. Gaskell, A. von Kriegsheim, H. F. Hebestreit, M. Mukherji, C. J. Schofield, P. H. Maxwell, C. W. Pugh, and P. J. Ratcliffe. 2001. 'Targeting of HIF-alpha to the von Hippel-Lindau ubiquitylation complex by O2-regulated prolyl hydroxylation', *Science*, 292: 468-72.
- Jadhav, G., D. Teguh, J. Kenny, J. Tickner, and J. Xu. 2016. 'Morc3 mutant mice exhibit reduced cortical area and thickness, accompanied by altered haematopoietic stem cells niche and bone cell differentiation', *Sci Rep*, 6: 25964.
- Jakobsson, L., C. A. Franco, K. Bentley, R. T. Collins, B. Ponsioen, I. M. Aspalter, I. Rosewell, M. Busse, G. Thurston, A. Medvinsky, S. Schulte-Merker, and H. Gerhardt. 2010. 'Endothelial cells dynamically compete for the tip cell position during angiogenic sprouting', *Nat Cell Biol*, 12: 943-53.

- Jin, S. W., D. Beis, T. Mitchell, J. N. Chen, and D. Y. Stainier. 2005. 'Cellular and molecular analyses of vascular tube and lumen formation in zebrafish', *Development*, 132: 5199-209.
- Jones, E. A., F. le Noble, and A. Eichmann. 2006. 'What determines blood vessel structure? Genetic prespecification vs. hemodynamics', *Physiology (Bethesda)*, 21: 388-95.
- Kewley, R. J., M. L. Whitelaw, and A. Chapman-Smith. 2004. 'The mammalian basic helix-loop-helix/PAS family of transcriptional regulators', *Int J Biochem Cell Biol*, 36: 189-204.
- Kimelman, D. 2006. 'Mesoderm induction: from caps to chips', *Nat Rev Genet*, 7: 360-72.
- Kobayashi, K., G. Ding, S. Nishikawa, and H. Kataoka. 2013. 'Role of Etv2-positive cells in the remodeling morphogenesis during vascular development', *Genes Cells*, 18: 704-21.
- Kohli, V., J. A. Schumacher, S. P. Desai, K. Rehn, and S. Sumanas. 2013. 'Arterial and venous progenitors of the major axial vessels originate at distinct locations', *Dev Cell*, 25: 196-206.
- Kok, F. O., M. Shin, C. W. Ni, A. Gupta, A. S. Grosse, A. van Impel, B. C. Kirchmaier, J. Peterson-Maduro, G. Kourkoulis, I. Male, D. F. DeSantis, S. Sheppard-Tindell, L. Ebarasi, C. Betsholtz, S. Schulte-Merker, S. A. Wolfe, and N. D. Lawson. 2015. 'Reverse genetic screening reveals poor correlation between morpholino-induced and mutant phenotypes in zebrafish', *Dev Cell*, 32: 97-108.
- Konantz, M., E. Alghisi, J. S. Muller, A. Lenard, V. Esain, K. J. Carroll, L. Kanz, T. E. North, and C. Lengerke. 2016. 'Evi1 regulates Notch activation to induce zebrafish hematopoietic stem cell emergence', *EMBO J*, 35: 2315-31.
- Krueger, J., D. Liu, K. Scholz, A. Zimmer, Y. Shi, C. Klein, A. Siekmann, S. Schulte-Merker, M. Cudmore, A. Ahmed, and F. le Noble. 2011. 'Flt1 acts as a negative regulator of tip cell formation and branching morphogenesis in the zebrafish embryo', *Development*, 138: 2111-20.
- Kume, T. 2010. 'Specification of arterial, venous, and lymphatic endothelial cells during embryonic development', *Histol Histopathol*, 25: 637-46.
- Lancrin, C., P. Sroczynska, C. Stephenson, T. Allen, V. Kouskoff, and G. Lacaud. 2009. 'The haemangioblast generates haematopoietic cells through a haemogenic endothelium stage', *Nature*, 457: 892-5.
- Lawson, N. D., A. M. Vogel, and B. M. Weinstein. 2002. 'sonic hedgehog and vascular endothelial growth factor act upstream of the Notch pathway during arterial endothelial differentiation', *Dev Cell*, 3: 127-36.
- Lee, D., C. Park, H. Lee, J. J. Lugus, S. H. Kim, E. Arentson, Y. S. Chung, G. Gomez, M. Kyba, S. Lin, R. Janknecht, D. S. Lim, and K. Choi. 2008. 'ER71 acts downstream of BMP, Notch, and Wnt signaling in blood and vessel progenitor specification', *Cell Stem Cell*, 2: 497-507.
- Lemus-Varela, M. L., M. E. Flores-Soto, R. Cervantes-Munguia, B. M. Torres-Mendoza, G. Gudino-Cabrera, V. Chaparro-Huerta, D. Ortuno-Sahagun, and C. Beas-Zarate. 2010. 'Expression of HIF-1 alpha, VEGF and EPO in peripheral blood from patients with two cardiac abnormalities associated with hypoxia', *Clin Biochem*, 43: 234-9.
- Leung, A., A. Ciau-Uitz, P. Pinheiro, R. Monteiro, J. Zuo, P. Vyas, R. Patient, and C. Porcher. 2013. 'Uncoupling VEGFA functions in arteriogenesis and hematopoietic stem cell specification', *Dev Cell*, 24: 144-58.
- Liao, W., B. W. Bisgrove, H. Sawyer, B. Hug, B. Bell, K. Peters, D. J. Grunwald, and D. Y. Stainier. 1997. 'The zebrafish gene cloche acts upstream of a flk-1 homologue to regulate endothelial cell differentiation', *Development*, 124: 381-9.

- Lieu, Y. K., and E. P. Reddy. 2009. 'Conditional c-myb knockout in adult hematopoietic stem cells leads to loss of self-renewal due to impaired proliferation and accelerated differentiation', *Proc Natl Acad Sci U S A*, 106: 21689-94.
- Lin, C., R. McGough, B. Aswad, J. A. Block, and R. Terek. 2004. 'Hypoxia induces HIF-1alpha and VEGF expression in chondrosarcoma cells and chondrocytes', *J Orthop Res*, 22: 1175-81.
- Ling, K. W., K. Ottersbach, J. P. van Hamburg, A. Oziemlak, F. Y. Tsai, S. H. Orkin, R. Ploemacher, R. W. Hendriks, and E. Dzierzak. 2004. 'GATA-2 plays two functionally distinct roles during the ontogeny of hematopoietic stem cells', *J Exp Med*, 200: 871-82.
- Lis, R., C. C. Karrasch, M. G. Poulos, B. Kunar, D. Redmond, J. G. B. Duran, C. R. Badwe, W. Schachterle, M. Ginsberg, J. Xiang, A. R. Tabrizi, K. Shido, Z. Rosenwaks, O. Elemento, N. A. Speck, J. M. Butler, J. M. Scandura, and S. Rafii. 2017. 'Conversion of adult endothelium to immunocompetent haematopoietic stem cells', *Nature*, 545: 439-45.
- Liu, F., M. Walmsley, A. Rodaway, and R. Patient. 2008. 'Flt1 acts at the top of the transcriptional network driving blood and endothelial development', *Curr Biol*, 18: 1234-40.
- Ma, M., and Y. J. Jiang. 2007. 'Jagged2a-notch signaling mediates cell fate choice in the zebrafish pronephric duct', *PLoS Genet*, 3: e18.
- Marcelo, K. L., L. C. Goldie, and K. K. Hirschi. 2013. 'Regulation of endothelial cell differentiation and specification', *Circ Res*, 112: 1272-87.
- Marcelo, K. L., T. M. Sills, S. Coskun, H. Vasavada, S. Sanglikar, L. C. Goldie, and K. K. Hirschi. 2013. 'Hemogenic endothelial cell specification requires c-Kit, Notch signaling, and p27-mediated cell-cycle control', *Dev Cell*, 27: 504-15.
- Marikawa, Y., D. A. Tamashiro, T. C. Fujita, and V. B. Alarcon. 2009. 'Aggregated P19 mouse embryonal carcinoma cells as a simple in vitro model to study the molecular regulations of mesoderm formation and axial elongation morphogenesis', *Genesis*, 47: 93-106.
- Massari, M. E., and C. Murre. 2000. 'Helix-loop-helix proteins: regulators of transcription in eucaryotic organisms', *Mol Cell Biol*, 20: 429-40.
- Matsuoka, R. L., M. Marass, A. Avdesh, C. S. Helker, H. M. Maischein, A. S. Grosse, H. Kaur, N. D. Lawson, W. Herzog, and D. Y. Stainier. 2016. 'Radial glia regulate vascular patterning around the developing spinal cord', *Elife*, 5.
- McMahon, S., M. Charbonneau, S. Grandmont, D. E. Richard, and C. M. Dubois. 2006. 'Transforming growth factor beta1 induces hypoxia-inducible factor-1 stabilization through selective inhibition of PHD2 expression', *J Biol Chem*, 281: 24171-81.
- Medvinsky, A., and E. Dzierzak. 1996. 'Definitive hematopoiesis is autonomously initiated by the AGM region', *Cell*, 86: 897-906.
- Missinato, M. A., M. Saydmohammed, D. A. Zuppo, K. S. Rao, G. W. Opie, B. Kuhn, and M. Tsang. 2018. 'Dusp6 attenuates Ras/MAPK signaling to limit zebrafish heart regeneration', *Development*, 145.
- Molina, G., A. Vogt, A. Bakan, W. Dai, P. Queiroz de Oliveira, W. Znosko, T. E. Smithgall, I. Bahar, J. S. Lazo, B. W. Day, and M. Tsang. 2009. 'Zebrafish chemical screening reveals an inhibitor of Dusp6 that expands cardiac cell lineages', *Nat Chem Biol*, 5: 680-7.
- Monahan-Earley, R., A. M. Dvorak, and W. C. Aird. 2013. 'Evolutionary origins of the blood vascular system and endothelium', *J Thromb Haemost*, 11 Suppl 1: 46-66.
- Monteiro, R., P. Pinheiro, N. Joseph, T. Peterkin, J. Koth, E. Repapi, F. Bonkhofer, A. Kirmizitas, and R. Patient. 2016. 'Transforming Growth Factor beta Drives

- Hemogenic Endothelium Programming and the Transition to Hematopoietic Stem Cells', *Dev Cell*, 38: 358-70.
- Mouse Genome Sequencing Consortium, R. H. Waterston, K. Lindblad-Toh, E. Birney, J. Rogers, J. F. Abril, P. Agarwal, R. Agarwala, R. Ainscough, M. Alexandersson, P. An, S. E. Antonarakis, J. Attwood, R. Baertsch, J. Bailey, K. Barlow, S. Beck, E. Berry, B. Birren, T. Bloom, P. Bork, M. Botcherby, N. Bray, M. R. Brent, D. G. Brown, S. D. Brown, C. Bult, J. Burton, J. Butler, R. D. Campbell, P. Carninci, S. Cawley, F. Chiaromonte, A. T. Chinwalla, D. M. Church, M. Clamp, C. Clee, F. S. Collins, L. L. Cook, R. R. Copley, A. Coulson, O. Couronne, J. Cuff, V. Curwen, T. Cutts, M. Daly, R. David, J. Davies, K. D. Delehaunty, J. Deri, E. T. Dermitzakis, C. Dewey, N. J. Dickens, M. Diekhans, S. Dodge, I. Dubchak, D. M. Dunn, S. R. Eddy, L. Elnitski, R. D. Emes, P. Eswara, E. Eyraas, A. Felsenfeld, G. A. Fewell, P. Flicek, K. Foley, W. N. Frankel, L. A. Fulton, R. S. Fulton, T. S. Furey, D. Gage, R. A. Gibbs, G. Glusman, S. Gnerre, N. Goldman, L. Goodstadt, D. Grafham, T. A. Graves, E. D. Green, S. Gregory, R. Guigo, M. Guyer, R. C. Hardison, D. Haussler, Y. Hayashizaki, L. W. Hillier, A. Hinrichs, W. Hlavina, T. Holzer, F. Hsu, A. Hua, T. Hubbard, A. Hunt, I. Jackson, D. B. Jaffe, L. S. Johnson, M. Jones, T. A. Jones, A. Joy, M. Kamal, E. K. Karlsson, D. Karolchik, A. Kasprzyk, J. Kawai, E. Keibler, C. Kells, W. J. Kent, A. Kirby, D. L. Kolbe, I. Korf, R. S. Kucherlapati, E. J. Kulbokas, D. Kulp, T. Landers, J. P. Leger, S. Leonard, I. Letunic, R. Levine, J. Li, M. Li, C. Lloyd, S. Lucas, B. Ma, D. R. Maglott, E. R. Mardis, L. Matthews, E. Mauceli, J. H. Mayer, M. McCarthy, W. R. McCombie, S. McLaren, K. McLay, J. D. McPherson, J. Meldrim, B. Meredith, J. P. Mesirov, W. Miller, T. L. Miner, E. Mongin, K. T. Montgomery, M. Morgan, R. Mott, J. C. Mullikin, D. M. Muzny, W. E. Nash, J. O. Nelson, M. N. Nhan, R. Nicol, Z. Ning, C. Nusbaum, M. J. O'Connor, Y. Okazaki, K. Oliver, E. Overton-Larty, L. Pachter, G. Parra, K. H. Pepin, J. Peterson, P. Pevzner, R. Plumb, C. S. Pohl, A. Poliakov, T. C. Ponce, C. P. Ponting, S. Potter, M. Quail, A. Reymond, B. A. Roe, K. M. Roskin, E. M. Rubin, A. G. Rust, R. Santos, V. Sapojnikov, B. Schultz, J. Schultz, M. S. Schwartz, S. Schwartz, C. Scott, S. Seaman, S. Searle, T. Sharpe, A. Sheridan, R. Shownkeen, S. Sims, J. B. Singer, G. Slater, A. Smit, D. R. Smith, B. Spencer, A. Stabenau, N. Stange-Thomann, C. Sugnet, M. Suyama, G. Tesler, J. Thompson, D. Torrents, E. Trevaskis, J. Tromp, C. Ucla, A. Ureta-Vidal, J. P. Vinson, A. C. Von Niederhausern, C. M. Wade, M. Wall, R. J. Weber, R. B. Weiss, M. C. Wendl, A. P. West, K. Wetterstrand, R. Wheeler, S. Whelan, J. Wierzbowski, D. Willey, S. Williams, R. K. Wilson, E. Winter, K. C. Worley, D. Wyman, S. Yang, S. P. Yang, E. M. Zdobnov, M. C. Zody, and E. S. Lander. 2002. 'Initial sequencing and comparative analysis of the mouse genome', *Nature*, 420: 520-62.
- Mucenski, M. L., K. McLain, A. B. Kier, S. H. Swerdlow, C. M. Schreiner, T. A. Miller, D. W. Pietryga, W. J. Scott, Jr., and S. S. Potter. 1991. 'A functional c-myb gene is required for normal murine fetal hepatic hematopoiesis', *Cell*, 65: 677-89.
- Mukherjee, T., W. S. Kim, L. Mandal, and U. Banerjee. 2011. 'Interaction between Notch and Hif-alpha in development and survival of Drosophila blood cells', *Science*, 332: 1210-3.
- Nakanishi, N., S. Sogabe, and B. M. Degnan. 2014. 'Evolutionary origin of gastrulation: insights from sponge development', *BMC Biol*, 12: 26.
- Nguyen, D., and T. Xu. 2008. 'The expanding role of mouse genetics for understanding human biology and disease', *Dis Model Mech*, 1: 56-66.
- Nguyen, H. C., H. Yang, J. L. Fribourgh, L. S. Wolfe, and Y. Xiong. 2015. 'Insights into Cullin-RING E3 ubiquitin ligase recruitment: structure of the VHL-EloBC-Cul2 complex', *Structure*, 23: 441-9.

- Nolan, D. J., M. Ginsberg, E. Israely, B. Palikuqi, M. G. Poulos, D. James, B. S. Ding, W. Schachterle, Y. Liu, Z. Rosenwaks, J. M. Butler, J. Xiang, A. Rafii, K. Shido, S. Y. Rabbany, O. Elemento, and S. Rafii. 2013. 'Molecular signatures of tissue-specific microvascular endothelial cell heterogeneity in organ maintenance and regeneration', *Dev Cell*, 26: 204-19.
- North, T. E., W. Goessling, C. R. Walkley, C. Lengerke, K. R. Kopani, A. M. Lord, G. J. Weber, T. V. Bowman, I. H. Jang, T. Grosser, G. A. Fitzgerald, G. Q. Daley, S. H. Orkin, and L. I. Zon. 2007. 'Prostaglandin E2 regulates vertebrate haematopoietic stem cell homeostasis', *Nature*, 447: 1007-11.
- Padron-Barthe, L., S. Temino, C. Villa del Campo, L. Carramolino, J. Isern, and M. Torres. 2014. 'Clonal analysis identifies hemogenic endothelium as the source of the blood-endothelial common lineage in the mouse embryo', *Blood*, 124: 2523-32.
- Paik, E. J., and L. I. Zon. 2010. 'Hematopoietic development in the zebrafish', *Int J Dev Biol*, 54: 1127-37.
- Parker, L., and D. Y. Stainier. 1999. 'Cell-autonomous and non-autonomous requirements for the zebrafish gene *cloche* in hematopoiesis', *Development*, 126: 2643-51.
- Pauli, A., E. Valen, M. F. Lin, M. Garber, N. L. Vastenhouw, J. Z. Levin, L. Fan, A. Sandelin, J. L. Rinn, A. Regev, and A. F. Schier. 2012. 'Systematic identification of long noncoding RNAs expressed during zebrafish embryogenesis', *Genome Res*, 22: 577-91.
- Peng, J., L. Zhang, L. Drysdale, and G. H. Fong. 2000. 'The transcription factor EPAS-1/hypoxia-inducible factor 2alpha plays an important role in vascular remodeling', *Proc Natl Acad Sci U S A*, 97: 8386-91.
- Pereira, L. A., M. S. Wong, S. M. Lim, A. Sides, E. G. Stanley, and A. G. Elefanty. 2011. 'Brachyury and related Tbx proteins interact with the Mixl1 homeodomain protein and negatively regulate Mixl1 transcriptional activity', *PLoS One*, 6: e28394.
- Peterson, S. M., and J. L. Freeman. 2009. 'RNA isolation from embryonic zebrafish and cDNA synthesis for gene expression analysis', *J Vis Exp*.
- Phng, L. K., and H. Gerhardt. 2009. 'Angiogenesis: a team effort coordinated by notch', *Dev Cell*, 16: 196-208.
- Pitulescu, M. E., I. Schmidt, B. D. Giaimo, T. Antoine, F. Berkenfeld, F. Ferrante, H. Park, M. Ehling, D. Biljes, S. F. Rocha, U. H. Langen, M. Stehling, T. Nagasawa, N. Ferrara, T. Borggreffe, and R. H. Adams. 2017. 'Dll4 and Notch signalling couples sprouting angiogenesis and artery formation', *Nat Cell Biol*, 19: 915-27.
- Potente, M., and T. Makinen. 2017. 'Vascular heterogeneity and specialization in development and disease', *Nat Rev Mol Cell Biol*, 18: 477-94.
- Pugsley, M. K., and R. Tabrizchi. 2000. 'The vascular system. An overview of structure and function', *J Pharmacol Toxicol Methods*, 44: 333-40.
- Pyati, U. J., A. E. Webb, and D. Kimelman. 2005. 'Transgenic zebrafish reveal stage-specific roles for Bmp signaling in ventral and posterior mesoderm development', *Development*, 132: 2333-43.
- Qian, F., F. Zhen, C. Ong, S. W. Jin, H. Meng Soo, D. Y. Stainier, S. Lin, J. Peng, and Z. Wen. 2005. 'Microarray analysis of zebrafish *cloche* mutant using amplified cDNA and identification of potential downstream target genes', *Dev Dyn*, 233: 1163-72.
- Rasighaemi, P., F. Basheer, C. Liongue, and A. C. Ward. 2015. 'Zebrafish as a model for leukemia and other hematopoietic disorders', *J Hematol Oncol*, 8: 29.
- Reischauer, S., O. A. Stone, A. Villasenor, N. Chi, S. W. Jin, M. Martin, M. T. Lee, N. Fukuda, M. Marass, A. Witty, I. Fiddes, T. Kuo, W. S. Chung, S. Salek, R. Lerrigo, J. Alsio, S. Luo, D. Tworus, S. M. Augustine, S. Mucenieks, B. Nystedt, A. J. Giraldez,



- G. P. Schroth, O. Andersson, and D. Y. Stainier. 2016. 'Cloche is a bHLH-PAS transcription factor that drives haemato-vascular specification', *Nature*, 535: 294-8.
- Rocha, S. F., and R. H. Adams. 2009. 'Molecular differentiation and specialization of vascular beds', *Angiogenesis*, 12: 139-47.
- Rossi, A., S. Gauvrit, M. Marass, L. Pan, C. B. Moens, and D. Y. R. Stainier. 2016. 'Regulation of Vegf signaling by natural and synthetic ligands', *Blood*, 128: 2359-66.
- Rossmann, M. P., Y. Zhou, and L. I. Zon. 2016. 'Development: For cloche the Bell Tolls', *Curr Biol*, 26: R890-R92.
- Ryan, H. E., J. Lo, and R. S. Johnson. 1998. 'HIF-1 alpha is required for solid tumor formation and embryonic vascularization', *EMBO J*, 17: 3005-15.
- Ryan, H. E., M. Poloni, W. McNulty, D. Elson, M. Gassmann, J. M. Arbeit, and R. S. Johnson. 2000. 'Hypoxia-inducible factor-1alpha is a positive factor in solid tumor growth', *Cancer Res*, 60: 4010-5.
- Sanchez, M. J., A. Holmes, C. Miles, and E. Dzierzak. 1996. 'Characterization of the first definitive hematopoietic stem cells in the AGM and liver of the mouse embryo', *Immunity*, 5: 513-25.
- Scheer, N., A. Groth, S. Hans, and J. A. Campos-Ortega. 2001. 'An instructive function for Notch in promoting gliogenesis in the zebrafish retina', *Development*, 128: 1099-107.
- Schoenebeck, J. J., B. R. Keegan, and D. Yelon. 2007. 'Vessel and blood specification override cardiac potential in anterior mesoderm', *Dev Cell*, 13: 254-67.
- Schulte-Merker, S., F. J. van Eeden, M. E. Halpern, C. B. Kimmel, and C. Nusslein-Volhard. 1994. 'no tail (ntl) is the zebrafish homologue of the mouse T (Brachyury) gene', *Development*, 120: 1009-15.
- Schumacher, J. A., J. Bloomekatz, Z. V. Garavito-Aguilar, and D. Yelon. 2013. 'tal1 Regulates the formation of intercellular junctions and the maintenance of identity in the endocardium', *Dev Biol*, 383: 214-26.
- Shalaby, F., J. Rossant, T. P. Yamaguchi, M. Gertsenstein, X. F. Wu, M. L. Breitman, and A. C. Schuh. 1995. 'Failure of blood-island formation and vasculogenesis in Flk-1-deficient mice', *Nature*, 376: 62-6.
- Sharma, R., M. E. R. Shafer, E. Bareke, M. Tremblay, J. Majewski, and M. Bouchard. 2017. 'Bmp signaling maintains a mesoderm progenitor cell state in the mouse tailbud', *Development*, 144: 2982-93.
- Shea, K., and N. Geijsen. 2007. 'Dissection of 6.5 dpc mouse embryos', *J Vis Exp*: 160.
- Shin, D., C. H. Shin, J. Tucker, E. A. Ober, F. Rentzsch, K. D. Poss, M. Hammerschmidt, M. C. Mullins, and D. Y. Stainier. 2007. 'Bmp and Fgf signaling are essential for liver specification in zebrafish', *Development*, 134: 2041-50.
- Simoës, F. C., T. Peterkin, and R. Patient. 2011. 'Fgf differentially controls cross-antagonism between cardiac and haemangioblast regulators', *Development*, 138: 3235-45.
- Soza-Ried, C., I. Hess, N. Netuschil, M. Schorpp, and T. Boehm. 2010. 'Essential role of c-myb in definitive hematopoiesis is evolutionarily conserved', *Proc Natl Acad Sci U S A*, 107: 17304-8.
- Stahl, A., K. M. Connor, P. Sapiëha, J. Chen, R. J. Dennison, N. M. Krah, M. R. Seaward, K. L. Willett, C. M. Aderman, K. I. Guerin, J. Hua, C. Lofqvist, A. Hellstrom, and L. E. Smith. 2010. 'The mouse retina as an angiogenesis model', *Invest Ophthalmol Vis Sci*, 51: 2813-26.
- Stainier, D. Y., B. M. Weinstein, H. W. Detrich, 3rd, L. I. Zon, and M. C. Fishman. 1995. 'Cloche, an early acting zebrafish gene, is required by both the endothelial and hematopoietic lineages', *Development*, 121: 3141-50.
- Stickney, H. L., M. J. Barresi, and S. H. Devoto. 2000. 'Somite development in zebrafish', *Dev Dyn*, 219: 287-303.

- Stott, D., A. Kispert, and B. G. Herrmann. 1993. 'Rescue of the tail defect of Brachyury mice', *Genes Dev*, 7: 197-203.
- Sumanas, S., and K. Choi. 2016. 'ETS Transcription Factor ETV2/ER71/Etsrp in Hematopoietic and Vascular Development', *Curr Top Dev Biol*, 118: 77-111.
- Swiers, G., M. de Bruijn, and N. A. Speck. 2010. 'Hematopoietic stem cell emergence in the conceptus and the role of Runx1', *Int J Dev Biol*, 54: 1151-63.
- Tang, N., L. Wang, J. Esko, F. J. Giordano, Y. Huang, H. P. Gerber, N. Ferrara, and R. S. Johnson. 2004. 'Loss of HIF-1alpha in endothelial cells disrupts a hypoxia-driven VEGF autocrine loop necessary for tumorigenesis', *Cancer Cell*, 6: 485-95.
- Thisse, B., and C. Thisse. 2014. 'In situ hybridization on whole-mount zebrafish embryos and young larvae', *Methods Mol Biol*, 1211: 53-67.
- Thomas, K. R., and M. R. Capecchi. 1987. 'Site-directed mutagenesis by gene targeting in mouse embryo-derived stem cells', *Cell*, 51: 503-12.
- Tian, H., R. E. Hammer, A. M. Matsumoto, D. W. Russell, and S. L. McKnight. 1998. 'The hypoxia-responsive transcription factor EPAS1 is essential for catecholamine homeostasis and protection against heart failure during embryonic development', *Genes Dev*, 12: 3320-4.
- Treangen, T. J., and S. L. Salzberg. 2011. 'Repetitive DNA and next-generation sequencing: computational challenges and solutions', *Nat Rev Genet*, 13: 36-46.
- Tsai, F. Y., G. Keller, F. C. Kuo, M. Weiss, J. Chen, M. Rosenblatt, F. W. Alt, and S. H. Orkin. 1994. 'An early haematopoietic defect in mice lacking the transcription factor GATA-2', *Nature*, 371: 221-6.
- Tsang, K. M., J. S. Hyun, K. T. Cheng, M. Vargas, D. Mehta, M. Ushio-Fukai, L. Zou, K. V. Pajcini, J. Rehman, and A. B. Malik. 2017. 'Embryonic Stem Cell Differentiation to Functional Arterial Endothelial Cells through Sequential Activation of ETV2 and NOTCH1 Signaling by HIF1alpha', *Stem Cell Reports*, 9: 796-806.
- Tsankov, A. M., H. Gu, V. Akopian, M. J. Ziller, J. Donaghey, I. Amit, A. Gnirke, and A. Meissner. 2015. 'Transcription factor binding dynamics during human ES cell differentiation', *Nature*, 518: 344-9.
- Tse, D., and R. V. Stan. 2010. 'Morphological heterogeneity of endothelium', *Semin Thromb Hemost*, 36: 236-45.
- Tual-Chalot, S., M. Mahmoud, K. R. Allinson, R. E. Redgrave, Z. Zhai, S. P. Oh, M. Fruttiger, and H. M. Arthur. 2014. 'Endothelial depletion of Acvrl1 in mice leads to arteriovenous malformations associated with reduced endoglin expression', *PLoS One*, 9: e98646.
- Vogel, A. M., and B. M. Weinstein. 2000. 'Studying vascular development in the zebrafish', *Trends Cardiovasc Med*, 10: 352-60.
- Vogeli, K. M., S. W. Jin, G. R. Martin, and D. Y. Stainier. 2006. 'A common progenitor for haematopoietic and endothelial lineages in the zebrafish gastrula', *Nature*, 443: 337-9.
- Weiss, O., R. Kaufman, N. Michaeli, and A. Inbal. 2012. 'Abnormal vasculature interferes with optic fissure closure in lmo2 mutant zebrafish embryos', *Dev Biol*, 369: 191-8.
- Westerfield, Monte. 1993. *The zebrafish book : a guide for the laboratory use of zebrafish (Brachydanio rerio)* (M. Westerfield: Eugene, OR).
- Wilkinson, R. N., M. J. Koudijs, R. K. Patient, P. W. Ingham, S. Schulte-Merker, and F. J. van Eeden. 2012. 'Hedgehog signaling via a calcitonin receptor-like receptor can induce arterial differentiation independently of VEGF signaling in zebrafish', *Blood*, 120: 477-88.

- Winnier, G., M. Blessing, P. A. Labosky, and B. L. Hogan. 1995. 'Bone morphogenetic protein-4 is required for mesoderm formation and patterning in the mouse', *Genes Dev*, 9: 2105-16.
- Wong, K. S., K. Proulx, M. S. Rost, and S. Sumanas. 2009. 'Identification of vasculature-specific genes by microarray analysis of *Etsrp/Etv2* overexpressing zebrafish embryos', *Dev Dyn*, 238: 1836-50.
- Xu, P., G. Zhu, Y. Wang, J. Sun, X. Liu, Y. G. Chen, and A. Meng. 2014. 'Maternal Eomesodermin regulates zygotic nodal gene expression for mesendoderm induction in zebrafish embryos', *J Mol Cell Biol*, 6: 272-85.
- Yamaguchi, T. P., K. Harpal, M. Henkemeyer, and J. Rossant. 1994. 'fgfr-1 is required for embryonic growth and mesodermal patterning during mouse gastrulation', *Genes Dev*, 8: 3032-44.
- Zape, J. P., and A. C. Zovein. 2011. 'Hemogenic endothelium: origins, regulation, and implications for vascular biology', *Semin Cell Dev Biol*, 22: 1036-47.
- Zhang, P., Q. Yao, L. Lu, Y. Li, P. J. Chen, and C. Duan. 2014. 'Hypoxia-inducible factor 3 is an oxygen-dependent transcription activator and regulates a distinct transcriptional response to hypoxia', *Cell Rep*, 6: 1110-21.
- Zhang, Y., H. Jin, L. Li, F. X. Qin, and Z. Wen. 2011. 'cMyb regulates hematopoietic stem/progenitor cell mobilization during zebrafish hematopoiesis', *Blood*, 118: 4093-101.

## **Acknowledgments**

During my PhD I have learnt a lot, even more than I could expect. My PhD was filled with highs and lows, and it really contributed in making my skin thicker and in becoming an adult. I met a lot of special people and I made a number of experiences that I will bring with me forever.

First of all and foremost I thank Claudia Gerri, my girlfriend, who helped me every minute, every hour, every day in basically EVERYTHING. With a lot of patience and wisdom, you were able to channel my energy towards the important things in life and I will be eternally grateful for the joyful moments we spent together despite the difficulties.

I also would like to thank:

Prof. Dr. Didier Stainier for the opportunity he gave me to work in such a wonderful lab.

Prof. Dr. Virginie Lecaudey because she was available to review my thesis and she invested her time in reading this work.

My colleagues who helped me during my PhD, mainly: Sven Reischauer, Oliver Stone and Aly Villaseñor for having involved me in a historical project, supporting my own project with valuable ideas. Rubén Marín-Juez, you have always been extremely helpful and open to discuss a multitude of projects and you have been able to identify the most critical aspects in every circumstance. Arica Beisaw, not only for your help in very important techniques but also for the discussions

beyond my own project. Ryota Matsuoka, because the countless hours I spent with you talking about experiments and papers, really helped me in understanding what I like the most in science. Francesca Luzzani, it was very enriching supervising you, even for a limited amount of time. Jason Lai and Kenny Mattonet: the nerdy friends that every nerd needs, it was great talking with you about science and philosophy! Ana Marta Romao Stone, you were one of the first people I met in the institute and you have been extremely helpful in showing me how to be positive in all situations.

I would also like to thank my old friends from Trieste, they have always been extremely helpful, providing advice but also giving me new reasons to laugh every day.

Moreover, I would like to thank the members of “il Genio™” group, because in the past 4 years they have been an invaluable source of support and entertainment. Especially Elvio Carini, I discussed every imaginable topic in the past 10 years with you, and it was very enriching.

I thank also all the other scientists, the technicians, the animal caretakers and the administrative staff because everyone I met played a role in my journey.

As per usual, in my acknowledgments, I thank my parents. My mom Renata Gregoretti and my dad Paolo Marass only care about my happiness and they've always been supportive in all the choices I made in my life. They have always been helpful and they will keep doing everything they can to guide and to encourage me in the future.

# CURRICULUM VITAE

## Work Experience

11/2014 - 09/2018

**PhD candidate.** Max Planck Institute, Germany – Didier Stainier Laboratory.

- Coordinated eight successful research projects
- Developed a collaboration network including researchers belonging to Francis Crick Institute, Weill Cornell Medicine, Duke University and Cleveland Clinic
- Supervised a PhD student, three master's students and a medical student
- Invented, designed and tested a synthetic protein of therapeutic interest, recently patented

10/2015 - 10/2017

**Committee member** of International Max Planck Research School

- Successfully organised two international conferences for over 40 people each, inviting a total of five influential professors as keynote speakers
- Planned and coordinated multiple soft skills seminars directed to PhD students regarding topics such as “scientific writing” and “time management”

10/2014

**Lecturer** at University of Parma

- I gave 3 lectures for the course of “molecular biology of model organisms”

03/2014 - 09/2014

**Intern.** Max Planck Institute, Germany — Didier Stainier Laboratory.

- I performed site-directed mutagenesis to identify the determinants of Vegf *in vivo*

04/2012 - 09/2012

**Intern.** University of Parma, Italy — Tiziana Lodi Laboratory

- I have worked on yeast genetics and molecular mechanisms controlling iron homeostasis

10/2011 - 10/2014

**Student Representative** for the course of “Industrial Biotechnology” and the course of “Biotechnology”

- Responsible for **Quality Assurance** for the course of “Industrial Biotechnology”

- Collaborated with the professors to improve students' satisfaction over three years

### **Education and Training**

10/2014 - 09/2018 (expected)

**PhD in Molecular Biology** Max Planck Institute for Heart and Lung Research,  
Germany

07/2017

**Summer School program:** Mars42 - Entrepreneurship for scientists  
SISSA, Trieste

- I have acquired the tools to transfer the scientific methodology to entrepreneurial projects

10/2012 - 10/2014

**Master's Degree in Industrial and Molecular Biotechnology**  
University of Parma

Grade: 110 *summa cum laude*

09/2009 - 09/2012

**Bachelor's Degree in Biotechnology**  
University of Parma

Grade: 110 *summa cum laude*

### **Organisational Skills**

**Team-oriented** and propensity to give helpful feedbacks

Experience in **project management** and leadership

**Communication** and public speaking skills

Successfully organised two **international conferences**

### **Computer Skills**

Able to efficiently analyse multiple large datasets in **Excel**

Basic **programming** skills: Java, Python

Proficient in **Adobe Creative Suite** (Photoshop, Illustrator, InDesign, Acrobat)

**Bioinformatics** softwares (IGV, VMD, GSEA) applied to NGS and RNA-seq data

## Prizes and Awards

Winner of the advanced European **Erasmus Placement Grant**

Awarded of the **International Max Planck Research School Fellowship**

**Inventor of the patent:** Modified vascular endothelial growth factor a (VEGF-A) and its medical use (EP 3216458)

**Invited** to the International FishMed Conference on Zebrafish Research, in 2016

Poster selected for a short talk in the **Gordon Conference** for Angiogenesis 2017

## Publications

- Hif-1 $\alpha$  and Hif-2 $\alpha$  regulate HE and HSC formation in zebrafish.  
Gerri C\* ,**Marass M\***, et al. ***Blood***, 2018 Jan. - \*joint first author
- Hif-1 $\alpha$  regulates macrophage-endothelial interactions during blood vessel development in zebrafish.  
Gerri C, Marín-Juez R, **Marass M** et al. ***Nature Communications***, 2017 May
- Radial glia regulate vascular patterning around the developing spinal cord.  
Matsuoka R, **Marass M** et al. ***Elife***, 2016 Nov.
- Fast revascularization of the injured area is essential to support zebrafish heart regeneration.  
Marín-Juez R, **Marass M** et al. ***PNAS***, 2016 Oct.
- Regulation of Vegf signaling by natural and synthetic ligands.  
Rossi A\*, Gauvrit S\*, **Marass M** et al. ***Blood***, 2016 Aug. - \*joint first author
- Cloche is a bHLH-PAS transcription factor that drives haemato-vascular specification.  
Reischauer S\*, Stone OA\*, Villasenor A\*, Chi N, Jin SW, Martin M, Lee MT, Fukuda N, **Marass M** et al. ***Nature***, 2016 Jul. - \*joint first author